Micro-scale variability of atmospheric particle concentration in the urban boundary layer

Kumulative Dissertation
zur Erlangung des akademischen Grades
doctor rerum naturalium
Dr. rer. nat.

im Fach Geographie

eingereicht an der Mathematisch-Naturwissenschaftlichen Fakultät
der Humboldt-Universität zu Berlin

von
M.Sc. Bastian Paas

Präsidentin der Humboldt-Universität zu Berlin: Prof. Dr.-Ing. Dr. Sabine Kunst
Dekan der Mathematisch-Naturwissenschaftlichen Fakultät: Prof. Dr. Elmar Kulke

Gutachter:
1. Prof. Dr. Christoph Schneider
2. Prof. Dr. Wilfried Endlicher
3. Prof. Dr. Stefan Weber

Tag der mündlichen Prüfung: 07.12.2017

List of publications

This thesis is presented in a cumulative form and is based on the following citation-indexed and peer-reviewed journal papers:

I. **Paas, B.**, Schmidt, T., Markova, S., Maras, I., Ziefle, M., & Schneider, C. (2016). Small-scale variability of particulate matter and perception of air quality in an inner-city recreational area in Aachen, Germany. *Meteorologische Zeitschrift*, *25*(3), 305–317. https://doi.org/10.1127/metz/2016/0704

II. **Paas, B.** & Schneider, C. (2016). A comparison of model performance between ENVI-met and Austal2000 for particulate matter. *Atmospheric Environment*, *145*, 392–404. https://doi.org/10.1016/j.atmosenv.2016.09.031

III. **Paas, B.**, Stienen, J., Vorländer, M., & Schneider, C. (2017). Modeling of Urban Near-Road Atmospheric PM Concentrations Using an Artificial Neural Network Approach with Acoustic Data Input. *Environments 2017, 4*(2), 26. https://doi.org/10.3390/environments4020026

The author made the following contributions to the journal papers on which this thesis is based:

I. Responsible for the study design, the fieldwork (except for the survey), the modeling (except for the CAD pre-work) and numerical simulations, the data preparation, the data analysis, all figures, the literature review, and the writing (except for a few lines regarding the survey)

II. Responsible for the study design, the fieldwork, the modeling and numerical simulations, the data preparation, the data analysis, all figures, the literature review, and the entire writing

III. Responsible for the study design, the fieldwork (except for microphone calibrations), the model development and testing, the data preparation (except for acoustic raw data pre-processing), the data analysis, all figures, the literature review, and the entire writing

The author also contributed to the following full paper publications (conference proceedings or peer-reviewed journal papers) related to the thesis, which are, however, of minor relevance to the thesis itself:

i. Stienen, J., Schmidt, T., **Paas, B.**, Schneider, C., & Fels, J. (2014). Evaluation of combined stress factors on humans in urban areas. *Proceedings of TECNIACUSTICA 2014, 45th Spanish Congress on Acoustics, 8th Iberian Congress on Acoustics, European Symposium on smart cities and environmental acoustics*. Murcia, Spain.

ii. Stienen, J., Schmidt, T., **Paas, B.**, & Fels, J. (2015). Noise as a Stress Factor on Humans in Urban Environments in Summer and Winter. In *Proceedings of the EuroNoise 2015*. Maastricht, Netherlands, 2445-2450.

iii. Schmidt, T., Maras, I., **Paas, B.**, Stienen, J., & Ziefle, M. (2015). Psychophysical observations on human perceptions of climatological stress factors in an urban environment. *Proceedings of the 19th Triennial Congress of the IEA*. Melbourne, Australia, 1-8.

iv. Maras, I., Schmidt, T., **Paas, B.**, Ziefle, M., & Schneider, C. (2016). The impact of human-biometeorological factors on perceived thermal comfort in urban public places. *Meteorologische Zeitschrift*, *25*(4), 407–420. https://doi.org/10.1127/metz/2016/0705

v. Daniels, B., Zaunbrecher, B., **Paas, B.**, Ottermanns, R., Ziefle, M., & Roß-Nickoll, M. (2017). Assessment of urban green space structures and their quality from a multidimensional perspective. In a review for *Science of the Total Environment*[1].

[1]Ms. Ref. No.: STOTEN-D-17-04181

Contents

Abbreviations

AA1	Test case Aachen 1
AA2	Test case Aachen 2
AABU	Urban background government monitoring station, Aachen-Burtscheid
ABL	Atmospheric Boundary Layer
ANN	Artificial Neural Network
Austal2000	German reference pollutant dispersion model, developed by Janicke Consulting Engineers for the German Federal Environmental Agency
CAD	Computer-aided design
CFD	Computational Fluid Dynamics
DAE	Aerodynamic diameter
ENVI-met	Numerical micro-climate model, developed by M. Bruse
FAIRMODE	Forum for Air Quality Modeling in Europe
FB	Fractional bias
FuEco	Future Ecosystem
Hörn	Permanent weather station in the outlying district of Hörn, in Aachen
IBC	Inflow Boundary Conditions
ILÖK	Institute of Landscape Ecology at the University of Münster
JRC	Joint Research Centre of the European Commission
LAD	Leaf Area Density
LANUV	North Rhine-Westphalian State Office for Nature, Environment, and Consumer Protection
MEF	Model efficiency score
MS1	Test case Münster 1
MS2	Test case Münster 2
MSGE	Urban background government monitoring station, Münster-Geist
NH_3	Ammonia
NO	Nitric oxide
NO_x	Oxides of nitrogen
NRW	North Rhine Westphalia
O_3	Ozone
OPC	Optical Particle Counter
PM	Particulate Matter
$PM_{(0.25\text{-}1)}$	Particle mass concentration of particles with an aerodynamic diameter between 0.25 µm and 1 µm

$PM_{(0.25\text{-}10)}$	Particle mass concentration of particles with an aerodynamic diameter between 0.25 µm and 10 µm
$PM_{(0.25\text{-}2.5)}$	Particle mass concentration of particles with an aerodynamic diameter between 0.25 µm and 2.5 µm
$PM_{(1\text{-}10)}$	Particle mass concentration of particles with an aerodynamic diameter between 1 µm and 10 µm
PM_{10}	Particle mass concentration of particles with an aerodynamic diameter <10 µm
PNC	Particle Number Concentration
$PNC_{(0.25\text{-}2.5)}$	Particle number concentration of particles with an aerodynamic diameter between 0.25 µm and 2.5 µm
Q-Q plot	Quantile-Quantile plot
RANS	Reynolds-Averaged Navier Stokes equations
rh	Relative humidity
RHC	Robust Highest Concentration
RQ	Research Question
SBSS	SOM-Based Stratified Sampling
sh	Specific humidity
SO_2	Sulfur dioxide
SOM	Self-Organizing Map
Ta	Air temperature
TalDIA	Wind field model of Austal2000
UFO	Urban Future Outline
VACW	Traffic-related government monitoring station, Aachen-Wilhelmsstrasse
VMS2	Traffic-related government monitoring station, Münster-Weselerstrasse
WD	Wind Direction
WHO	World Health Organization
WS	Wind Speed
z_0	Roughness length
Δ PM_{10}	PM_{10} remainder

Figures

Tables

Abstract

Knowledge about the micro-scale variability of airborne particles is a crucial criterion for air quality assessment within complex terrains such as urban areas. Due to the significant costs and time consumption related to the work required for standardized measurements of particle concentrations, dense monitoring networks are regularly missing. Models that simulate the transmission of particles are often difficult to use and/or computationally expensive. As a result, information regarding on-site particle concentrations at small scales is still limited.

This thesis explores the micro-scale variability of aerosol concentrations in space and time using different methods. Experimental fieldwork, including measurements with mobile sensor equipment alongside a survey, and modeling approaches were conducted. Applied simulation studies, a performance assessment of two popular particle dispersion models, namely Austal2000 and ENVI-met, as well as the development of an ANN model are presented. The cities of Aachen and Münster were chosen as case studies for this research.

Unexpected patterns of particle mass concentrations could be observed, including the identification of diffuse particle sources inside a park area with strong evidence that unpaved surfaces contributed to local aerosol concentration. In addition, vehicle traffic was proved to be a major contributor of particles, particularly close to traffic lanes. Results of the survey reveal that people were not able to distinguish between different aerosol concentration levels. Austal2000 and ENVI-met turned out to have room for improvement in terms of the reproduction of observed particle concentration levels, with both models having a tendency toward underestimation. The newly developed ANN model was confirmed to be a fairly accurate tool for predicting aerosol concentrations in both space and time, and demonstrates the principal ability of the approach also in the domain of air quality monitoring.

Keywords: Air quality; Austal2000; ENVI-met; Environmental acoustics; Machine learning; Micro-scale simulations; Model performance; Neural networks; Particle dispersion; Particulate matter; Personal exposure

Zusammenfassung

Für die Luftqualitätsbewertung in urbanem Gelände sind Informationen zur raumzeitlichen Variabilität luftgetragener Feinstaubpartikel auf kleiner Skala von wichtiger Bedeutung. Standardisierte Messverfahren, zur Bestimmung von Partikelkonzentrationen, sind mit hohem Zeit- und Kostenaufwand verbunden, weshalb dichte Messnetze selten vorhanden sind. Simulationsmodelle zur Berechnung des Partikeltransports sind kompliziert in der Anwendung und/oder benötigen hohe Computerrechenleistung. Infolgedessen gibt es bezüglich örtlicher Partikelkonzentrationen noch große Informationslücken.

Diese Arbeit untersucht die mikroskalige Variabilität von Aerosolen in Raum und Zeit mit Hilfe unterschiedlicher Methoden. Für Feldexperimente wurden Messwerterhebungen mit mobilen Sensoren und eine Passantenbefragung durchgeführt. Weiterhin wurden Modellierungsansätze angewendet. In dieser Arbeit wurden die Partikeltransportmodelle ENVI-met und Austal2000 einerseits in ihrer Leistung bewertet und andererseits in angewandten Studien eingesetzt. Weiterhin wurde ein neuronales Netzwerk zur Vorhersage von Partikelkonzentrationen entwickelt. Die Untersuchungen wurden exemplarisch in den Städten Aachen und Münster durchgeführt.

Es konnten unerwartete Verteilungsmuster hinsichtlich der Massekonzentration von Partikeln beobachtet werden. In einem innerstädtischen Park wurden diffuse Partikelquellen identifiziert, mit einem deutlichen Hinweis darauf, dass feuchtgelagerte Wegedecken einen maßgeblichen Anteil an lokalen Partikelimmissionen hatten. Weiterhin wurde Straßenverkehr als wichtiger Beitrag zum städtischen Aerosol identifiziert, insbesondere in der Nähe von Verkehrswegen. Ergebnisse der Befragungen ergaben, dass Passanten, die verschiedenen Partikelkonzentrationen ausgesetzt waren, diese durch Wahrnehmung nicht unterscheiden konnten. Die Modelle Austal2000 und ENVI-met zeigten bei Simulationen Ungenauigkeiten in Form von Unterschätzungen im Vergleich zu Messwerten. Das neu entwickelte neuronale Netzwerk prognostizierte Partikelkonzentrationen teilweise mit hoher Genauigkeit. Der entwickelte Ansatz zeigt das große Potenzial von neuronalen Netzen für die Vorhersage von Partikelkonzentrationen, auch für den Bereich der Luftqualitätsüberwachung, in räumlicher und zeitlicher Ausdehnung auf.

Keywords: Aerosol; Akustik; Austal2000; Belastung; ENVI-met; Feinstaub; Individuelle Exposition; Luftqualität; Mikroskalige Simulation; Modellleistung; Neuronales Netz; Partikelverteilung; Umwelt

1. Introduction

1.1 Structure of the thesis

This thesis is based on the content of three citation-indexed and peer-reviewed journal papers. The main outcomes of the publications are summarized in this synthesis, which puts the results of the individual studies in the broader context of the RQs listed in Sect. 1.5. The presented synthesis is intended to be a stand-alone document; however, a similarity to some degree with the content of the three papers is inevitable.

Sect 1. **Introduction**

provides a short overview of the current scientific challenges in the research area of the thesis. It defines the framework as well as the open research questions and respective objectives of the thesis.

Sect 2. **The field experiment analysis**

outlines the motivation for the multidisciplinary framework of the field experiment study, presents the study design and research sites, and illustrates the main outcomes that could be reached by analysis of field experiment data.

Sect 3. **Deterministic modeling of particle distribution in the urban ABL**

justifies the comparison of two different deterministic simulation tools, and presents the test case environments, configuration choices, and recommendations for successful modeling, as well as a performance analysis, where predictions were compared to observations. It furthermore includes the presentation of two applied studies, quantifying resuspension source emissions of particles and assessing the influence of vegetation elements on ground-level aerosol concentrations.

Sect 4. **Prediction of particle concentrations using a newly developed statistical model**

describes the motivation for the development of the ANN model, discusses the testbed environment as well as technical steps that should be considered during ANN model development, and outlines the performance and ability of the approach presented.

Sect 5. **Conclusions and outlook**

concludes the thesis and identifies directions for future research.

The synthesis is followed by the thesis papers, which are reproduced in their original journal format, and an appendix:

Journal paper I, *Small-scale variability of particulate matter and perception of air quality in an inner-city recreational area in Aachen, Germany*

Journal paper II, *A comparison of model performance between ENVI-met and Austal2000 for particulate matter*

Journal paper III, *Modeling of Urban Near-Road Atmospheric PM Concentrations Using an Artificial Neural Network Approach with Acoustic Data Input*

Appendix A, *Micro-scale variability of PM_{10} – Influence of vegetation elements on ground-level aerosol concentrations*; A conference poster presented at the European Geoscience Union, EGU – General Assembly, 2016, April 2016.

1.2 Perspective

Poor air quality as a result of air pollutants like particulate matter (PM) is a major environmental risk to health (WHO, 2013). Results of epidemiological studies suggest that both long-term and even short-term stays at locations with high atmospheric PM concentrations, for example while commuting or relaxing, could have significant impacts on health and are linked with issues such as respiratory and cardiovascular diseases (Brunekreef and Holgate, 2002; Pope et al., 2002; von Klot, 2005; Chow et al., 2006; Raaschou-Nielsen et al., 2013). In cities, particles emitted through anthropogenic activities, such as industrial works, domestic heating, or vehicle traffic, which often include toxic, carcinogenic, or mutagenic materials (Kelly and Fussell, 2012), contribute to the urban aerosol (Lenschow, 2001), leading to increased particle concentrations that can even be visually recognized at times, as in the example shown in Fig. 1. Not only are levels of particle concentrations observed to be higher in urban spaces but they also affect a considerably larger number of people in comparison to rural areas. Over half of the world's population lives in cities. In Europe urbanization is even more progressed. Nowadays, over 70 % of European citizens live in cities with a future perspective of further increasing urbanization (United Nations, 2014). In general, urban citizens are influenced by numerous environmental stressors, one of the major ones being PM, due to the time they spend close to the respective sources (Vlachokostas et al., 2012). It is estimated that in European cities life expectancy at age 30 is reduced by up to 22 months solely due to the fact that outdoor particle concentrations exceed the World Health Organization (WHO) air quality guidelines (Pascal et al., 2013). The combination of both regular exceedances of air quality standards in cities (EEA, 2016) and the fact that throughout the world the majority of people live in urban areas highlights the importance of the research area at hand concerning the issue of urban air pollution through PM and its respective distribution.

The individual outdoor exposure to airborne particles is complex to describe and is highly dependent on the specific whereabouts (Dons et al., 2011; Broich et al., 2012; Steinle et al., 2013; Bekö et al., 2015; Spinazzè et al., 2015; Van den Bossche et al., 2016). In cities vehicle traffic has been identified as a major contributor to the aerosol strain near roads (Morawska et al., 1999; Karagulian et al., 2015; Manousakas et al., 2017) due to both exhaust and non-exhaust inputs (Ketzel et al., 2007; Amato et al., 2014). High levels of particle concentrations are found to occur mostly within street canyons (Wurzler et al., 2016). However, knowledge of aerosol distribution patterns in complex terrain on the urban micro-scale and their related drivers is still limited (Kumar et al., 2009).

Fig. 1: Photograph of the Guanabara Bay area of Rio de Janeiro, Brazil, showing considerably polluted air up to a few hundred meters AGL, capped by a late morning temperature inversion. The photograph has been taken from the viewpoint of the statue *Christ the Redeemer* during a field trip at a project workshop of RWTH Aachen University and the Universidad Federal do Rio de Janeiro in 2014.

Observation of particle concentrations with reference methods is an important task due to the surveillance of air quality standards. However, traditional monitoring of particle concentrations may not accurately characterize the spatial variability in the surrounding area and may thus not be representative of the city as a whole (Wilson et al., 2005). Reference instrumentation is expensive and, therefore, dense monitoring networks to overcome this issue are regularly missing (Laden et al., 2006). As a result, information on micro-scale particle concentrations and the distribution of particles derived from field data is limited. Recently developed economic micro-sensors have until now been unable to mitigate the poor availability of information in the dimension of space since this generation of micro-sensor platforms still shows mostly poor performance for PM in particular (Borrego et al., 2016).

Air pollution dispersion modeling is an important additional tool in urban air-quality regulation and planning throughout the world (El-Harbawi, 2013). Models simulate the concentration of air pollutants at specific times and locations, and can be cost- and time-effective integrative alternatives to field measurements. Numerous methods have been developed and these can be divided into two main approaches: namely, deterministic and statistical modeling (Massmeyer, 1999). Deterministic models describe the physical processes that determine the particle transportation in the atmosphere (Daly and Zannetti, 2007; Lateb et al., 2016). Statistical methods rest on data analysis, forging empirical relationships between predictive values and predictor variables (e.g., Santos and Fernández-Olmo, 2016). Until now, despite successful application, modeling approaches of both deterministic and statistical

methods show room for improvement with regard to their performance (Blocken et al., 2013).

As already identified, besides various air pollutants, individuals are simultaneously exposed to several other environmental stressors, such as noise or thermal stress. There is a need to address co-exposure in a more integrated way due to a current lack of multi-disciplinary environmental studies (Mauderly et al., 2010; Vlachokostas et al., 2012, 2014). Focusing on the development of innovative solutions for the cities of the future, the research project UFO (*Urban Future Outline*[2]) was initiated within the Project House HumTec (*Human Technology Centre*[3]) at RWTH Aachen University, funded by the German federal and state governments' Excellence Initiative, in order to establish a multi-disciplinary platform for research on urban spaces. The FuEco sub-project (*Future Ecosystem*[4]), part of UFO, focused on the assessment of combined stresses in urban public spaces and brought together scientists from various backgrounds, including humanities/social sciences, engineering, and natural sciences. The work presented in this thesis took place within the frame of the FuEco project.

[2] www.humtec.rwth-aachen.de/index.php?article_id=881&clang=1. The UFO project, led by C. Schneider (now at HU Berlin) and M. Ziefle, was initially funded for two years.

[3] http://www.humtec.rwth-aachen.de/index.php?article_id=1&clang=1. Project House HumTec at RWTH Aachen.

[4] http://www.humtec.rwth-aachen.de/index.php?article_id=1055&clang=1. The FuEco project, led by C. Schneider (now at HU Berlin) and M. Ziefle, and coordinated by the author of this thesis, integrated five chairs at RWTH Aachen (Communication Science, Physical Geography and Climatology, Technical and Medical Acoustics, Computer Aided Architectural Design, & Virtual Reality).

1.3 Case study environments

As ideal examples of mid-sized cities with around 250,000 inhabitants in Germany, the cities of Aachen and Münster were chosen as case studies for this thesis. Both cities are located in the west of Germany (Fig. 2) and feature a population of around 250,000 inhabitants (IT.NRW, 2015). The cities are characterized by a mild oceanic climate with cool summers and moderately cool winters (Köppen, 1936). Precipitation is evenly dispersed around the year with a

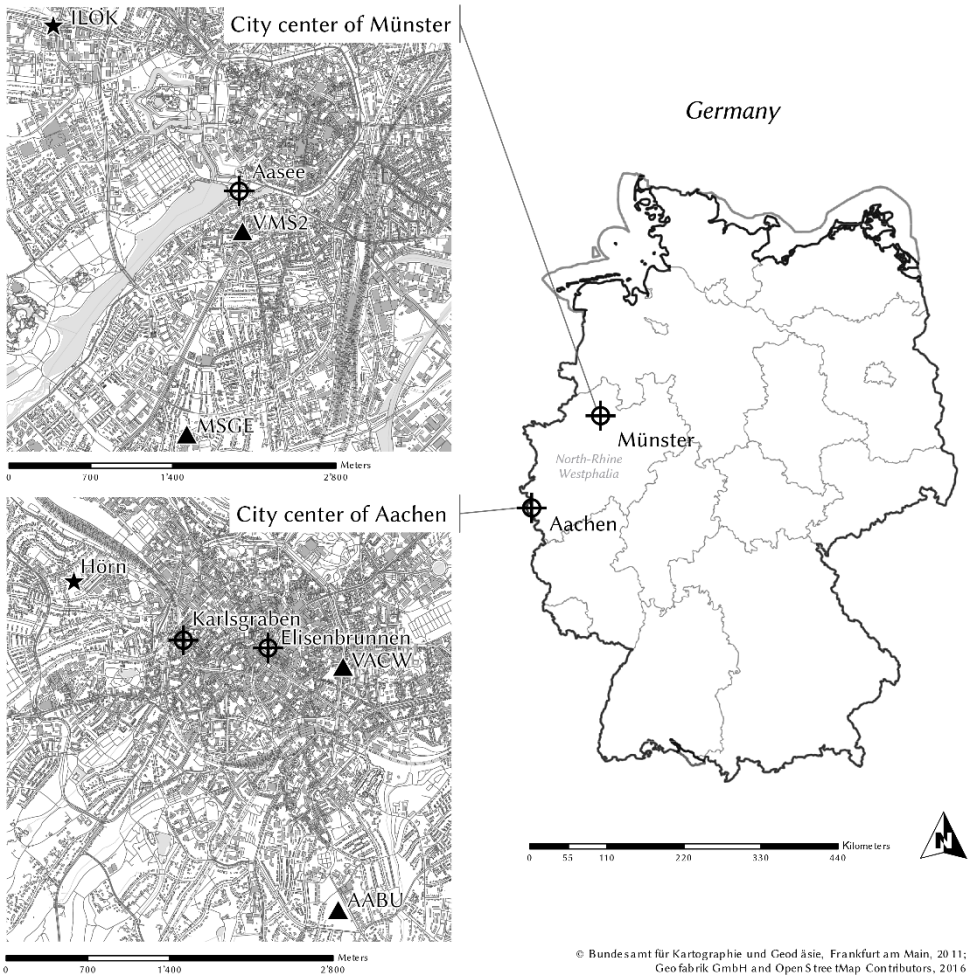

Fig. 2: The cities used as case studies and their locations in Germany (right illustration) with close-ups of the city centers of Münster (upper left illustration) and Aachen (lower left illustration) including depictions of the research sites (crosshair cursors), government air quality monitoring stations (triangles) and weather stations (stars). Reworked after journal paper III.

mean quantity of rainfall of 782 mm and 914 mm for Münster and Aachen, respectively. The mean air temperature in both cities was found to be 10 °C, valid for the period of the years 1981–2010 (DWD, 2012). However, the cities of Aachen and Münster are characterized by different topographies. Aachen is situated in the tri-border region close to the Netherlands and Belgium, 60 kilometers to the west of Cologne (see Fig. 2). The city of Aachen is characterized by distinct relief, with the city center lying in a basin north of the foothills of the low Eifel mountain range. The maximum altitude range in the municipal area is 200 m (150–350 m ASL). The city center is identified by densely built up perimeter development with buildings that generally contain 4–5 floors. The annual mean concentration of urban background PM_{10} in the city of Aachen has been found to be 15 µg m^{-3} (LANUV, 2015). Münster, meanwhile, is located 40 kilometers north of the Ruhr area (see Fig. 2). It is characterized by almost entirely flat terrain (65 m ASL). The urban area features two main water bodies: Aasee, a lake located to the west of the city center, and the Dortmund–Ems Canal, an inland navigation channel that divides the municipal area of Münster to the east of the city center in a north–south direction. The urban fabric contains mixed development with areas that feature isolated, freestanding buildings with 2–3 floors (mostly in the outlying areas) and a small city core, as well as the neighborhood around the port that is more densely built up with perimeter development. In the city of Münster the annual mean concentration of urban background PM_{10} has been determined to be 19 µg m^{-3} (LANUV, 2015).

1.4 Framework

Atmospheric particle concentrations not only differ between a city and its rural surroundings but also vary spatially within urban areas. Cities are, by definition, characterized by a complex terrain that leads to increased surface roughness, including varying ground levels as well as numerous obstacles such as buildings and vegetation elements that prevent both air from moving uniformly and conditions of laminar flow in the boundary layer atmosphere. Thus, particle transport, mainly driven by the wind vector, underlies the chaotic system of turbulence even more than in rural areas and is therefore highly variable in both space and time (Lien et al., 2008). Dominant turbulent transmission and dispersion processes make the nature of examinations focusing on the spatial micro-scale variability of particle concentrations within cities challenging (Lateb et al., 2016). The definition of the micro-scale in particular includes the spatial resolution of single buildings; single vegetation elements; or street canyons (see Fig. 3). From the perspective of particle sources within this type of scale, single point, line, or area sources such as vehicle traffic emissions must be resolved as well. Furthermore, single micro-scale elements,

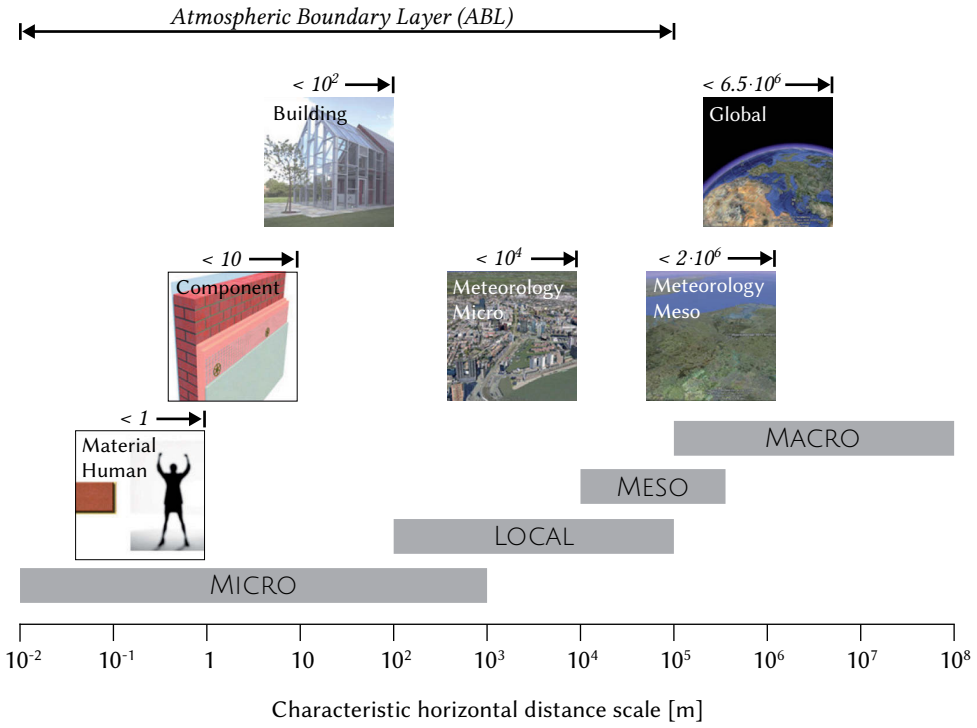

Fig. 3: Relevant distance scales of atmospheric phenomena and pollutant dispersion. Reworked after Oke (1987) and Blocken (2013).

the entire city representing the meso-scale, as well as macro-scale aspects, such as long-range background particle transport or synoptic weather conditions, interact in complex ways (Oke, 1987; Gosling et al., 2007). Processes on all the mentioned spatial scales together have a combined impact on local particle concentrations. This thesis focuses on phenomena that can be observed on the micro-scale; under consideration of local-, meso-, and macro-scale interactions. The main approach employs methods of experimental fieldwork, and deterministic and statistical modeling. Experimental designs for all studies conducted in this thesis incorporated the requirements that arise on research that focuses on the urban micro-scale as described above.

1.5 Research questions

This thesis is designed to explore the micro-scale variability of aerosol concentrations in space and time using different methodical approaches. The work is built around the following research questions (RQs):

RQ 1. How are airborne particles distributed within typical inner-city park areas in Germany? Which areas show the highest concentrations of PM? Is it possible to identify the main drivers that lead to specific concentration patterns?

RQ 2. Can humans identify different concentration levels of particle metrics in concentration magnitudes that can be expected in urban areas in Germany?

RQ 3. How can the problem of scarce particle concentration data in both space and time on the micro-scale within urban areas be overcome?

RQ 4. What performance regarding predictions of particle concentration can be expected from deterministic pollution dispersion models of both well-established reference models and newly available micro-climate models when faced with real-world situations? Which initial conditions lead to poor/good performance? What can be done to improve the performance of pollution dispersion models?

RQ 5. Is statistical modeling an option to predict non-linear phenomena such as the distribution of particles in the Atmospheric Boundary Layer (ABL)? What accuracy can be reached with non-linear approaches? Can non-linear statistical modeling help to address the gap mentioned in RQ 3?

1.6 Objectives & related approaches

The following objectives are defined to answer the main RQs of this thesis, formulated in Sect. 1.5. Within this thesis a combination of various approaches, using methods of experimental fieldwork and modeling tools, whose results are inter-compared, has been applied to reach the designated objectives (see Fig. 4).

The first objective of the thesis is to present an insight of micro-scale dispersion of airborne particles on the micro-scale by the use and the analysis of experimental field data in order to address the first part of RQ 1. Experimental research has been conducted at two inner-city park areas using portable instrumentation able to sample at high temporal resolution concerning the collection of meteorological and aerosol data, respectively. Furthermore, due to the use of mobile sensor equipment, the data collection approach enabled spatial investigations. Additionally, an on-site survey was carried out to assess the human perception of air quality. A comparison with aerosol concentration data reveals the ability of humans to distinguish between different levels of particle exposure in order to address RQ 2.

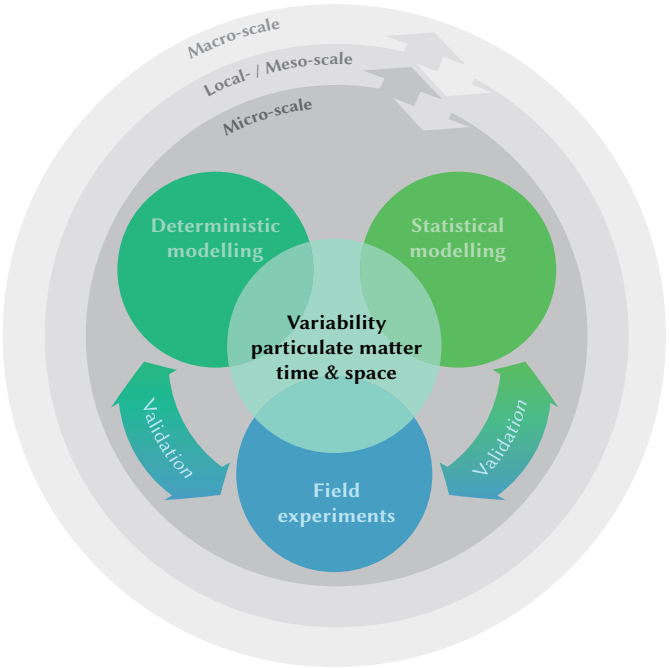

Fig. 4: Scheme of the research approach of the thesis.

The second objective of this thesis is to evaluate the performance of two different deterministic pollutant dispersion models in real-world situation case studies concerning RQ 4. The comparison with field data reveals the accuracy that can be expected in complex urban environments from the models used, namely the reference dispersion model Austal2000 and the micro-climate model ENVI-met. Different case studies were set up to highlight the atmospheric conditions that lead to poor/good performance, as well as to find possible drivers to improve the models' accuracy. For the purpose of finding possible answers to the second and third parts of RQ 1, modeling results were compared to field data again. The goal was also to demonstrate practical applications, such as the influence of green elements on ground-level aerosol concentrations. Overall, the assessment of deterministic model performance gives partial answers to RQ 3.

One major goal of this thesis is to outline approaches to gain more detailed spatial and temporal information on local particle concentration beyond field data from immovable sensors (RQ 3). Therefore, a non-linear statistical model based on the artificial neural network (ANN) approach has been developed using acoustic and meteorological data as well as data representing background particle transport as input variables. Comparison with field data demonstrates the capabilities of the approach regarding the temporal and spatial prediction of particle concentrations in order to address RQ 5 and thus to give partial answers to RQ 3. The added value of the ANN model approach to predicting atmospheric particle concentrations is discussed, and limitations and uncertainties are presented.

2. The field experiment analysis

This section describes the analysis of the intra-urban particle distribution that was observed using field experiment data. Data were derived from mobile sensors that were used to collect different particle concentration metrics. Furthermore, an investigation of the perception of different levels of particle exposure is presented herein. This chapter is based on results also described and discussed in journal paper I. Section 2.1 provides a brief introduction. Here, the current state of the art concerning field experiments in the context of aerosol distribution on the urban micro-scale is highlighted and the motivation for the study is outlined. Section 2.2 provides a description of the study design, including an introduction to the research site and an explanation of the field methods that were used to collect the data set. The results with regard to micro-scale particle distribution are presented in Sect. 2.3, while Sect. 2.4 details the main outcomes of the perception analysis.

2.1 Context and motivation to carry out field experiments

Mobile sensor platforms are increasingly used to assess the variability of, for example, particle concentration within the urban environment and to elaborate the concentration levels people are effectively exposed to (Peters et al., 2014). Experimental studies have shown that aerosols are dispersed in highly variable ways, especially inside cities and even within tens of meters in space. Evidence has been provided from opportunistic mobile monitoring studies using people's common daily routines to move measurement devices around the city (Dons et al., 2011; Broich et al., 2012; Van den Bossche et al., 2016) on the local city scale by using temporary installed sensors (Birmili et al., 2013b) and from studies using portable instrumentation, either along fixed measurement routes (Birmili et al., 2013a) or recurrently at different locations, respectively (Merbitz et al., 2012c, 2012b). In this chapter, a field study seeking to obtain a deeper understanding of the micro-scale distribution of particles was conducted within an inner-city park area. Park areas fulfill a variety of important ecosystem functions inside urban environments, including reducing the risk of flooding, mitigation of heat stress, and having a positive effect on air quality through filtration of polluted air (Baumgardner et al., 2012; Andersson-Sköld et al., 2015).

One of the most important functions of inner-city parks, alongside the effects on the urban micro-climate, is the way in which they serve as recreational areas for citizens. Besides actual conditions of environmental stressors, for example of particle concentrations and their respective influence on health (Venn et al., 2001), there is a basic question of whether people are able to perceive their exposure to particles. It is not yet understood whether there is a relationship between the physical stressor (i.e., aerosol concentration) and the specific perception of air quality, and/or whether there is a relationship between the physical stressor and the integrative evaluation of on-site comfort. Most of the work focusing on the perception of environmental stressors has focused on thermal comfort (Chen and Ng, 2012; Johansson et al., 2014). When perception was linked to air pollution, usually perceived risks were addressed or epidemiological studies were performed (Badland and Duncan, 2009). Most studies have been carried out through social and public opinion surveys that focused almost exclusively on people's awareness or level of concern about air pollution (Nikolopoulou et al., 2011). Brody et al. (2004) started empirical research to examine the local level. Even in this case, the data was collected and analyzed at the neighborhood level and not assessed on the pedestrian scale.

2.2 Study design

The field experiment analysis was designed to explore the spatial distribution patterns of urban atmospheric aerosol using portable instrumentation to determine different metrics of particle concentration, in combination with a parallel survey examining urban park users' sensation and perception of air quality. A simplified description of the study design (i.e., a description of the research site and the basic principle of data collection and analysis) is outlined in the following sections. A more comprehensive picture of, for example, the principle of operation regarding the sensors used, and the survey and data quality (including uncertainties) is given in the introduction and methodology sections of journal paper I.

2.2.1 Areas under study

The inner-city park area *Elisenbrunnen* in the city of Aachen was determined as the research site for the field experiment case study. The area is remote from industrial estate and features complex terrain. "Complex terrain" is hereinafter used to refer to the complex urban geometry of street canyons and squares that are characterized by numerous obstacles such as houses with varying height and

ground levels (see Fig. 5). The park area is surrounded by dense perimeter development with buildings generally comprised of 4–5 floors. One of the most frequented roads by public transit buses (Friedrich-Wilhelm-Platz), inaccessible for individual private vehicles and boasting four main bus stops (102 coach connections per hour on weekdays), leads through the investigation area. The park is surrounded by infrequently used roads to the northeast (industrial vehicles for delivery only) and southeast (Hartmannstrasse), and a highly frequented street used mainly by private cars (Ursulinerstrasse). Unsurfaced footpaths subdivide the green area, which contains mainly small flowerbeds and a lawn surface that is surrounded by deciduous London plane trees (*Platanus x hispanica*). Six monitoring sites were chosen inside the study area for measurements and surveys. Sites E and F were characterized as typical recreational spots within the green area (marked with green circles in Fig. 5). Site C features a prominent bus station, whereas site B was located in proximity to the intersection of Friedrich-Wilhelm-Platz and Ursulinerstrasse, which is dominated by moving traffic (indicated by red circles in Fig. 5). Monitoring sites A and D were chosen as places influenced by both traffic and the green area, respectively (depicted with blue circles in Fig. 5).

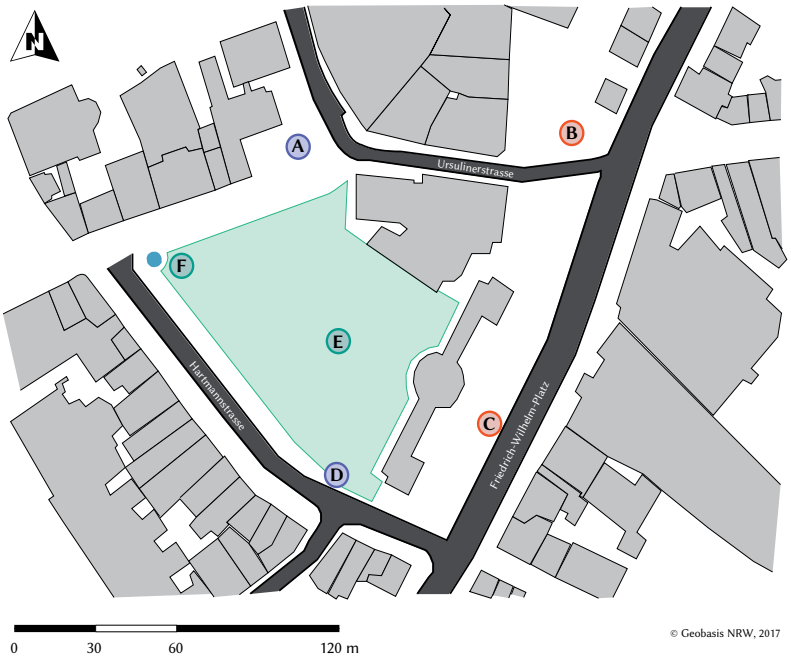

Fig. 5: Research site *Elisenbrunnen* in Aachen, including depicted measurement locations A–F (colored circles). The park area is marked with a green color field, whereas the light blue color field represents a water body. Gray areas depict buildings and black areas represent traffic arterials. Reworked after journal paper I.

2.2.2 Particle concentration measurements

Particle concentration measurements were carried out pursuing two different approaches by the use of a mobile optical particle counter (OPC) to determine different metrics of mass concentration of suspended particles with aerodynamic diameters (DAE) between 0.25 µm and 10 µm inside the park area *Elisenbrunnen*:

a) Time-series (weekdays, 10:00–17:00, 10-minute mean values of $PM_{(0.25–10)}$) measurements were performed in parallel to the survey (see below Sect. 2.2.3) at locations A, B, C, E, and F on chosen weekdays during a typical wintertime in February 2014, as well as at locations A, B, E, and F during summer in July 2014.

b) A semi-parallel approach was taken, using the single OPC recurrently at all described measurement locations (A–F) during seven selected weekdays (10:00–17:00) in February, May, and September 2014. The measurement location was changed every 5 minutes along a fixed measurement route with the OPC. One-minute means of mass fractions of particles with a DAE of 0.25 µm and 1 µm ($PM_{(0.25–1)}$), as well as of 1 µm and 10 µm ($PM_{(1–10)}$) were determined (n = 56).

Initial conditions for all measurement campaigns were chosen to be the same for both periods, including weather conditions with only partly clouded skies, no precipitation, and southwesterly winds (prevailing wind direction in the area under study (Merbitz et al., 2010); see also Fig. 3 in journal paper I).

2.2.3 Survey

A survey was performed in parallel to the time-series measurements of particle concentrations (see Sect. 2.2.2). A mixed-method interview study with on-site users was carried out in order to identify perceptions of air quality and on-site comfort. Overall, the sample consisted of 300 participants who volunteered to take part, representing an even gender distribution (see Sect. 2.6 in journal paper I for details). The perception of their own weather comfort, air quality, and on-site comfort was questioned and compared with the measured physical data. Data were analyzed using paired sample t-tests in order to detect seasonal differences of particulate matter concentration and mean rating for perceived air quality (results are not shown here; for further details see Sect. 3.3 in journal paper I). Further, the relationship between particulate matter and perceived on-site comfort was analyzed using bivariate analysis (Spearman's rank).

2.3 Micro-scale distribution of particles

Considering the semi-parallel approach of data collection (see Sect. 2.2.2) the distribution of $PM_{(1\text{-}10)}$ was found to be surprising. The highest mean concentration was revealed inside the green area at measurement locations E and F (arithmetic mean: 22.5 µg m^{-3} and 18.9 µg m^{-3}, respectively; geometric mean: 9.3 µg m^{-3} and 6.5 µg m^{-3}, respectively). As shown in Fig. 6, the lowest mean concentrations of $PM_{(1-10)}$ were found curbside of the main traffic arterials at locations B and C (arithmetic mean: 7.5 µg m^{-3} and 8.7 µg m^{-3}, respectively; geometric mean: 5.8 µg m^{-3} and 6.5 µg m^{-3}, respectively). Results of trend-corrected (for the methodology, see Sect. 2.5.1 in journal paper I) time-series measurement data ($PM_{(0.25-10)}$) indicate a similar distribution of coarse particles (not shown here; see Sect. 3.1 in journal paper I). Besides vehicle traffic that is expected to have a major influence on the

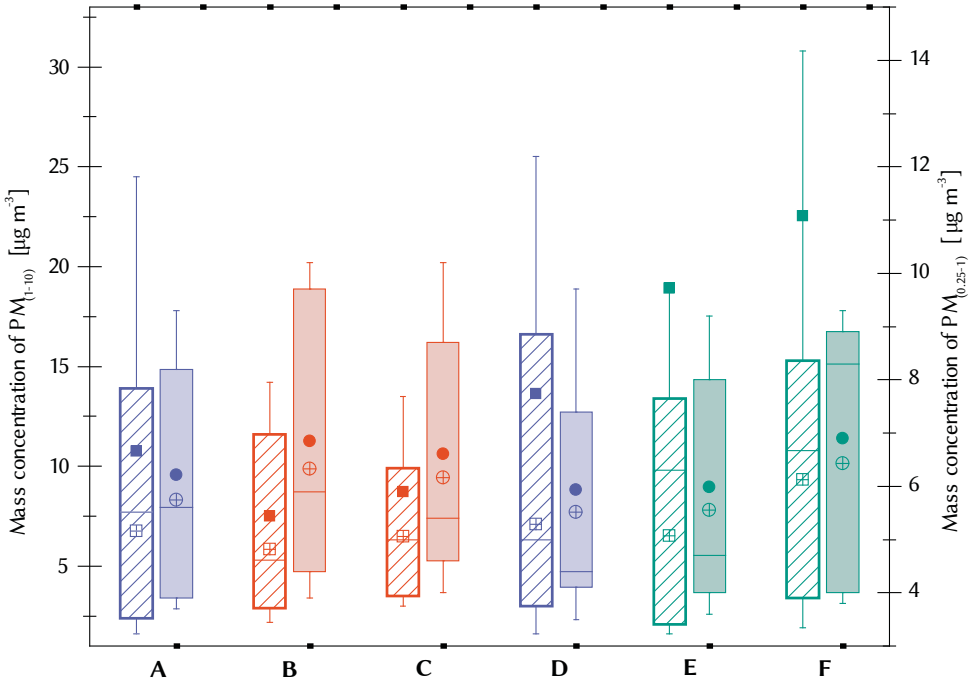

Fig. 6: Boxplot diagram of particle mass concentrations [µg m^{-3}] measured with a semi-parallel approach at different locations (A-F) inside the area under study *Elisenbrunnen* (1-minute means; n = 56). $PM_{(1\text{-}10)}$ concentrations are displayed in hatched boxes (left ordinate) whereas $PM_{(0.25\text{-}1)}$ concentrations are shown in planar boxes (right ordinate). Boxes display 25%/75% quantiles and medians (Red boxes: traffic related locations; Green boxes: green area locations; Blue boxes: transition locations). Filled squares and circles represent arithmetic means, crossed squares and circles represent geometric means, and whiskers show the standard deviation. Modified after journal paper I.

particle concentration near roads (Karagulian et al., 2015), it can be assumed that especially inside the park area additional diffuse particle sources are present. The green area at the Elisenbrunnen site is characterized by a surface of dry grass and unsurfaced footpaths containing loose and dry top coating material (during the summer season in particular). It may well be that those surfaces made a dominant contribution to airborne particles of $PM_{(1–10)}$ due to resuspension, as supposed by other studies (e.g., Birmili et al., 2013a).

Particle fractions of $PM_{(0.25–1)}$ were found to be equally distributed within the research site *Elisenbrunnen* (arithmetic mean: 6.0–6.9 µg m^{-3}). A poorly distinctive spatial pattern could be observed considering arithmetic mean $PM_{(0.25–1)}$ values with comparatively small differences between measurement locations, probably within the range of uncertainty of measurements. However, the highest average $PM_{(0.25–1)}$ concentrations were detected in the direct vicinity of the traffic arterials (locations B and C) and at location F inside the green area, respectively (see Fig. 6). It can be stated that vehicle traffic had a more dominant impact on $PM_{(0.25–1)}$ mass concentration due to emissions of, for example, brake and tire abrasion (Ketzel et al., 2007; Amato et al., 2014) as well as secondary accumulation mode particles arising from combustion processes during the case study (Gidhagen et al., 2004; Ketzel and Berkowicz, 2005).

Overall, observations similar to earlier studies (e.g., Broich et al., 2012; Birmili et al., 2013a) could be repeated. Aerosols were found variably distributed at very small scales. Different particle metrics were found to be distributed in various ways as already described by Zhu et al. (2006), Ning and Sioutas (2010) and Shu et al., (2014). A gradient with weak but declining concentrations of PM_{10} metrics with increased distance from traffic arterials, as found by other studies (e.g., Zhu et al., 2006), could not be confirmed at the research site *Elisenbrunnen*. Within the area under investigation the park site was surprisingly identified as featuring higher concentrations of $PM_{(1–10)}$ or $PM_{(0.25–10)}$ in comparison to traffic-related locations such as street canyons.

2.4 Perception of particle exposure

A detailed comparison of physically measured $PM_{(0.25–10)}$ data against survey results regarding the perception of air quality reveals that mass concentrations of $PM_{(0.25–10)}$ were not reliably assessed during the periods of data collection (see Fig. 7). In fact, park users described perceived air quality as good, neutral, or bad regardless of the factually measured mean $PM_{(0.25–10)}$ concentrations (ranging from 11.3 to 36.2 µg m^{-3} during the winter campaign and 17.0 to 129.9 µg m^{-3} during the summer campaign). This was the case in both investigated seasons (albeit it was

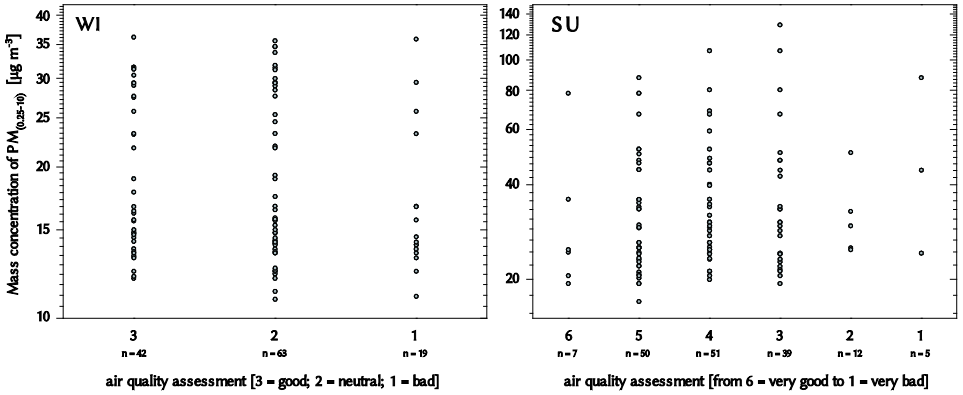

Fig. 7: Scatter plot diagrams of measured $PM_{(0.25\text{-}10)}$ concentrations [µg m^{-3}] vs. air quality assessments on a 3-point Likert scale (3 = good, 2 = neutral, 1 = bad) during the winter campaign (left illustration "WI") and vs. air quality assessments on a 6-point Likert scale (from 6 = very good to 1 = very bad,) during the summer campaign (right illustration "SU"). Modified from journal paper I.

worked with a refined Likert scale range from 1.0 = very bad air quality to 6.0 = very good air quality during the summer campaign). Consequently, no significant correlation was found between measured $PM_{(0.25–10)}$ and perceived air quality during both the winter season and the summer season (winter: r 0.13; summer: r -0.20).

In marked contrast to findings from Nikolopoulou et al. (2011), who claimed a significant positive correlation between PM concentrations and perception of air quality during a similar study in similar PM concentration magnitudes, it can be concluded that perception of air quality was imprecise and unrelated to the factually measured exposure. Nevertheless, data revealed a close relationship between the awareness of air quality and on-site comfort (data not shown here; for more details see Sect. 3.3 of journal paper I), thus corroborating the sensitivity of pedestrians to perception of urban stressors. Due to an undersized sample this study lacks deeper investigation into what actually formed the park users' opinion on air quality and on-site comfort, which is probably influenced more by factors such as sense of place (Brody et al., 2004) or acoustic occurrences than by actual air quality conditions.

3. Deterministic modeling of particle distribution in the urban ABL

This chapter describes the analysis of intra-urban particle distribution calculated by micro-scale pollutant dispersion models. It is based mainly on results described in journal paper II, shows results of journal paper I that could be obtained from the comparison of model predictions to field experiment data, and depicts outcomes presented on a poster presentation presented in Appendix A. Section 3.1 provides a short review of the current state of the art regarding deterministic dispersion modeling and puts the analyses made into context. Section 3.2 describes the performance analysis of two dispersion models including the motivation that justifies the investigation made, a brief introduction of the study design and the main results of the work of journal paper II. Sections 3.3 and 3.4 give results of two applied studies that were conducted with the modeling software codes ENVI-met and Austal2000, respectively, including brief motivation and methodology sections. Section 3.5 summarizes the main findings that were obtained by the use of deterministic modeling approaches.

3.1 Context

Deterministic air pollution models up to full numerical solutions describe the physical phenomena that determine the transportation of pollutants in the atmosphere and are powerful approaches for predicting the distribution of pollutants (Lateb et al., 2016). Highly resolved information can be gathered in time and space (Daly and Zannetti, 2007). This is one main advantage over information from field data, for instance data derived from point measurements that are only representative of the location where the measurements are taken (Wilson et al., 2005; Broich et al., 2012). Dispersion models are used intensively for scientific applications in order to better understand the spatial distribution of, for example, pollutants such as PM in the atmosphere (Tominaga and Stathopoulos, 2013). However, current challenges for the exploitation of deterministic modeling tools are manifold. Software codes are either expensive and/or difficult to use. Background knowledge of, for example, the physics behind fluid dynamics or pollutant dispersion is an essential precondition to avoid misinterpretation of modeling

results (Langner and Klemm, 2011). Massive computational effort is still needed to solve the equations that describe the turbulent air flow that is typically observed in the urban ABL (Stull, 1988) since numerous disturbing features are present in complex urban environments, such as buildings of different heights and shapes (Lateb et al., 2016). The transportation of pollutants is strongly influenced by the superposition and interaction of the turbulent flow patterns induced by urban obstacles (Chang and Meroney, 2001). As a result, extensive input information is needed, such as three-dimensional geometric information of obstacles in the domain (e.g., CAD data of buildings or/and vegetation elements), local meteorological data, and emission rates of pollutants to initiate deterministic models. Sometimes, input information is insufficiently available (e.g., Grimmond et al., 1998) to run those models successfully. This is especially true for scientific applications of deterministic models in complex terrains like urban areas. Consequently, deterministic modeling approaches are still far from straightforward operational tools when seeking to accurately predict the pollutant dispersion around buildings that qualify for, for example, urban air quality regulation and planning (Lateb et al., 2016).

3.2 Analysis of model performance between ENVI-met and Austal2000

3.2.1 Motivation for the model performance assessment

In this context (Sect. 3.1), a performance analysis is made between ENVI-met, a sophisticated computational fluid dynamics (CFD) modeling tool (Bruse and Fleer, 1998) that is popular in the research area of human bio-meteorology (e.g., Ambrosini et al., 2014; Jänicke et al., 2015), and Austal2000, the German reference dispersion model (Janicke, 2011). As of late, ENVI-met also features a pollutant dispersion module that is becoming more and more popular in air pollution research (Wania et al., 2012; Vos et al., 2013; Morakinyo and Lam, 2016). In comparison with numerous other models (e.g., Austal2000) ENVI-met is one of the first that offers ease of use—even for non-experts—as a result of a graphical user interface and useful editing tools contained in the software package. In addition, ENVI-met is available free of charge[5]. The features entail both chances and risks. Considering the risks, misinterpretation of results is possible, for instance when ENVI-met is used by those unfamiliar with the complex physics behind the dispersion simulation. This problem is likely to occur when model predictions are not reliable and accurate (Langner and Klemm, 2011). There is an urgent necessity that models are properly evaluated before their results can be used with confidence (Chang and Hanna, 2004). Until now, the performance of ENVI-met regarding the distribution of particles has rarely been assessed (Nikolova et al., 2011) and the performance in real-world applications in comparison with reference models is widely unknown. The accuracy and reliability of dispersion models such as CFD are of concern; thus, verification and validation of simulation results are imperative (Blocken et al., 2013). As a result, field measurements appear unquestionably necessary for assessing the quality of CFD simulations (Abohela et al., 2013).

[5] Up to version 3 and a temporarily restricted beta version 4, ENVI-met was free of charge including full functionality. The current version featuring unlimited usage is subject to a charge.

3.2.2 Study design

A more comprehensive description of the summarized study design outlined hereinafter (i.e., of the research sites, the modeling strategy, and settings) can be found in the introduction and methodology sections of journal paper II.

The modeling software used

In journal paper II the dispersion models Austal2000 and ENVI-met are compared to each other. Austal2000 is based on the Lagrangian approach and is designed for long-term sources and continuous buoyant plumes. The model is capable of calculating the dispersion of multiple point, line, and area sources of odorous substances and pollutants (e.g., SO_2, NO, NO_2, NH_3, PM) and includes dry deposition algorithms. Austal2000 is widely used for short-range transport of particles and gases in both applied studies (Merbitz et al., 2012b; Schiavon et al., 2015; Dias et al., 2016; Pepe et al., 2016) and in model performance research (Langner and Klemm, 2011; Letzel et al., 2012). The implemented model TALdia calculates a wind field library for cases with complex terrain input data. Such cases require input parameters of both the geometric information of the research domain (CAD data) and meteorological input data taken from ground-based measurements (Janicke, 2011).

ENVI-met, meanwhile, is a prognostic three-dimensional micro-climate model that is designed to simulate surface–plant–air interactions in urban environments with a typical resolution down to 0.5 m in space and 1–5 s in time (Bruse and Fleer, 1998), and features a pollution dispersion module according to simulate numerous point, line, and area sources of substances (e.g., NO, NO_2, O_3, and PM). It includes processes of particle sedimentation depending on size and mass, and deposition at surfaces. A simple upstream advection approach is used to calculate the pollutant dispersion. The CFD core of ENVI-met solves the Reynolds-averaged non-hydrostatic Navier–Stokes equations (RANS) for each spatial grid cell and time step. For initialization purposes, parameters of meteorological initial conditions must be provided as well as geometric information data similar to the requirements of Austal2000. For specific humidity (sh) input parameters, information from upper air soundings must be used (values from 2500 m AGL must be provided) whereas all other parameters can be obtained from ground-based measurements.

Test cases

Overall, four test cases were set up for the model performance analysis in the cities of Aachen and Münster, respectively (see Fig. 2 in Sect. 1.3). Two test cases were set up for the research site in Aachen modeling one computational domain with a spatial resolution of 2 m resembling the inner-city park area *Elisenbrunnen*. Two test cases were set up for the research site, *Aasee*, in the city of Münster, featuring one computational domain that represents the park area in 2 m spatial resolution (see Fig. 8). Dispersion simulations of both models, Austal2000 and ENVI-met, were performed using inflow boundary conditions (IBCs) in comparison with the time periods of semi-parallel particle concentration measurements that were carried out using a single OPC (for details see Sect. 2.2.2 and Sect. 3.5 in journal paper II) at different locations within the study domains (Fig. 8).

Two different test cases for each research site result from different meteorological actuations of the models using meteorological input data from different weather stations. For the first test case of the Aachen research site, meteorological data from the distant weather station *Hörn* (see Fig. 2) initiated the

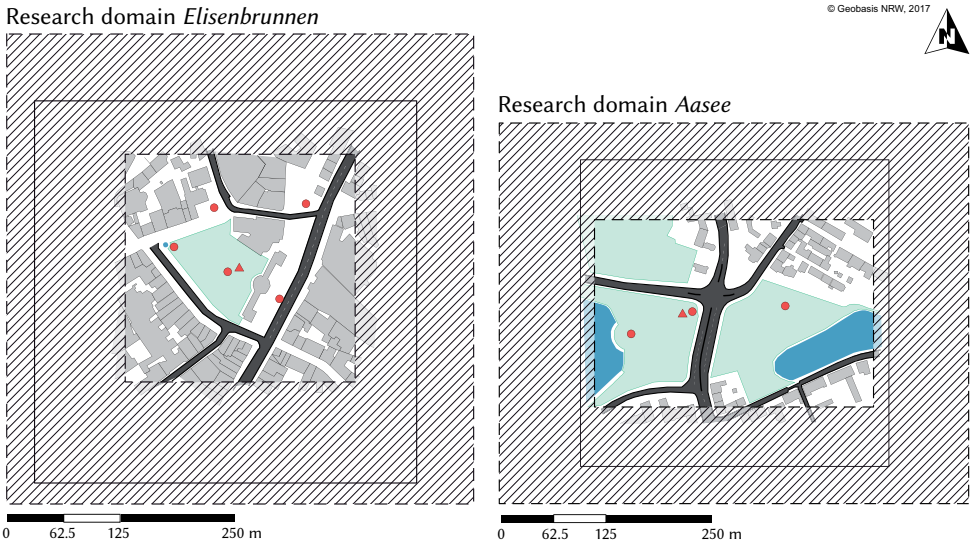

Fig. 8: Close-ups of the research domains in Aachen (left ill.) and in Münster (right ill.), including the receptor points where measurements of PM concentrations were carried out (red dots) and where meteorological input data were taken (red triangles). Park areas are marked with green color fields. Blue color fields represent water bodies. Gray areas depict buildings. Black areas represent traffic arterials. Frames mark the computational domain sizes of the two models used (black continuous line: Austal2000; black dashed line: ENVI-met; hatched areas represent the nesting grid sizes). Reproduced from journal paper II.

model runs (test case AA1). Local measurement data, collected during the particle concentration measurements within the study domain (see Fig. 8), were used as IBCs for the second test case of the Aachen research site (test case AA2). For the first test case of the Münster research site, meteorological data from the distant weather station *ILÖK* (see Fig. 2) initiated the model runs (test case MS1). Again, local measurement data from within the study domain (see Fig. 8) were used as IBCs for the second test case of the Münster research site (test case MS2). A short summary of the four different test cases is given in Tab. 1. Emission rates for all test cases and simulation tools were calculated by multiplying emission factors (µg vehicle^{-1} m^{-1}), referring to the guidelines published by Keller and de Hahn (2004) and Lohmeyer et al. (2004) with prevailing traffic intensity data (vehicles s^{-1}) that were derived from traffic counts.

Tab. 1: Summary of the four test cases that were conducted in the model performance analysis. Reproduced from journal paper II.

Research site	General setting	Study periods	IBC data	Test case
Aachen – *Elisen-brunnen*	Inner-city park area, complex terrain, varying ground surface, dense perimeter development, 3 area sources (traffic lanes)	9 selected weekdays in February, July 2014	Distant weather station, *Hörn*	AA1
			Local measurements in the area under study	AA2
Münster – *Aasee*	Inner-city park area, open space, varying ground surface, surface water, isolated freestanding buildings, 4 area sources (traffic lanes)	6 selected weekdays in February, July, August 2015	Distant weather station, *ILÖK*	MS1
			Local measurements in the area under study	MS2

3.2.3 Performance analysis

The performance of both models was assessed, comparing the simulation results of both models against each other as well as comparing simulation results to observations on the basis of 1-hour averages using different metrics of statistics and performance measures, as recommended in the literature. Namely, Q-Q plots (Venkatram et al., 2001), the fractional bias, FB (Cox and Tikvart, 1990), and the robust highest concentration, RHC (Perry et al., 2005), were used. Further details and a mathematical description of FB and RHC can be found in Sect. 4 of journal paper II.

Spatial distribution

As presented in Fig. 9, which shows 1-h averages of Austal2000 and ENVI-met PM_{10} predictions of depicted model runs, both models simulated similar patterns of particle dispersion, including highest PM_{10} concentrations close to particle sources, i.e., traffic arterials (see Fig. 8). Corresponding simulated PM_{10} concentrations seem to decline rapidly further from the traffic lanes in both models. Wind vector input data are one of the key meteorological drivers for dispersion models (Lateb et al., 2016) and make for higher PM_{10} concentrations in the north of the model area of the *Elisenbrunnen* test cases (see Fig. 9 a) and b)). In this case, with winds from the south, Austal2000 predicted a situation where particles tend to accumulate in, for example, the narrow passage in the north of the computational domain as well as in areas downwind from emission sources where particles get dammed up at obstacles.

In comparison, ENVI-met results showed more smoothly dispersed PM_{10} concentrations that rapidly decline further from the sources. Dispersion results of both models calculated for the *Aasee* test case where urban obstacles are present show, to a lesser extent, a more even distribution of the PM_{10} concentration. Particles seem to be transported with the wind away from the traffic lanes in both models. Overall, it is clear that Austal2000 predicted about two times higher PM_{10} concentrations throughout most parts of the computational domain in comparison with ENVI-met (see Fig. 9).

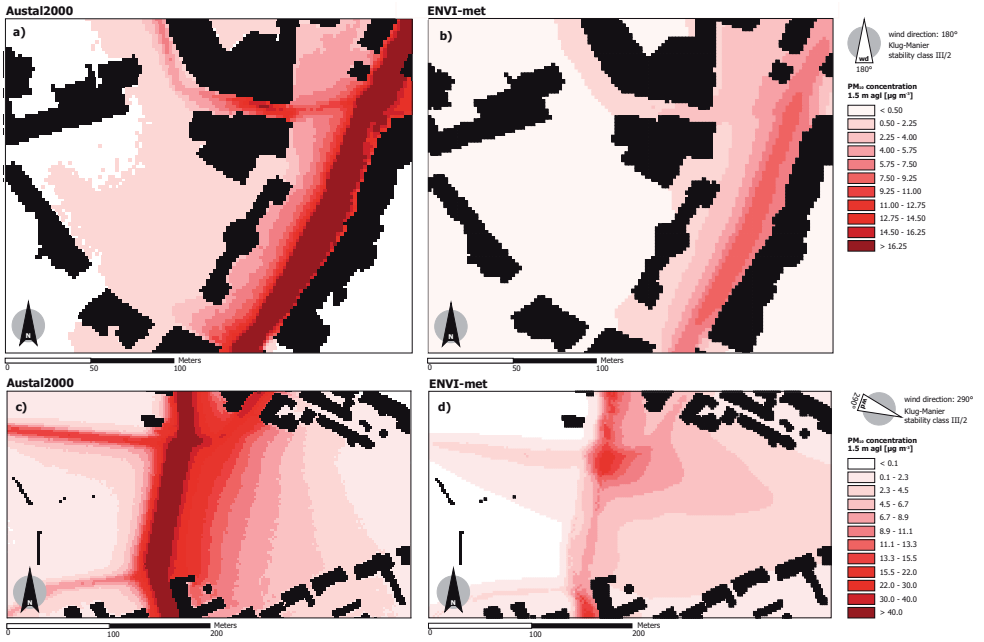

Fig. 9: Predicted traffic-induced PM_{10} concentration distribution of selected situations in 1.5 m agl of (a) Austal2000 and (b) ENVI-met for the Aachen test case (AA2) with inflow boundary conditions (IBC) defined by local meteorological measurements (1-hour average; prevailing wind direction = 180°; Klug-Manier stability class III/2) and of (c) Austal2000 and (d) ENVI-met for the Münster test case (MS2) with inflow boundary conditions (IBC) defined by local meteorological measurements (1-hour average; prevailing wind direction = 290°; Klug-Manier stability class III/2).

Predictions in comparison with observations

When compared to field data, both models almost constantly underestimated observations by a considerable amount, regardless of inflow boundary conditions and the areas under study (see Fig. 10). ENVI-met predictions were almost always less accurate compared to Austal2000; this was particularly the case in the low

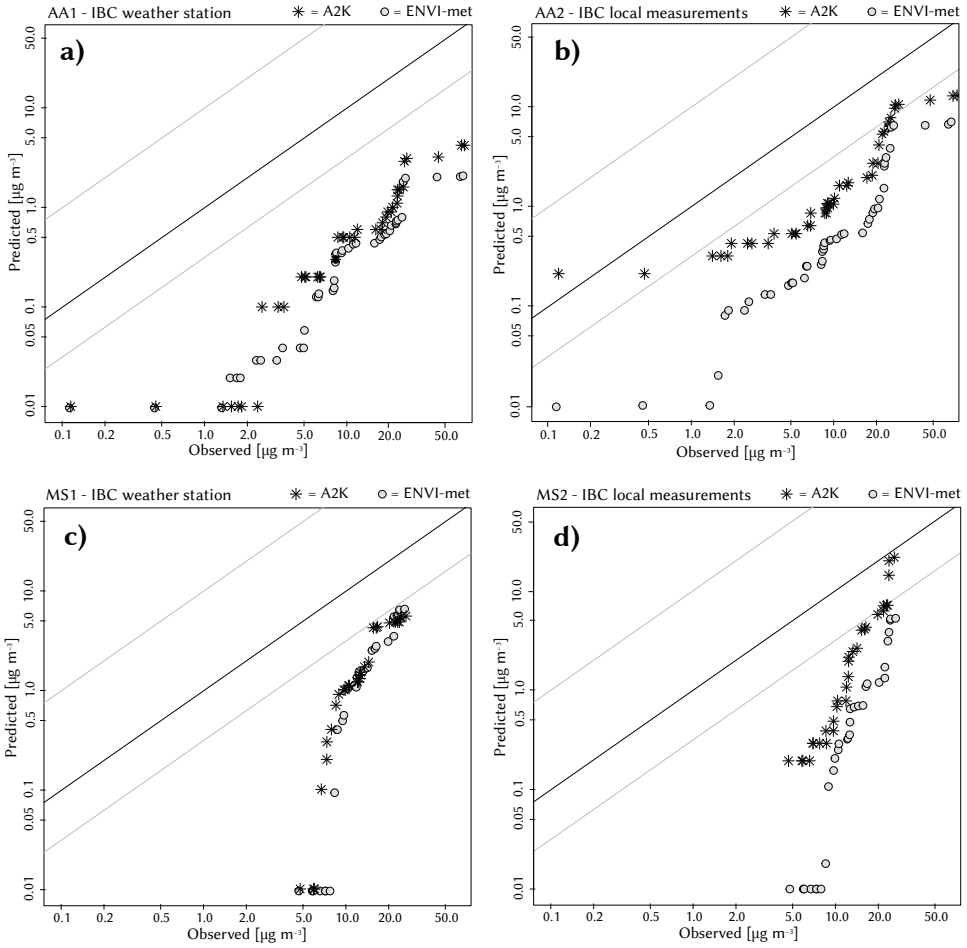

Fig. 10: Q-Q plot for predicted PM_{10} concentrations of all the receptor points of (a) the AA1 test case (IBC: data from the distant weather station), of (b) the AA2 test case (IBC: data from local measurements), of (c) the MS1 test case (IBC: data from the distant weather station) and of (d) the MS2 test case (IBC: data from local measurements) as 1-hour averages. Black stars represent predicted PM_{10} concentrations of Austal2000. Gray circles show predicted PM_{10} concentration of ENVI-met. The black line indicates the 1:1 rank correlation of the distributions. The gray lines depict the factor of two over- and underestimates. Reproduced from journal paper II.

concentration range. In the important upper concentration range ENVI-met results are closer to the simulation results of Austal2000 and the underestimations of both models were less marked. The analysis of the calculated RHCs confirms the former findings for the upper concentration range as well (see Tab. 2). Both models continued to underestimate the observed concentrations over the entire study period. RHCs for measurement data were calculated to be 73.6 µg m^{-3} for the Aachen test cases (AA1, AA2) and 33.1 µg m^{-3} for the Münster test cases (MS1, MS2), respectively. In particular, during the AA1 test case the RHC calculated from observations was seriously underestimated by both models (Austal2000 RHC: 4.8 µg m^{-3}; ENVI-met RHC: 2.5 µg m^{-3}). When considering RHCs it becomes evident that both models produced results closer to observations in the Münster test cases, with underestimation of both models being of a lesser extent. Austal2000 simulated results in the important upper concentration range with an RHC of 21.4 µg m^{-3}, which was very close to the RHC derived from observations. The underestimation of Austal2000 (35 % in comparison to observations) was confirmed by Schiavon et al. (2015), though was found to be related to the annual mean concentration of NO_X.

Tab. 2: RHC and standard deviations of the highest concentration values (SDHC; in brackets) in µg m^{-3} of observed and predicted PM_{10} concentrations for all four test cases. Reproduced from journal paper II.

	AA1	AA2	MS1	MS2
Observed	73.6 (±25.8)		33.1 (±2.8)	
Austal2000	4.8 (±1.2)	18.0 (±3.2)	6.1 (±0.4)	21.4 (±6.7)
ENVI-met	2.5 (±0.7)	9.3 (±2.5)	9.5 (±1.6)	5.2 (±1.7)

Importance of model input and initial conditions

The transportation of pollutants in the urban environment is strongly related to the flow field (Huang et al., 2009), which in turn is mainly dominated by meteorological conditions and urban morphology (Moonen et al., 2012). Therefore, meteorological inflow boundary conditions and, in particular, the wind vector are of distinct importance for dispersion modeling. Under all of the tested conditions the comparison of model predictions to observations shows that both models gained accuracy when the simulation runs were initiated with IBCs of local atmospheric measurements instead of initiations using data from weather stations several hundred meters away from the research sites (see Fig. 10). In the cases where local IBC data were used as inputs, underestimation was less marked. In the test case MS2, ENVI-met is an exception to this rule; no performance enhancement could be

observed by using local measurement data. With locally measured wind speeds two times lower compared to measurement data from the distant weather stations (see Sect. 3 of journal paper II), higher predicted PM_{10} concentrations are to be expected (Gromke et al., 2008; Wania et al., 2012). Dilution of pollutants (i.e., the horizontal air mass exchange) is reduced under conditions with lower horizontal wind speeds. Perry et al. (2005) verified that uncertainty in wind direction can cause disappointing simulation results as well. A slight alteration of wind direction could be observed when comparing data from local measurements to data from the distant weather stations (see Sect. 3 of journal paper II).

While FBs indicate underestimation by both models throughout the entire study, it is apparent that both models performed better under neutral stratification conditions of the atmosphere (Klug–Manier stability classes III/1 and III/2) most of the time (see Tab. 3). Results of both models show mostly poor performance under unstable and very unstable stratification regimes (Klug–Manier stability classes IV and V) in all test cases (FB: 1.16–1.95). It seems possible that both models had difficulty in calculating an accurate mixing of the atmosphere under unstable and very unstable conditions, with possibly an overestimation of the dilution rate regarding PM_{10} concentrations.

Tab. 3: FB for all four test cases segregated in atmospheric stability classes after Klug–Manier. Reproduced from journal paper II.

Test case	**AA1**		**AA2**		**MS1**		**MS2**	
Atmospheric stability (Klug–Manier)	Austal 2000	ENVI-met	Austal 2000	ENVI-met	Austal 2000	ENVI-met	Austal 2000	ENVI-met
III/1 (neutral)	1.58	1.75	-	-	1.32	1.20	0.58	1.62
III/2 (neutral)	1.85	1.90	0.91	1.28	1.56	1.46	0.98	1.64
IV (unstable)	1.93	1.95	-	-	1.17	1.45	1.16	1.38
V (very unstable)	-	-	1.68	1.93	1.42	1.55	1.47	1.86
Total	1.81	1.88	1.41	1.71	1.44	1.46	1.12	1.71

3.3 Particle emissions out of resuspension sources

3.3.1 Motivation to quantify resuspension source emissions using Austal2000

A simulation of particle dispersion was conducted using Austal2000 to investigate the unexpected distribution patterns concerning $PM_{(0.25-10)}$ and $PM_{(1-10)}$ that were found during field experiments within the Aachen *Elisenbrunnen* campaign (see Sect. 2.3). Birmili et al. (2013a) assumed that surfaces of, for example, dried-out soil or gravel paths within park areas may be significant sources of coarse airborne particles such as PM_{10}. Austal2000 has been used to inversely proof the supposition that resuspension is responsible for the unusual and unexpected distribution patterns within the area under study. Therefore, the dispersion of traffic-induced particles was investigated to rule out the possibility that adverse effects, such as specific flow conditions or vortices (Ahmad et al., 2005; Li et al., 2006), could have led to an accumulation of traffic-induced coarse particles and thus could have induced the increased concentrations of $PM_{(0.25-10)}$ and $PM_{(1-10)}$ inside the park area.

3.3.2 Methods

The simulation study was conducted using the simulation tool Austal2000 with the settings of the test case AA1 (as described in Sect. 3.2.2) to calculate the distribution of road traffic emissions only (including emissions from combustion processes and blown-up dust, as well as tire and break abrasions) in a computational domain extending 420 m by 420 m representing the area *Elisenbrunnen* in Aachen (see Sect. 2.2.1). Inflow boundary conditions were determined using meteorological data from the weather station *Hörn*, which were taken during the same period of time in which semi-parallel concentration measurements were carried out (see Sect. 2.2.2). Mean concentrations of Austal2000's predictions, averaged over the entire period of investigation, have been analyzed and compared to the mean values of observations as well as urban background particle concentrations derived from government monitoring stations. Following Lenschow (2001) it has been assumed that the factually measured concentration of PM_{10} at a given intra-urban location might be a mixture of: (a) rural background particle transport, (b) urban background concentration, and (c) local emissions (see Fig. 11). Consequently, it was possible to approximate a PM_{10} remainder (ΔPM_{10}) at a specific location, representing the resuspension source emissions, by subtracting the aerosol contribution of urban backgrounds (taken from the government station AABU, representing (a) and (b);

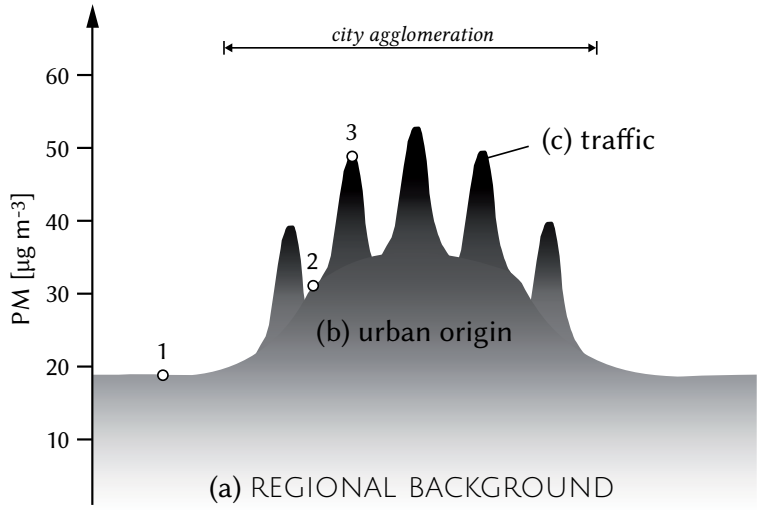

Fig. 11: Schematic horizontal profile of the ambient PM concentration (**1**: regional background monitoring station, measurements of (a); **2**: urban background monitoring station, measurements of (a) and (b); **3**: traffic-related monitoring station, measurements of (a), (b) and (c)). Modified after Lenschow (2001).

see Sect. 1.3) and local traffic-induced emissions (determined by simulation results, representing (c)) from on-site measured concentrations, subject to certain data quality (for details concerning measurement data quality see Sect. 2.5.2 in journal paper I).

3.3.3 Main results

Averaged simulation results (arithmetic means averaged over the entire study period) under conditions representing prevailing wind conditions show different patterns of particle distribution in comparison with observations (see Sect. 2.2.2). The highest simulated concentrations of PM_{10} were found close to the traffic lanes while the lowest concentrations were simulated to be inside the park area (see Fig. 12). As far as the simulation results are concerned, it could be proved that no specific flow pattern was responsible for the extraordinary high concentrations of traffic-induced particles concerning PM_{10} inside the green area. According to the simulation outcomes, the direct impact of local vehicle traffic on PM_{10} concentrations inside the park tends to be negligible.

Approximations of PM_{10} remainders (ΔPM_{10}) indicate that local diffuse particle sources contributed to local PM_{10} concentrations of up to 17.9 µg m^{-3} inside the

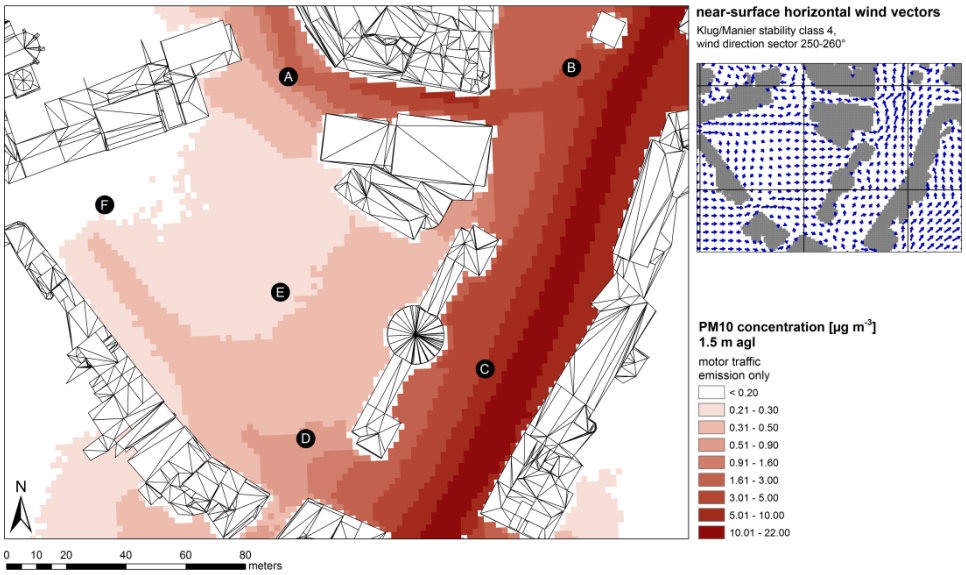

Fig. 12: Contour plot of the simulated distribution of average PM_{10} concentrations induced by motor traffic only [µg m^{-3}] at 1.5 m AGL for the research site *Elisenbrunnen*, Aachen, for different chosen weekdays in February, May, and September 2014, 10:00–17:00, during cyclonic weather conditions including depicted measurement locations A–F (black dots). Upper right plot shows near-surface horizontal wind vectors (blue arrows) representative for mean inflow boundary conditions (Klug–Manier stability class 4, wind direction sector 250–260°). Reproduced from journal paper I.

green area, whereas the impact on measurement locations in the vicinity of the main roads (measurement locations B and C, see Fig. 12) from local resuspension other than traffic sources was calculated to be close to zero (see Tab. 4). From this analysis we may conclude that resuspension of PM from unpaved ground within the green park area was a major contribution to the elevated measured $PM_{(0.25–10)}$ and $PM_{(1–10)}$ levels at sites E and F and possibly also at sites A and D within the limits of specified uncertainties (see Sect. 2.2.2). However, uncertainties must be taken into account that arise when data of different measurement techniques are compared to each other (for more details see Sect. 2.5.2 in journal paper I) as well as model uncertainty. The relatively poor performance of the Austal2000 model could be proved, including considerable underestimation within the model performance analysis of journal paper II (see Sect. 3.2). Therefore, results concerning ΔPM_{10} should be interpreted with caution.

Tab. 4: Mean PM_{10} remainder (Δ PM_{10}) for monitoring locations A–F calculating the difference between arithmetic mean $PM_{(0.25–10)}$ values of the semi-parallel measurements and the sum of arithmetic mean PM_{10} data out of the simulation and the arithmetic mean background PM_{10} concentration recorded at the rural background air quality monitoring station *Burtscheid* (AABU). Reproduced from journal paper I.

	monitoring location					
	A	B	C	D	E	F
Mean $PM_{(0.25-10)}$ measured	17.0	14.4	15.3	19.6	24.9	29.4
Mean PM_{10} simulated	0.5	2.7	4.3	0.6	0.2	0.2
Mean rural background PM_{10} (AABU)			11.4			
Δ PM_{10}	5.0	0.2	-0.4	7.6	13.3	17.9

3.4 Influence of vegetation elements on ground-level aerosol concentrations

3.4.1 Motivation

The draft towards an integrated analysis arose out of both the discussion points of journal paper II regarding dispersion models and their by definition non-exhaustive consideration of variables that affect particle concentration at a specific time and location (Venkatram, 2008), and the ability of ENVI-met to extend the input variable set-up by the use of information on vegetation. Vegetation elements are considered important design elements, particularly in cities, by virtue of the ecosystem services they can provide (Janhäll, 2015). These include impacts on the urban micro-climate, as plants tend to decrease temperature differences in urban areas (Lee and Park, 2007), among others (Oberndorfer et al., 2007). Vegetation has also been taken into account, as elements that can help to remove airborne particles from the atmosphere due to a large reactive surface area per unit volume correlative to ambient air (Litschke and Kuttler, 2008). Significant filter processes due to enhanced deposition on foliage have been observed (Sæbø et al., 2012; Roupsard et al., 2013). At larger scales, beyond isolated specie specific investigations (Sæbø et al., 2012), authors have investigated the effect of vegetation on ground-level aerosol concentrations in the atmosphere, for instance with the help of wind tunnel experiments (Gromke et al., 2008; Roupsard et al., 2013) or CFD simulations studying the idealized environment of a street canyon (Buccolieri et al., 2011; Gromke and Blocken, 2015). ENVI-met has been used in this regard as well (Wania et al., 2012) and also to investigate idealized spaces between buildings (Vos et al., 2013). Few studies have assessed environments with settings considering real-world configurations by the use of experimental fieldwork (e.g., Yli-Pelkonen et al., 2017).

3.4.2 Methodical approach

A simulation study investigating the influence of vegetation elements on pedestrian-level aerosol concentrations considering a real-world situation of an inner-city park area and the surroundings, including street canyons, was conducted using the modeling tool ENVI-met (see Appendix A).

The same computational domain mentioned in Sect. 3.2.2 (described also in more detail in Sect. 3 of journal paper II), resembling the park area *Elisenbrunnen* in the city of Aachen, was used and extended by the inclusion of information on vegetation elements within the computational domain (i.e., geometric information and species characteristics, including the leaf area density, LAD). A three-dimensional rendering of the computational domain used, including vegetation data, is shown in Fig. 13. A comparison was made between the simulation results of ENVI-met calculated using computational domains with and without vegetation elements. All other criteria of inflow boundary conditions were set equally and as described in Sect. 3 of journal paper II, using input data from local meteorological measurements during the summer season. Furthermore, the simulation results have been compared to data collected during field experiments by the use of Q-Q plots, the FB, and the RHC (see Sect. 3.2.3).

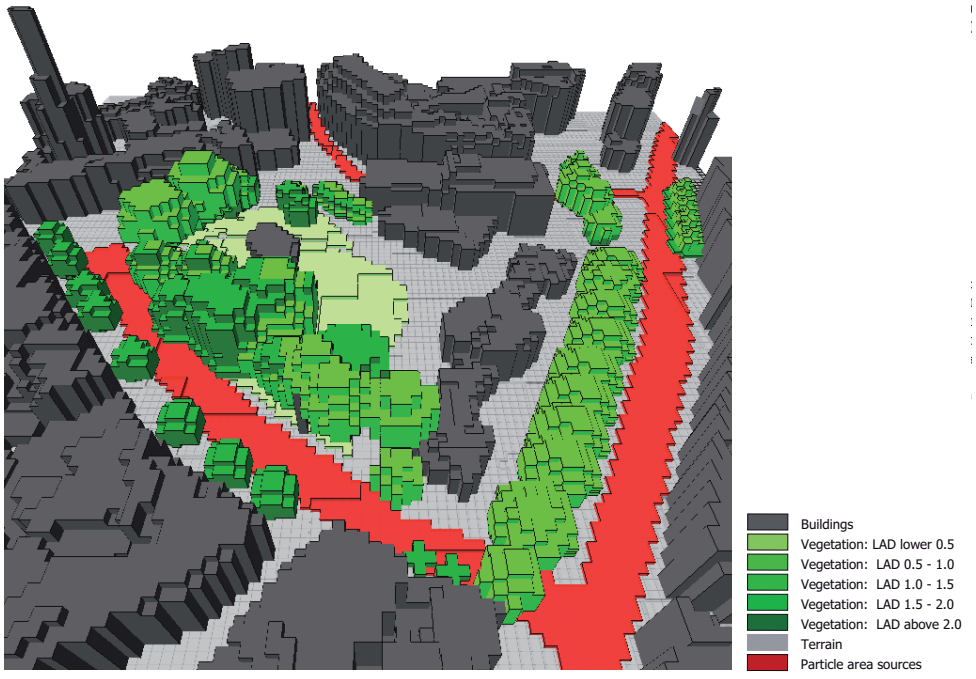

Fig. 13: 3D rendering of the used ENVI-met core model domain representing the area under study *Elisenbrunnen*. Reproduced from Appendix A.

3.4.3 Main results

Simulation runs that contained vegetation elements (i.e., shrubs and trees > 1 m) indicate higher ground-level concentrations of PM_{10} (1.5 m AGL) close to the particle sources in particular in comparison with predictions out of simulations without the consideration of plants (see Fig. 14). The results show that in real-world environments similar to the set-up of the case study the effect of reduced vertical and horizontal air mass exchange (that can be responsible for accumulation of PM in the near-ground atmosphere) due to plants can be rated dominant in comparison with the effect of deposition, where vegetation filters ambient air and acts as a sink for airborne particles, as discussed earlier (Janhäll, 2015). However, the overall effect of vegetation on ground-level aerosol concentration was found to be small and in the same order of magnitude as in findings from studies focusing on street canyon environments (Gromke and Blocken, 2015). When compared to observations, the consideration of plants, as an additional variable and factor of influence in the model calculations of ENVI-met, helped to slightly enhance the otherwise poor model performance, expressed by the considerable underestimation observed earlier (see journal paper II and Sect. 3.2.3) and indicated by both an improved FB (1.60 including plants; 1.65 without plants) as well as an enhanced RHC. However, the model performance was still far from acceptable when predictions were compared to observations (for details see Tab. 1 and Fig. 5 of Appendix A).

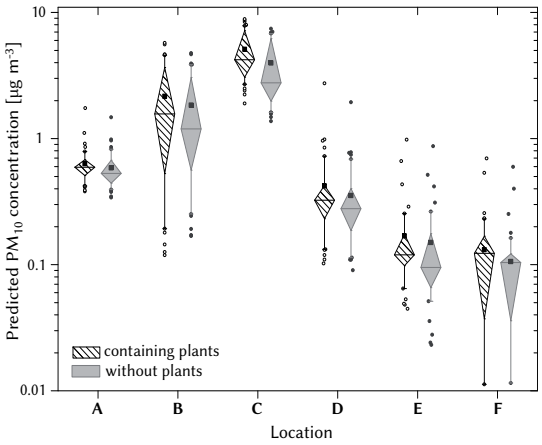

Fig. 14: Boxplot diagram of predicted PM_{10} concentrations for all monitoring locations (A–F), comparing data of simulation runs that were conducted without plants (gray boxes) to predictions that were calculated containing plants (black boxes). Filled squares represent arithmetic means; boxes show 25–75 percentiles; whiskers represent 10–90 percentiles; outliers are marked with circles. Reproduced from Appendix A.

3.5 Summary

i. Deterministic models were found to be valid methods in terms of spatial simulations of particle distribution; however, there is room for improvement with regard to their performance. Mixed performance could be observed when assessing the effectiveness of ENVI-met and Austal2000, with both models underestimating results by a considerable margin. In comparison, and by the use of the same IBCs determined in the model set-up stage, Austal2000 outperformed ENVI-met in almost every aspect concerning model performance.

ii. Both models gained accuracy in the upper concentration range, which is particularly important for regulatory purposes. It was found that the use of local meteorological measurement data instead of data from distant weather stations as inputs to actuate the dispersion models considerably improved the performance of both models. Predictions by both models were more accurate under neutral atmosphere stratification regimes. Both models had problems with significant underestimation under unstable or very unstable atmospheric conditions.

iii. The simulation results of traffic-induced particle emissions conducted using Austal2000 did not support the unusual findings concerning distribution patterns that were observed through the field data analysis (see Sect. 2.3), encouraging the hypothesis that local resuspension within the park area caused the unexpected spatial pattern revealed by the observations.

iv. Approximations of ΔPM_{10}—although interpreted with caution—imply that the contribution of diffuse resuspension particle sources within the park area of the research site Elisenbrunnen to the measured total mass concentration of $PM_{(0.25–10)}$ was between 13.3 and 17.9 $\mu g\ m^{-3}$ during the period of data collection.

v. In a real-world environment, simulation results of ENVI-met indicate that trees and shrubs had an influence on ground-level particle concentrations and particle distribution. Vegetation elements lead to increased levels of near-ground PM_{10} concentrations. As a result, the performance of ENVI-met that included vegetation elements in the computational domain improved the model performance. However, the influence was found to be small, as confirmed by other studies (Gromke and Blocken, 2015).

4. Prediction of particle concentrations using a newly developed statistical model

Section 4 presents the development of a non-linear statistical model to predict different metrics of particle concentrations using inputs of standard meteorological data and background concentration of PM_{10}, as well as acoustic data. This chapter is based on journal paper III. Section 4.1 puts the model development and performance study into context of atmospheric pollution and the respective state of the art concerning statistical modeling. The motivation for the model development is highlighted therein. Section 4.2 gives a brief description of the model concept and the main steps that should be taken into consideration to develop such models. The main outcomes of the performance assessment of the different models proposed are presented in Sect. 4.3.

4.1 Context and motivation to develop an ANN model

Statistical modeling is an objective estimation technique in the sense that the method is based on statistical data analysis establishing empirical relationships between predictive values such as ambient pollutant concentrations and predictor variables such as meteorological parameters (Vlachogianni et al., 2011; Santos and Fernández-Olmo, 2016) or land use patterns (Merbitz et al., 2012a, 2012c). Many popular approaches, such as regression modeling, apply linear dependences between predictive and predictor variables (Vlachogianni et al., 2011). Unfortunately, these solutions are not applicable for the non-linear problems often found to be true in environmental contexts. The relationship between, for example, meteorology or acoustic and pollutant concentrations is complex and potentially multi-scale in nature (Gardner and Dorling, 1998; Weber, 2009; Can et al., 2011). This initial situation makes the complex nature of the problem highly suitable for an artificial neural network (ANN) approach (Kukkonen, 2003). The ability of ANNs to learn underlying data generating processes without the requirement of prior knowledge of the nature of relationships between variables, given sufficient data samples, has led to popular usage in applications such as prediction and forecasting of air quality in environmental studies (Kukkonen, 2003; Hooyberghs et al., 2005; Cai et al., 2009; Santos and Fernández-Olmo, 2016), among others (Gardner and Dorling, 1998; Wu

et al., 2014). In comparison with deterministic modeling, the application of statistical approaches such as ANN models is computationally efficient and equally cost-effective, given that input variables are carefully chosen using appropriate site- and time-specific data. However, until now ANN models have rarely been applied successfully concerning spatial predictions of pollutants in the atmosphere (Kukkonen, 2003).

4.2 Concept

In this context an ANN model approach using input data of sound and meteorological parameters, as well as background particle concentrations, has been developed to predict concentrations of different particle metrics ($PM_{(0.25–1)}$, $PM_{(0.25–2.5)}$, $PM_{(0.25–10)}$, and $PNC_{(0.25–2.5)}$). The networks were developed, validated, and tested in a case study environment of a street canyon in the direct vicinity of a road arterial at the Aachen research site *Karlsgraben* (see Fig. 15). In a second step, the validated ANN models were applied and tested by the use of a data set collected within the open green area of the Münster research site *Aasee* (see Fig. 2 and Fig. 8). Here the approach was to test for the first time the ability of the ANN approach to gather spatial information on particle concentrations other than from the direct vicinity of traffic lanes. Furthermore, the networks developed were assessed with regard to their performance against the more traditional ANN approach of using only meteorological data and background aerosol concentrations as predictor variables.

Hereinafter, a brief description is presented introducing the Aachen research site *Karlsgraben* and the different steps that were conducted for the network development of the ANN models. Details regarding the Münster research site *Aasee* are presented in Sect. 3.2.2 and in Sect 3.1 of journal paper II. A more comprehensive description of data collection as well as pre- and post-processing of data and, in particular, of the detailed technical steps that should be taken into consideration when developing such models is offered within the methodology sections of journal paper III.

4.2.1 Areas of investigation

The development and validation of the proposed ANN model approach took place with a dataset that was collected in an isolated street canyon at the Aachen research site *Karlsgraben* (see 1.3). The buildings that enclose the street canyon mostly consist of 4–5 floors and are in the main residential in use. Only very

occasional business—an electronic hardware store as well as two restaurants—is present in the research site. The building-height(h)-to-street-width(w) aspect ratio of the street canyon h/w is ~1. The Karlsgraben road is a loop arterial oriented in the north–south direction in the area under study with two traffic lanes (two-way) and an average traffic volume of approximately 501 vehicles per hour in the daytime, comprising 93% passenger cars, 2% busses (diesel), 4% delivery vehicles, and 1% mostly diesel-powered heavy duty vehicles (manually counted for seven randomly picked hours at different times of the day during the period of investigation). The observed vehicle fleet apportionment represents the approximate average traffic composition in the state NRW (Kraftfahrtbundesamt, 2012).

The stretch of road under study covers a range of 200 m and is located between two intersections that are controlled with traffic lights. The Karlsgraben road has a speed limit of 50 km h^{-1}; however, because most of the vehicle traffic is between accelerating and slowing down due to the traffic lights at the beginning and the end of the stretch of road under study, the average vehicle speed was

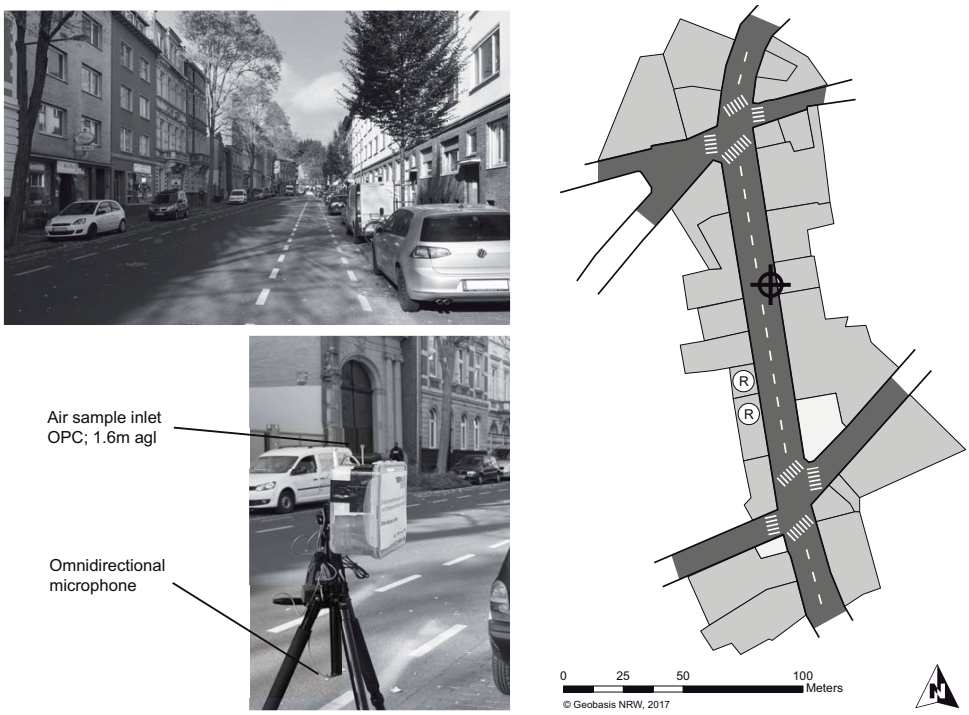

Fig. 15: Scheme of the *Karlsgraben* research site in Aachen (right illustration) including depictions of the measurement location (crosshair cursor) and locations of two restaurants (marked with "R") as well as images of both the street canyon of *Karlsgraben* road (upper left image) and the installed on-location measurement equipment (lower left image). Reproduced from journal paper III.

estimated to be ~ 30 km h^{-1} (mostly fluent) in front of the data collecting sensors. Field data collection took place halfway between two traffic lights eastward next to the traffic lane (1 m off-street). For details concerning the Münster research site *Aasee*, see Sect. 3.2.2.

4.2.2 ANN model development strategy

ANN models are universal approximators with the ability to generalize through learning non-linear relationships between provided variables of input(s) and output(s) (Hájek and Olej, 2012). The objective of all ANN prediction models is to find an unknown functional relationship f(X, W) that links the input vectors in X to the output vectors in Y (Gardner and Dorling, 1998). All ANN models are based on the form described with the equation (Eq. 1) given by (Maier et al., 2010):

$$Y = f(X, W) + \varepsilon \qquad 1)$$

where W is the vector of model parameters (connection weights) and ε represents the vector of model errors. Thus, in order to develop the ANN model, the vector of model inputs (X), the form of the functional relationship ($f(X, W)$), which is governed by the network architecture and the model structure (e.g., the number of hidden layers, number of neurons, and type of transfer function), and the vector of model parameters (W), which includes the connection and bias weights, have to be defined (Maier et al., 2010). A multi-layer perceptron (MLP) was selected as the network basis to predict the aerosol mass concentrations of particles as it is the most commonly used ANN model architecture (Maier et al., 2010; Razavi and Tolson, 2011) and has been found to perform well for applications such as the prediction of air pollutant concentrations (Kukkonen, 2003; Cai et al., 2009). Details regarding model architecture can be found in Sect. 2.2.1 in journal paper III.

ANN model development includes numerous different steps that must be followed carefully (see Fig. 16). One of the most important steps comprises the selection of a suitable set of input variables with maximum predictive power and the respective collection of data. In the study of journal paper III, the input selection process was divided into two different actions to determine an appropriate set of inputs. In the first step, input significance was justified using an ad hoc approach where potential input variables (i.e., candidates) were determined based on a priori knowledge considering the nature of the problem and available data. Following Lenschow (2001) and Cai et al. (2009), physically, local particle concentrations are dependent on both sources of particles (i) and the distribution of particles at the time when they are airborne (ii). Furthermore, (i) depends on both background particle transport, represented by urban background government monitoring data used as an input variable in the proposed modeling approach, and local particle

sources, represented by sound pressure level variables in the proposed modeling approach, respectively. Vehicle traffic emissions both in terms of the amount of combustion processes and blown-up dust as well as tire and break abrasions are identified to be a major source of particles near urban arterials (Morawska et al., 1999; Karagulian et al., 2015; Manousakas et al., 2017). Vehicular emissions are related to the volume of traffic, vehicle type, and speed (Cai et al., 2009), which, in turn, are assumed to be attributable to traffic sound. The transmission of particles (ii) depends on meteorology (Can et al., 2011). An extensive set of input variable candidates was considered using different metrics of acoustic data collected during the measurement campaign and standard meteorological data from continuously operated weather stations, as well as urban background concentrations of PM_{10} from government monitoring stations. For details concerning field data collection and processing see Sect. 2.3 of journal paper III.

In the second step, an analysis of partial mutual information (PMI) was applied to prove the relevance and independency of the proposed initial candidate set of input variables. The goal was to sample out a set of variables with maximum predictive power and minimum redundancy (Maier et al., 2010; Stamenković et al., 2015). Details concerning PMI are extensively described in Sect. 2.2.3 of journal

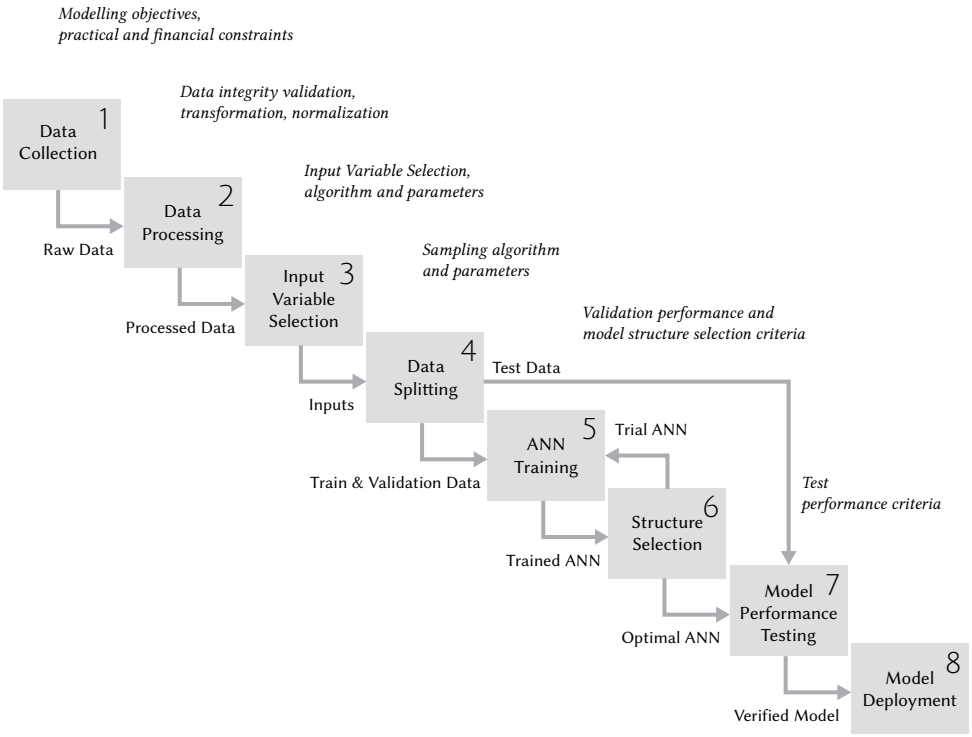

Fig. 16: ANN development workflow. Modified after May (2014).

paper III. All considered variable candidates as well as the determined input variables for the ANN models used are given in Table 2 of journal paper III.

The valid data set, including the selected input and output variables, were divided into training, validation, and testing subsets, in order to ensure the best possible generalization of the ANN model on unknown input data. In this study, a method based on stratified sampling of the self-organizing map (SOM) over simple random sampling was used to split the data set into subsamples, ensuring that the statistical properties of the subsets are similar (May et al., 2010). Details regarding SOM-based stratified data splitting (SBSS) can be found in Sect. 2.2.3 of journal paper III.

Together with the ANN model architecture, the model structure defines the functional relationship $f(X,W)$ between model inputs and outputs (cf. Eq. (1)). Model structure selection includes the determination of the optimum number of neurons in the hidden layer and how they process incoming signals by the use of suitable transfer functions (May et al., 2010). For the development of the ANN models a stepwise iterative process was conducted to find out the optimal number of neurons in the hidden layer and the best suitable transfer function (Maier et al., 2010). Details concerning the tuning of the network structure are extensively described in Sect. 2.2.4 of journal paper III.

The process of finding a set of connection weights between neurons of the network ("training") was conducted using the back-propagation algorithm (Rumelhart et al., 1986). Details regarding the training of the network are presented in Sect. 2.2.5 of journal paper III.

4.2.3 Performance measures

The performance of both the traditional model approach using only meteorological and background concentration data and the novel model approach using additionally input data of sound was assessed comparing the simulation results to observations using scatter plot diagrams as well as different metrics of statistics and performance measures, as recommended in recent literature. Again the FB was used (see Sect. 3.2.3) complemented by the root mean squared error (RMSE) and the model efficiency score (MEF), including the target approach first presented by Pederzoli et al. (2011). The methodology of the target diagram bases on the main principle of Taylor (2001) and was modified by the Joint Research Centre (JRC) of the European Commission within the framework of the Forum for Air Quality Modelling in Europe (FAIRMODE) to develop a harmonized methodology to evaluate model results based on a consensus set of statistical indicators. Further details concerning the interpretation of the performance measures used, as well as their mathematical description, can be found in Sect. 2.5 of journal paper III.

4.3 Performance evaluation of the developed ANN models

The proposed ANN models using inputs of background particle transport, meteorology, and acoustics to predict atmospheric concentrations of $PM_{(0.25–1)}$, $PM_{(0.25–2.5)}$, $PM_{(0.25–10)}$, and $PNC_{(0.25–2.5)}$ show mixed results in terms of their performance. The best-performing ANN models within the Karlsgraben test case were found to be for predicting concentrations of $PM_{(0.25–10)}$ and $PNC_{(0.25–2.5)}$, indicated by, for example, positive MEF values (MEF: 0.25–0.31) that result in the target values depicted inside the circumference of the target diagram, as shown in Fig. 17. However, the variation within the prediction sample was considerably lower

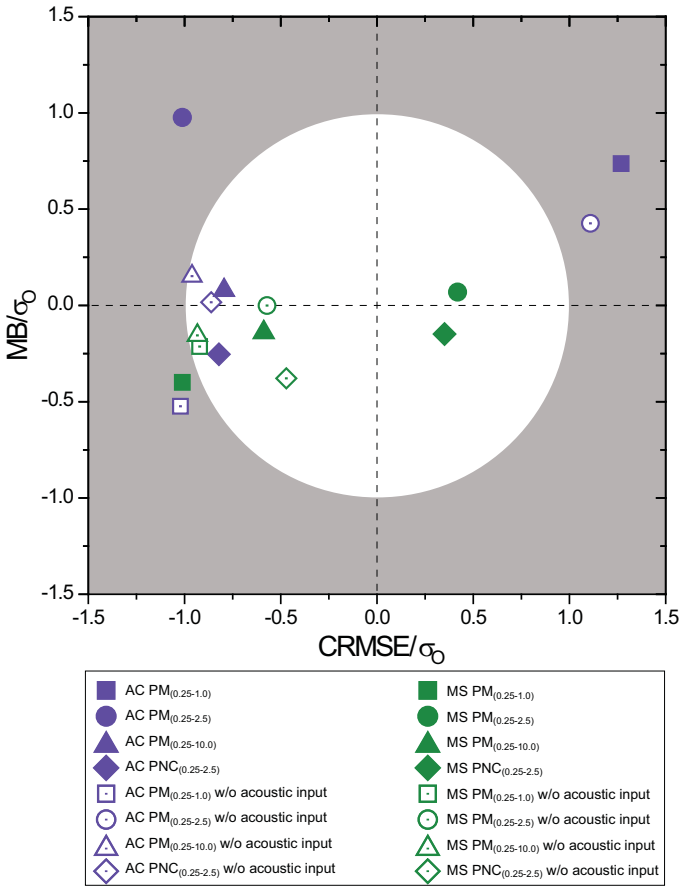

Fig. 17: Target diagram of ANN model results for $PM_{(0.25–1)}$ (rectangles), $PM_{(0.25–2.5)}$ (circles), $PM_{(0.25–10)}$ (triangles) and $PNC_{(0.25–2.5)}$ (rhombuses). Purple markers depict Aachen "Karlsgraben" test case results. Green markers depict Münster- "Aasee" test case results. Filled and hollow markers differentiate between model results using acoustic input data and calculations without acoustic data input. Reproduced from journal paper III.

compared to observations (see Fig. 18). Using data from the *Aasee* test case, the ANN model to predict concentrations of $PM_{(0.25–10)}$ turned out to perform fairly well, with a MEF of 0.64 (R^2 of 0.78). Models to predict concentrations of $PM_{(0.25–2.5)}$ and $PNC_{(0.25–2.5)}$ reproduced rather accurate observations over the entire concentration range considering high MEF scores (MEF: 0.82–0.85) and coefficients of determination close to 1.0 (R^2: 0.87–0.89). However, up to now air quality modelers have not yet agreed upon the magnitude of standards for judging model performance (Yassin, 2013). Chang and Hanna (2004) advised that a model should be considered acceptable when most of its predictions are within a factor of two of the observations. ANN models to predict concentrations of $PM_{(0.25–2.5)}$ and $PNC_{(0.25–2.5)}$ within the park area case in Münster surpass this requirement (see Fig. 19). A more comprehensive set of statistics and performance measures are given in the results (Sect. 3) of journal paper III.

Taking into account the more comprehensive target approach of the MEF (described in Sect. 2.5 of journal paper III), recommended by the JRC of the European Commission, it is guaranteed that the ANN model is a better predictor of

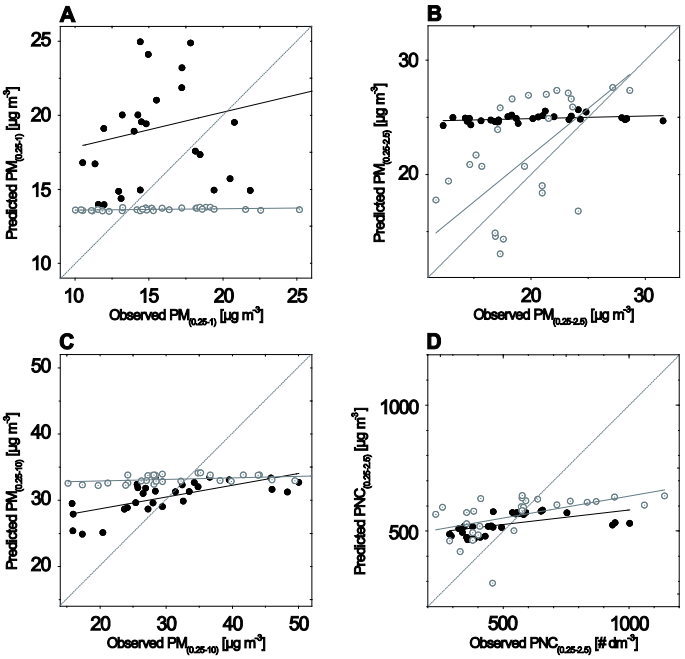

Fig. 18: Scatter plot diagram showing *Karlsgraben* ANN model predictions of (A) $PM_{(0.25–1)}$, (B) $PM_{(0.25–2.5)}$, (C) $PM_{(0.25–10)}$, and (D) $PNC_{(0.25–2.5)}$ over respective observations. Dashed lines illustrate a 1:1 reproduction of model predictions over observations; thin solid lines indicate linear regression results between the samples of predictions and observations; black marks depict model results using additional acoustic data inputs; gray marks indicate model results of using inputs without acoustic data. Reproduced from journal paper III.

the observations than a constant value set to $\overline{C_O}$ when target values are depicted inside the circumference of the target diagram, i.e., when the MEF is >0 (Stow et al., 2009). Using this measure, the best-performing ANN models developed in this study fulfill the requirements for estimations in terms of uncertainty and accuracy for mean value predictions according to Thunis et al. (2012).

Concentration predictions of $PM_{(0.25–1.0)}$ and $PM_{(0.25–2.5)}$ within the *Karlsgraben* test case as well as of $PM_{(0.25–1)}$ within the *Aasee* test case cannot be considered satisfactory, given negative MEF values throughout (see Fig. 17), as well as a seriously limited variation range of prediction values over observations (see Fig. 18 and Fig. 19). Reasons for poor performance in these cases were felt to be both methodology, especially concerning the sample size used to train and validate the network (Johnson and Jurs, 1999), and physical conditions the model cannot account for. For more details see Sect. 4 of journal paper III.

Overall, it could be proved that acoustic data input contributes to ANN model accuracy regarding the prediction of particle concentrations for almost all test cases (cf. Fig. 18 and Fig. 19).

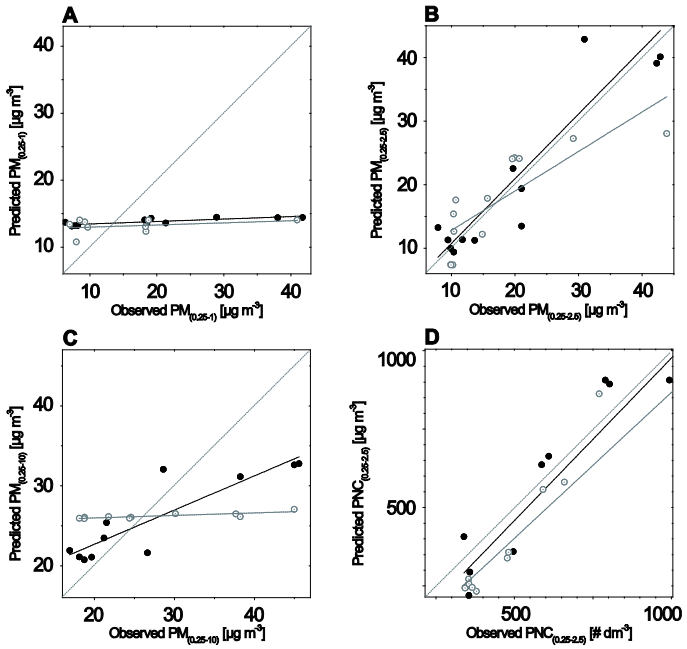

Fig. 19: Scatter plot diagram showing *Aasee* ANN model predictions of (A) $PM_{(0.25–1)}$, (B) $PM_{(0.25–2.5)}$, (C) $PM_{(0.25–10)}$, and (D) $PNC_{(0.25–2.5)}$ over respective observations. Dashed lines illustrate a 1:1 reproduction of model predictions over observations; thin solid lines indicate linear regression results between the samples of predictions and observations; black marks depict model results using additional acoustic data inputs; gray marks indicate model results of using inputs without acoustic data. Reproduced from journal paper III.

5. Conclusions and outlook

In this thesis, several issues have been addressed in a multi-methodological study in order to better understand the micro-scale variability of atmospheric particle concentration in the urban boundary layer. Three main approaches, the field experiment analysis using mobile sensor equipment alongside a survey, the performance assessment of two popular particle dispersion models, and the development of an ANN model have been presented for this purpose.

Results of both field data analyses and deterministic modeling tools provide evidence that airborne particles are distributed in highly varied and complex ways, even on small spatial scales, as also discovered by numerous other studies (e.g., Merbitz et al., 2012b; Birmili et al., 2013a, 2013b). As a result, it was difficult to identify single drivers that lead to specific concentration patterns. However, it could be proved that vehicle traffic had a huge impact on particle concentrations, especially near road arterials. Additional diffuse sources of particles could be determined, especially inside the park area in Aachen, where surfaces of dried-out grass and unpaved gravel paths contributed to the local aerosol concentration, resulting in unexpectedly high mean concentration levels of $PM_{(0.25-10)}$ that were, in fact, higher than the concentration levels in the direct vicinity of traffic lanes. It became obvious that fixed-site aerosol instrumentation lacks representative information on the concentration levels people are effectively exposed to (Peters et al., 2014) and that PM_{10} as a single metric is a questionable measure for air quality regulation regarding aerosols inside cities since different particle size fractions with different impacts on the human body (Kreyling et al., 2006) can be distributed in various ways, even on small spatial scales (Ning and Sioutas, 2010).

In marked contrast to findings from Nikolopoulou et al. (2011) this thesis highlights that people were not able to distinguish between different levels of particle exposure of $PM_{(0.25-10)}$ on-site; at least within the concentration ranges found in this study. This finding emphasizes the problem of public awareness regarding spatial and temporal distribution of air pollution such as PM. It highlights the necessity of accurately quantifying the spatial and temporal highly variable particle concentrations in the atmosphere, since otherwise the exposure to PM will remain beyond judgement in daily life. Current levels of PM concentrations are still rated as deleterious and should be further reduced (Pascal et al., 2013).

Today, deterministic models provide chances to broaden the knowledge of spatial pollutant distributions such as particles, especially considering user-friendly

tools such as ENVI-met. The simulation tools Austal2000 and ENVI-met were found to be powerful and well suited to determining the spatial information of aerosol concentrations on the micro-scale, solving issues posed in domains of complex urban environments including obstacles such as buildings or vegetation elements. However, the performance of both models turned out to have room for improvement when it comes to the task of reproducing observed concentration levels of particles. The results of this thesis will help model users from the scientific community, as well as those carrying out applied studies when investigating atmospheric composition concerning aerosols, to understand what performance they can expect from the simulation tools ENVI-met and Austal2000 in real-world applications. The analyses will support model developers in identifying the weaknesses of the evaluated models and conditions where the models do not perform satisfactorily. The results provide indications regarding the uncertainty that is present in the PM concentration prediction of ENVI-met and Austal2000 in comparison with field data under different atmospheric conditions. Furthermore, new options for model performance enhancement are given; i.e., by the advice on how to run both models successfully with recommendations in the part of atmospheric input data. Input data of pollutant emission rates, however, are still of concern. In the future, model performance should be enhanced in this particular case through inverse modeling, for example (Birmili et al., 2009). Further improvements can be obtained with the help of inflow boundary conditions derived from sophisticated wind field models (Letzel et al., 2012). Currently, the output data of Austal2000 and in particular of ENVI-met, must, as in any case with predictive models, be interpreted with caution.

A new computational- and cost-efficient ANN modeling approach has been presented to predict aerosol concentrations effective for areas where permanent sensor operation is not possible or feasible. By the use of information on sound, background concentration of PM_{10}, and meteorology as inputs, the approach turned out to be useful and at least in parts a fairly accurate tool for predicting aerosol concentrations in both time and space (cf. Kukkonen, 2003). Steps that should be considered when setting up an ANN prediction model successfully are outlined in detail. However, up to now the ANN model approach presented is still far from an operational tool due to its several limitations. The restricted development environment used in this thesis featuring simplified conditions (e.g., avoidance of rainy periods) should be enlarged towards real-world conditions. Currently, the approach presented is limited to “now-cast” (Maier et al., 2010). However, the performance assessment in this thesis demonstrates the principal ability of non-linear statistical models in the research domain of air quality monitoring. For the purpose of developing a forecasting tool for near-future particle concentrations based on the approach presented input vectors of data derived from urban acoustic

models and numerical weather prediction models, as well as meso-scale background particle transport models, might be used. The approach presented can be used to establish supplementary alternatives to measurements or deterministic modeling in order to enhance spatial and/or temporal availability of information on particle concentrations in the urban atmospheric boundary layer.

Thesis papers

Journal paper I

Small-scale variability of particulate matter and perception of air quality in an inner-city recreational area in Aachen, Germany

DOI:10.1127/metz/2016/0704

Meteorologische Zeitschrift, Vol. **25**, No. 3, 305–317 (published online April 29, 2016)

Mettools IX

Small-scale variability of particulate matter and perception of air quality in an inner-city recreational area in Aachen, Germany

Bastian Paas[1,4*], Teresa Schmidt[2,4], Stanimira Markova[3,4], Isabell Maras[1,4], Martina Ziefle[2] and Christoph Schneider[5]

[1]Department of Geography, RWTH Aachen University, Germany
[2]Communication Science, RWTH Aachen University, Germany
[3]Computer Aided Architectural Design, RWTH Aachen University, Germany
[4]Project house HumTec, RWTH Aachen University, Germany
[5]Department of Geography, Humboldt-Universität zu Berlin, Germany

(Manuscript received April 30, 2015; in revised form December 22, 2015; accepted December 23, 2015)

Abstract

Spatial micro-scale variability of particle mass concentrations is an important criterion for urban air quality assessment. In this study we present results from detailed spatio-temporal measurements in the urban roughness layer along with a survey to determine perceptions of citizens regarding air quality in an inner city park in Aachen, Germany. Particles were sampled with two different approaches in February, May, July and September 2014 using an optical particle counter at six fixed measurement locations, representing different degrees of outdoor particle exposure that can be experienced by a pedestrian walking in an intra-urban recreational area. A simulation of aerosol emissions induced by road traffic was conducted using the German reference dispersion model Austal2000. The mobile measurements revealed unexpected details in the distribution of urban particles with highest mean concentrations of $PM_{(1;10)}$ inside the green area 100 m away from bus routes (arithmetic mean: 22.5 µg m^{-3} and 18.9 µg m^{-3}; geometric mean: 9.3 µg m^{-3} and 6.5 µg m^{-3}), whereas measurement sites in close proximity to traffic lines showed far lower mean values (arithmetic mean: 7.5 µg m^{-3} and 8.7 µg m^{-3}; geometric mean: 5.8 µg m^{-3} and 6.5 µg m^{-3}). Concerning simulation results, motor traffic is still proved to be an important aerosol source in the area, although the corresponding concentrations declined rapidly as the distances to the line sources increased. Further analysis leads to the assumption that particularly coarse particles were emitted through diffuse sources e.g. on the ability of surfaces to release particles by resuspension which were dominantly apparent in measured $PM_{(1;10)}$ and $PM_{(0.25;10)}$ data. The contribution of diffuse particle sources and urban background transport to local $PM_{(0.25;10)}$ concentrations inside the green area were quantified to be up to 17.9 µg m^{-3}. The analysis of perception related experiments demonstrate that particle concentrations in form of $PM_{(0.25;10)}$ were inconsistent with park user opinions regarding perception of air quality. At least in investigated concentration magnitudes there proved to be no connection between user assessment and physical values at all.

Keywords: particulate matter, micro-scale, air quality perception, vehicle emissions, dispersion modelling, Austal2000, recreational area, environmental pollution, personal exposure

1 Introduction

Particulate matter (PM) is an important environmental risk to health (WHO, 2013). Results of epidemiological studies suggest that both long-term and even short-term stays, e.g. during commuting or relaxing, at locations with high PM concentrations could have significant impacts on health such as respiratory and cardiovascular diseases (Pope et al., 2002; von Klot, 2005; Chow et al., 2006). The major proportion of the world's population lives in cities (United Nations, 2014), where exceedances of air quality standards occur regularly. In general, town citizens are particularly affected due to their frequent exposure to pollution emitters and other environmental stressors.

The individual exposure to airborne particles outdoors is complex to describe and is highly dependent on the specific whereabouts (Dons et al., 2011; Broich et al., 2012; Steinle et al., 2013, Bekö et al., 2015) and meteorological conditions (Padró-Martínez et al., 2012; Birmili et al., 2013b). Although traffic has been identified as a major contributor to the aerosol strain near roads due to both exhaust and non-exhaust inputs (Merbitz et al., 2012b; Birmili et al., 2013a, Quiros et al., 2013), most evidence on aerosol health effects has been derived from measurements of particle mass concentrations from fixed sites (Laden et al., 2006). By definition, quantities of particle mass measures from immovable sensors, however, are not able to identify site

*Corresponding author: Bastian Paas, Department of Geography, Wüllnerstaße 5b, RWTH Aachen University, Germany, e-mail: bastian.paas@geo.rwth-aachen.de

DOI 10.1127/metz/2016/0704
Gebrüder Borntraeger Science Publishers, Stuttgart, www.borntraeger-cramer.com

dependent particle exposure on the spatial micro-scale. Nonetheless, to approximate the personal PM exposure representative for entire city areas (e.g. for legislative reasons), fixed monitoring sites are regularly used due to the lack of dense monitoring networks. In ambient air the characterization of spatial PM exposure is complex since different particle size classes show divergent spatial distribution patterns (Birmili et al., 2013b). Explaining mass concentrations of fine particles and particle number as a function of time and location appears to be specifically challenging (Kozawa et al., 2012; Mishra et al., 2012; Spinazzè et al., 2015) due to the fact that combustion sources from traffic processes and industry emit mainly small particles situated in nucleation mode (Quiros et al., 2013; Ning and Sioutas, 2010). These aerosol fractions change their physical characteristics rapidly as a consequence of growth processes. Further, accumulation mode particles tend to have long residence time in the atmosphere and therefore dominate particle mass (Seinfeld and Pandis, 2006). These complex physical processes are applicable to the urban roughness layer in particular. In urban environments numerous diffuse particle sources can be found and dispersion is difficult to describe due to a variety of different surface structures and numerous spatial obstacles.

Beyond the factual health risk of PM (Venn et al., 2001), it is a basic question whether people are able to perceive the exposure to PM in the perceived climate comfort. On the one hand, not all people might show the same sensitivity or awareness for those stressors (Shirom et al., 2000), especially as city pedestrians might differ in age or health status and therefore might have a different responsiveness to climate stressors in general and aerosol concentrations in particular (Brook et al., 2010). On the other hand, it is well possible that people have established an overall perception of the on-site comfort as a holistic evaluation with particulate matter being an integral though unconscious part of it. Both hypotheses implicate different consequences. It is therefore important to understand whether there is a relationship between the physical stressor (i.e. aerosol concentration) and the specific perception of air quality and/or whether there is a relationship between the physical stressor and the integrative evaluation of on-site comfort. Numerous studies can be found concerning human perception of the urban environment. However, most of the work has focused on thermal comfort (Chen and Ng, 2012; Johansson et al., 2014). When perception was linked to air pollution, usually perceived risks were addressed or epidemiological studies were performed (Badland and Duncan, 2009). Most studies have been carried out through social and public opinion surveys which focused almost exclusively on people's awareness or level of concern about air pollution (Nikolopoulou et al., 2011). Brody et al. (2004) started empirical research to examine the local level. Even in this case, the data was collected and analyzed at the neighborhood level and not measured or assessed at the local pedestrian level. Only recently have investigations on individual perception of exposure to PM been conducted on the micro-scale (Nikolopoulou et al., 2011). Local-scale studies have provided some information on place-specific conditions and evaluated how the location and its surroundings are important in the experience of air pollution but these studies disagree when it comes to an evaluation of air pollution sensation (Brody et al., 2004; Nikolopoulou et al., 2011).

Other impacts, for instance noise or thermal stress, influence human wellbeing and health in a variety of complex ways as well (Raimbault and Dubois, 2005; Yang and Kang, 2005; Gabriel and Endlicher, 2011; Maras et al., 2014). It is evident that monitoring, maintenance and planning of urban areas require an integrative approach to combine methods from natural sciences, engineering and social sciences. Taking this into account, a better understanding of highly-resolved distribution patterns of aerosols under given microclimate conditions in combination with the perception and sensation of urban space users regarding air quality parameters will help to achieve better environmental health standards inside cities at a local level (e.g. in intra-urban recreational areas).

This interdisciplinary work was designed to explore the spatial distribution patterns of the urban atmospheric aerosol by portable instrumentation in combination with a parallel survey to examine the sensation and perception of urban park users regarding air quality. We investigated different situations of outdoor exposure experienceable by a town citizen in an inner-city recreational area, in a generic medium-sized German city like Aachen. We identified localities of different particle exposure inside the exemplarily considered research site "Elisenbrunnen", and examined seasonal differences regarding concentrations of particulate matter and overall perception of air quality. Furthermore, we considered the question whether or not urban park users are intuitively able to distinguish between dissimilar particle mass concentrations. We used the Austal2000 simulation tool to investigate the influence of emissions induced only by motor traffic at the research site. We compared the outcomes with physically measured values collected during measurements. The analysis focuses on the question whether the green area "Elisengarten" inside the recreational area "Elisenbrunnen" in the city of Aachen has a positive impact on local atmospheric particle concentrations compared to the surrounding urban fabric structure. Bio-meteorological stress factors, i.e. thermal stress, and a psychophysical investigation on human perceptions of climatological stress factors were analyzed in related publications by Maras et al. (2016) and Schmidt et al. (2015).

2 Methods

2.1 Study area

Field experiments were carried out inside an inner-city public open space in the city of Aachen (pop. 245,000),

Figure 1: Research site "Elisenbrunnen" in Aachen. The image shows summer conditions of deciduous trees, with the photographer standing at the northern ending of the recreational area pointing to the south with the camera.

a typical German medium-sized town sitting in the triborder region close to the Netherlands and Belgium. The investigation site spans an area of about 0.02 km^2 and is characterized by a well-attended inner city park, enclosed with buildings generally comprised of 4–5 floors. One of the most frequented roads by public transport buses ("Friedrich-Wilhelm-Platz"), inaccessible for individual private vehicles, including four main bus stops (102 coach connections per hour on weekdays), leads through the investigation area. The park is surrounded by sparsely busy roads in the Northeast (industrial vehicles for delivery only) and Southeast ("Hartmannstr.") and a highly frequented alleyway used mainly by private cars ("Ursulinerstr."). Unsurfaced footpaths subdivide the green area which contains mainly small flowerbeds and a lawn surface that is surrounded by deciduous trees (*Platanus x hispanica*) (Fig. 1). Six monitoring sites were chosen inside the study area for measurements and surveys featuring different surroundings (Fig. 2). Sites E and F were characterized as typical recreational spots inside the green area. Location C features a main bus station, whereas site B was located in proximity to the intersection "Friedrich-Wilhelm-Platz"/"Ursulinerstr." dominated by moving traffic. Monitoring sites A and D have been chosen in between to capture transfer passages from surroundings into the green area to provide a gradient.

2.2 Experimental design

Local measurements were conducted to determine mass concentration of suspended particles with aerodynamic diameters (DAE) between 0.25 µm and 10 µm ($PM_{(0.25;10)}$). Simultaneously, questionnaires accounting for an overview of the perception of urban park users were filled in.

Firstly, physical data were collected with the entire described measurement equipment at location A, B, C, E and F as one-day time series (weekdays, 10:00–17:00, 10-minute mean values) alongside the survey during a typical wintertime in February 2014. A similar approach was conducted at locations A, B, E and F during summer in July 2014. Initial conditions for each measurement campaigns were chosen to be the same for both periods, including radiation weather conditions with only partly clouded skies and no precipitation.

Further particle measurements were carried out at locations A–F with a semi-parallel approach using again a mobile single measurement device. Measurements were conducted during 7 selected weekdays (10:00–17:00) in February, May and September 2014 that were characterized by meteorological conditions prevailing at the study area with no precipitation in cyclonic weather situations and south-westerly winds (Fig. 3). The measurement location was changed every 5 minutes in an identi-

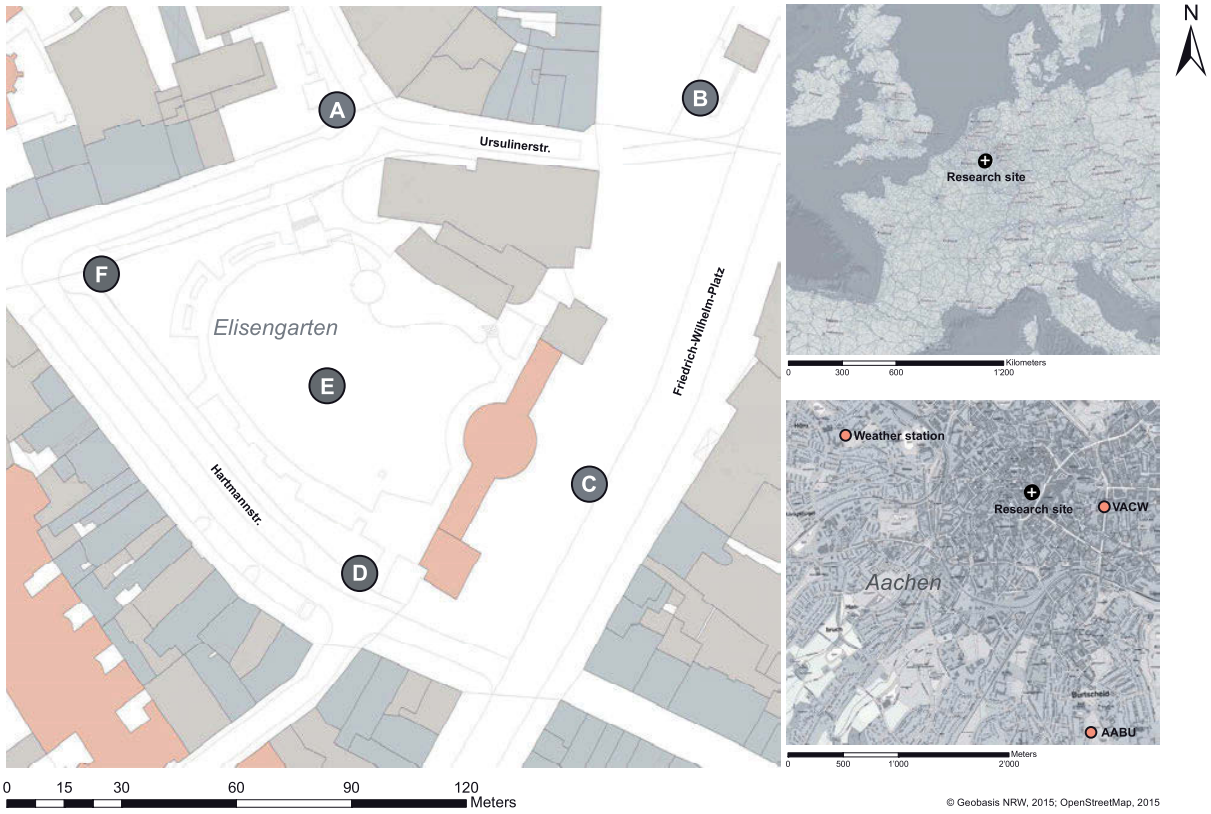

Figure 2: Research site "Elisenbrunnen" in Aachen (left illustration) including depicted measurement locations A–F (grey circles) and the area under study (white cross on black circle) located in Central Europe (upper right illustration) and located in Aachen (lower right illustration) including the weather station "Aachen-Hörn", traffic related air quality monitoring station "Wilhelmstrasse" (VACW) and rural background air quality monitoring station "Burtscheid" (AABU) operated by the Northrhine-Westfalian State Office for Nature, Environment, and Consumer Protection (LANUV) marked with red dots.

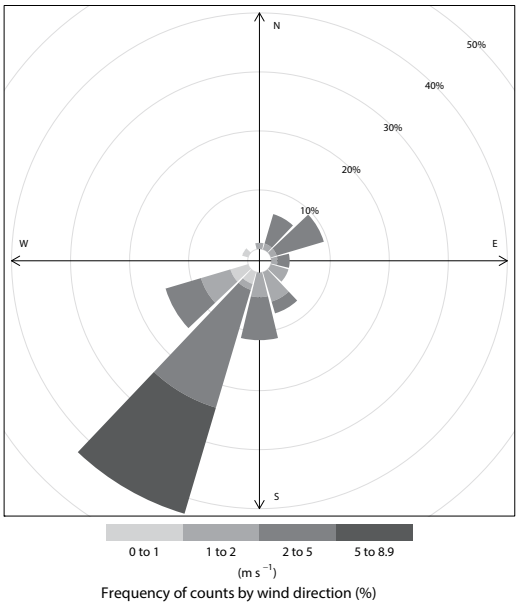

Figure 3: Wind rose representing data collected during semi parallel measurements in February, May and September 2014 at the weather station "Aachen-Hörn" also used as inflow boundary conditions for traffic induced PM_{10} distribution modelling.

cal chronological order (clockwise starting at location F, cf. Fig. 2), with the mobile particle counter circulating among the different locations. Data were sampled as 1-minute averages. Every first mean value of a sample was discarded from further analysis. For the analysis a sample consisting of 56 1-minute averages was used.

A simulation of particle dispersion under given meteorological initial conditions was conducted to reveal the effects of only motor traffic induced particle emissions using the simulation tool Austal2000 (see 2.4).

2.3 Instrumentation

2.3.1 Grimm mobile optical particle counter

The particle measurements were taken using a mobile optical particle counter (OPC, Model EDM 107G, Grimm GmbH, Ainring, Germany). The OPC integrates the approaches of light scattering technology with single particle counting. A pulse height analyzer classifies the scattered light pulse signals into a size distribution in the range between 0.25–32 µm DAE containing 31 different size channels. Internally, the particle number size distribution is converted into mass concentrations of e.g.

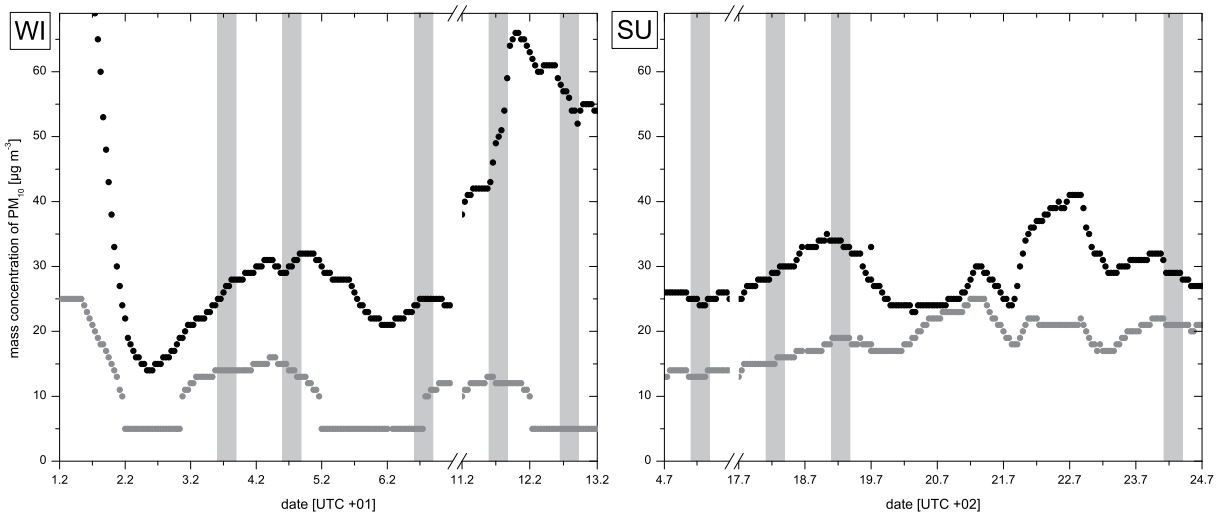

Figure 4: Time periods of $PM_{(0.25;10)}$ time series measurements (light grey bars) in comparison to 60-minute average concentrations of PM_{10} at the government air quality site "Burtscheid" (dark grey dots) and "Wilhelmstrasse" in Aachen during the winter campaign (left illustration "WI") and during the summer campaign (right illustration "SU"). Time and date is indicated in local time (UTC+01 during winter and UTC+02 during summer).

$PM_{(0.25;10)}$ for an indicated time interval. The sensor operates at a volumetric flow rate of 1.2 L min^{-1} and a time resolution of 6 s. All measurements with the OPC were carried out at the mean respiratory height of 1.6 m agl and stored as 1-minute mean values.

The OPC used had been factory calibrated on a regular basis (VDE standard 0701–0702) within the calibration validity period and was calibrated last time on 13/01/2015. Before calibration the latest inspection showed a deviation of $-0.6\,\mu g\,m^{-3}$ (−4.2 %) for $PM_{(0.25;10)}$ and a deviation of $-0.3\,\mu g\,m^{-3}$ (−2.7 %) for $PM_{(0.25;1)}$ of the OPC to the factory's reference unit 107 S/N.

2.3.2 Fixed weather station Aachen-Hörn

Inflow boundary conditions as entry criteria for the modelling tool were set using data from the permanent weather station "Aachen-Hörn", located in the outlying area of Aachen (6 ° 03 ′ 40 ″ E, 50 ° 46 ′ 44 ″), at 1800 m linear distance to the research site. Required values of wind speed and wind direction were collected as 10-minute averages (Schneider and Ketzler, 2015).

2.4 Simulation

The dispersion simulation of traffic related PM_{10} emissions were performed with version 2.6.11 of Austal2000, a Langrangian particle model according to the Technical Instructions on Air Quality Control (TA Luft), appendix 3 (BMU, 2002). Road traffic emissions only (including emissions from combustion processes, blown up dust as well as tire and break abrasions) were simulated in a domain extending 420 m by 420 m with a spatial resolution of 2 m.

For a best possible comparison with field observations, the semi-parallel measurements taken during the same period of time were considered regarding the initial conditions for the simulation run (cf. 2.2). Corresponding meteorological data from "Aachen-Hörn" (see 2.3.2) actuated the preceded and implemented model TALdia to calculate a wind and turbulence field library. In situ traffic counts were conducted to initiate particle source emission rates. Aerosol discharges for differentiated vehicle classes for each street leading to the investigation area (Fig. 2) were then calculated using the guideline published by Keller et al. (2004) and Lohmeyer et al. (2004). The simulation domain considered the complex conditions of the research site in terms of a spatially high-resolved (1 m) terrain model (soil surface) and georeferenced CAD-model data (urban fabric and obstacles). Vegetation elements such as trees were not considered. Georeferencing of CAD data and displaying of the results were realized using ESRI software ArcGIS version 10.2.2.

2.5 Measurement data handling

2.5.1 processing

There is a temporal variability of PM concentrations as a result of changing meteorological conditions and consequently an altering background particle transport towards the area under study during time series measurement campaigns (see Fig. 4). Therefore a daily correction factor for trend elimination and normalization of time series $PM_{(0.25;10)}$ values (cF_{PM10}) was developed. Therefore, the basic idea of Merbitz et al., 2012b was used and slightly modified. The correction factor $cF_{PM10}(d)$ is calculated separately for each day (d) at

the time when measurements took place as described in Eq. (2.1)

$$cF_{\mathrm{PM10}}(d) = \frac{1}{2}\left[\left(\frac{\sqrt[n]{\prod_{i=1}^{n} c_{i(AABU)}}}{c_{d(AABU)}}\right) + \left(\frac{\sqrt[n]{\prod_{i=1}^{n} c_{i(VACW)}}}{c_{d(VACW)}}\right)\right] \quad (2.1)$$

Hence, daily geometric mean values (c_d) of PM_{10} from the suburban monitoring site Aachen Burtscheid (AABU) and the traffic related monitoring site Aachen Wilhelmstrasse (VACW), operated by the Northrhine-Westfalian State Office for Nature, Environment, and Consumer Protection (LANUV), were set in relation to monthly averages c_i (geometric means) and averaged arithmetically over both sites, covering the whole periods of both measurement campaigns in February and September 2014. The calculated correction factors ($cF_{PM10}(d)$) for all measuring days (d) are further used by multiplying $cF_{PM10}(d)$ with the measured values on associated days (d) to remove meteorological bias from mere time series measurements collected at different locations and different times in order that these values become comparable. It is expected that the daily variability of urban PM-levels is better represented by a combination of both the suburban background station (AABU) and the traffic related air quality station (VACW) than by using only one reference site for daily normalization, since the area under study is situated among both regimes.

2.5.2 Data quality

In this study we compared measurement data from a mobile particle sensor with data sampled at government air quality stations that use a different principle of measurement. This implies that deterioration might be accepted when it comes to data quality.

To give an impression of data quality we made a comparison of the instruments at the government air quality monitoring site AABU in ambient air. The mobile OPC was compared there with the fixed-site SHARP instrument (continuous ambient particulate monitor consisting of a C14 source, detector and a light scattering Nephelometer (Thermo Fisher Scientific, Inc., Waltham (MA), U.S.)) operated by the LANUV for continuous air quality monitoring. Between 28/08/2015 and 30/09/2015, a total of 25 hours of comparison measurements were collected. One-hour averaged OPC data compared reasonably to the SHARP instrument values (slope 0.42, R^2 0.46, Fig. 5). Effectively, the OPC consistently overestimated PM10 data and measured on average 135 % of the PM_{10} indicated by the SHARP instrument including large scatter in the sample. The overestimation came as a surprise since the OPC features a sizing limit of 0.25 µm (see 2.3.1). Therefore, particles in the size range below 0.25 µm are not accessible to the OPC. Consequently, hereafter measurement data

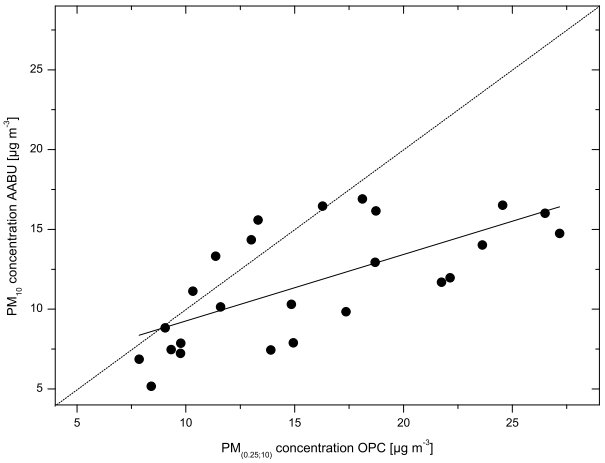

Figure 5: Comparison of 1 hour averages of PM_{10} derived from the SHARP instrument at the government air quality station AABU and $PM_{(0.25;10)}$ collected with the mobile opticle particle counter (OPC) in µg m^{-3} (slope: 0.42; R^2: 0.46). Data coverage is 25 hours between 28/08/2015 and 30/09/2015.

from the mobile OPC were analyzed as fraction values $PM_{(0.25;1)}$, $PM_{(0.25;10)}$ and $PM_{(1;10)}$.

2.6 Survey

2.6.1 Sample

A mixed method interview study with on-site users was carried out in order to identify perceptions towards air quality and on-site comfort. The questionnaire structure enabled a seasonal comparison regarding mass concentration of $PM_{(0.25;10)}$ and participants' perception. Overall, in both measurement campaigns 300 participants volunteered to take part. The mean age was 35.0 years (SD = 17.9) and the participants were between 10 and 95 years old. Of all participants 47.8 % were male and 52.2 % were female. In the winter campaign 124 pedestrians participated. The mean age was 37.0 years (SD = 19.3), with 65 women (53.3 %) and 57 men (46.7 %). In the summer campaign 176 pedestrians participated. The mean age was 33.6 years (SD = 16.7) with 90 women (51.4 %) and 85 men (48.6 %). Overall this represents an even gender distribution. Urban park users were examined as they incidentally crossed our measurements site in the inner urban area.

2.6.2 Method perception measurements and data analysis

In questionnaire-based interviews with pedestrians, demographic data as well as information on their individual social and living situations were assessed. In addition, the position of every participant was noted, i.e. whether they were sitting or standing, while they were being interviewed on perception of environmental condiditons. The perception of their own weather comfort, air quality as well as on-site comfort was questioned and compared to measured physical data.

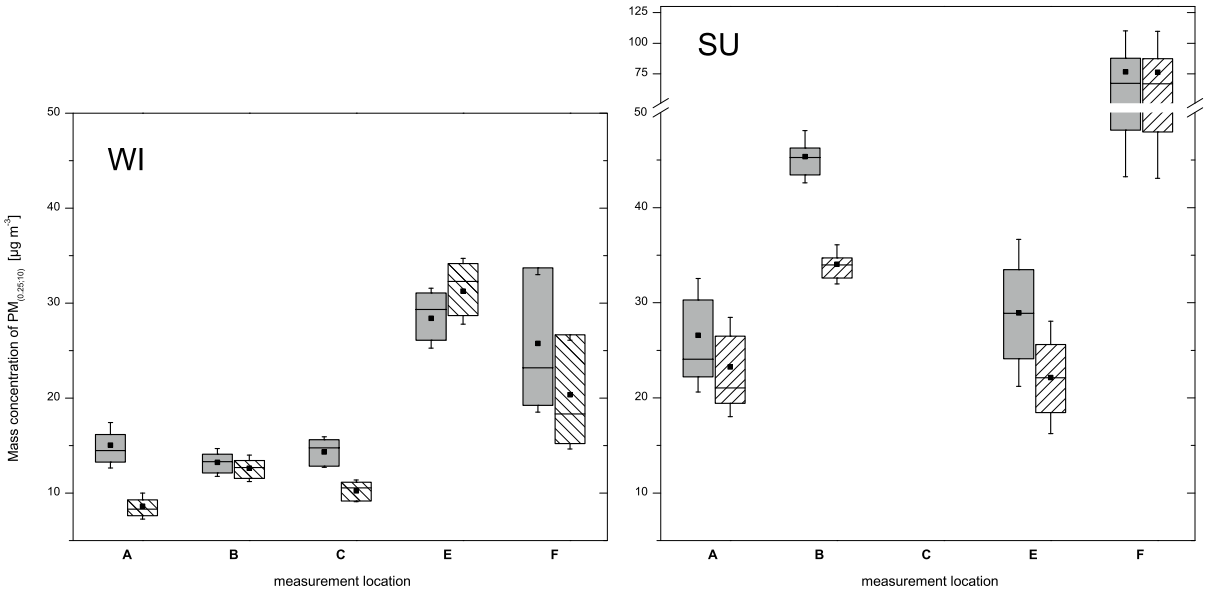

Figure 6: Boxplot diagram of $PM_{(0.25;10)}$ concentrations in $\mu g\,m^{-3}$ measured as time series at different locations (A, B, C, E, F) inside the area under study "Elisenbrunnen" in Aachen during different weekdays in winter (left illustration "WI") and in summer (right illustration "SU") 2014. Raw measurement values are shown in grey boxes whereas normalized values are shown in black/white boxes (10-minute mean values). Boxes display 25 % / 75 % quantiles and medians. Squares represent the arithmetic mean and whiskers show the standard deviation.

Data were analyzed using paired sample t-tests in order to detect seasonal differences of particulate matter concentration and mean rating for perceived air quality. Further, the relationship between particulate matter and perceived on-site comfort was analyzed by using bivariate analysis (spearman rank).

3 Results and discussion

3.1 Measurement results – spatial distribution of particle mass concentration

Results of trend corrected $PM_{(0.25;10)}$ mass concentration time series unveiled surprisingly the highest arithmetic mean values (20.4–31.3 $\mu g\,m^{-3}$) at monitoring locations E and F inside the green area during wintertime (Fig. 6). Three times less average $PM_{(0.25;10)}$ concentrations were found at monitoring positions in proximity to busy roads (B, C). Experiments during summer revealed both overall higher particle concentration regarding $PM_{(0.25;10)}$ and a slightly altered $PM_{(0.25;10)}$ distribution pattern (Fig. 6). Measurement location F featured outstanding mean $PM_{(0.25;10)}$ concentrations (76.4 $\mu g\,m^{-3}$) as well as the highest median (67.7 $\mu g\,m^{-3}$) whereas at sites A and E concentrations around 22.5 $\mu g\,m^{-3}$ were detected. Slightly higher trend corrected aerosol concentrations (34.0 $\mu g\,m^{-3}$) were measured during summer at the motor traffic governed monitoring site B. In comparison, sites A and E hat the comparatively lowest variations. In general, measurement values of $PM_{(0.25;10)}$ scattered mostly at monitoring sites inside the green area both in wintertime as well as during the summer campaign. Inside the park only, outliers with metered 10-minute mean values of $PM_{(0.25;10)}$ exceeding 100.0 $\mu g\,m^{-3}$ were recorded frequently.

Due to the unforeseen findings during the first measurement campaign during February 2014 we subsequently made a different approach to particle measurements (see Section 2.2). Surprisingly, measurement results of $PM_{(1;10)}$ regarding the semi-parallel approach show unexpected effects as well (Fig. 7) as compared to the observed time series results (cf. Fig. 6). For instance, the concentration of coarse particle fractions ($PM_{(1;10)}$) were higher at the park site E and F (arithmetic mean: 22.5 $\mu g\,m^{-3}$ and 18.9 $\mu g\,m^{-3}$; geometric mean: 9.3 $\mu g\,m^{-3}$ and 6.5 $\mu g\,m^{-3}$), 100 m away from motor traffic, than on the sidewalk in close vicinity to the main road at locations B and C (arithmetic mean: 7.5 $\mu g\,m^{-3}$ and 8.7 $\mu g\,m^{-3}$; geometric mean: 5.8 $\mu g\,m^{-3}$ and 6.5 $\mu g\,m^{-3}$). Due to the proximity to vehicles travelling at speeds between stop-and-go and 30 km h^{-1}, which cause significant turbulence, one would expect resuspended coarse particles and emissions from brake and tire abrasions to play a significant role at site B and C regarding $PM_{(1;10)}$. In contrast, the direct environment at park sites E, F and partly D featured a surface of dry grass and unsurfaced footpaths containing loose and dry top coating material. It can be stated that those surfaces made a dominant contribution to airborne particles of $PM_{(1;10)}$ due to resuspension. That gives an approach to explain the unexpected spatial pattern at the monitoring locations inside the park and the motor traffic related sites B and C. The observation of the largest

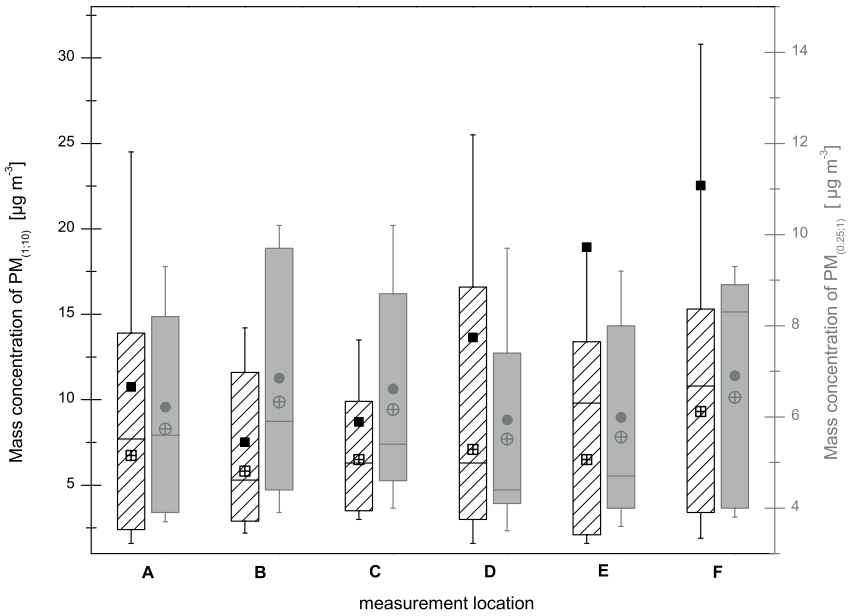

Figure 7: Boxplot diagram of PM concentrations in $\mu g\,m^{-3}$ measured with a semi parallel approach at different locations (A, B, C, D, E, F) inside the area under study "Elisenbrunnen" in Aachen during different weekdays in February, May and September 2014, 10:00–17:00, during cyclonic weather conditions. Measurement data of $PM_{(1;10)}$ concentrations are displayed in black/white boxes (left ordinate) whereas $PM_{(0.25;1)}$ concentrations are shown in grey boxes (right ordinate) collected as 1-minute mean values (n = 56). Boxes display 25 % / 75 % quantiles and medians. Filled squares and circles represent arithmetic means, crossed squares and circles represent geometric means and whiskers show the standard deviation.

scatter in measured $PM_{(1;10)}$ concentrations at sites D, E and F support our assumption of the subsistence of coarse particles emitters through diffuse sources e.g. on the ability of surfaces to release particles by resuspension. Consistently, during different days 1-minute mean concentrations of $PM_{(1;10)}$ far exceeded $50\,\mu g\,m^{-3}$. This was probably due to recurrent gusting wind that blew up dust from unpaved surfaces.

By contrast, particle fractions of $PM_{(0.25;1)}$ were distributed equally at all measuring points (arithmetic mean: 6.0–6.9 $\mu g\,m^{-3}$). Merely, a poorly distinctive spatial pattern was observed considering arithmetic mean $PM_{(0.25;1)}$ values with comparatively small differences between measurement locations. The highest average $PM_{(0.25;1)}$ concentrations were detected in proximity to the main road "Friedrich-Wilhelm-Platz" at monitoring sites B and C (arithmetic mean: 6.9 $\mu g\,m^{-3}$ and 6.6 $\mu g\,m^{-3}$; geometric mean: 6.3 $\mu g\,m^{-3}$ and 6.1 $\mu g\,m^{-3}$) and at measuring point F inside the green area (arithmetic mean: 6.9 $\mu g\,m^{-3}$; geometric mean: 6.4 $\mu g\,m^{-3}$), respectively. The observed pattern with the highest $PM_{(0.25;1)}$ concentrations in vicinity to motor traffic emitters was expected to be due to medium-sized particles out of brake and tire abrasion as well as secondary accumulation mode particles arising from combustion processes. However, the $PM_{(0.25;1)}$ mass concentration findings at site F made an exception. At least here it seems that the former described diffuse particle source inside the park has an impact on $PM_{(0.25;1)}$ mass concentrations as well – albeit to a vastly lesser extent.

Overall, it is evident that such small-scale spatial gradients of particle concentrations in the urban roughness layer can usually not be captured by single stationary measurements.

3.2 Simulation results – influence of traffic on PM_{10} concentrations at the research site

Simulation results of excessive motor traffic emissions generated with meteorological conditions initially similar to the semi-parallel measurements reveal the highest traffic-related PM_{10} concentrations in close vicinity to traffic lines particularly at the main road "Friedrich-Wilhelm-Platz" and the alleyway "Ursulinerstr.", with the average contribution to the total mass concentration of PM_{10} being in the range of 10.0 – 22.0 $\mu g\,m^{-3}$ (Fig. 8). Corresponding concentrations seem to decline rapidly further from the traffic sources. The average contribution of traffic-induced airborne particles to the total aerosol concentration at the research site under given meteorological conditions decreases to 3.0–10.0 $\mu g\,m^{-3}$ at distances as little as 10 m away from the two mentioned roads. According to simulation outcomes the direct impact of local motor traffic on PM_{10} concentrations inside the park tends to be negligible. At inner park sites, the additions to rural and urban background concentrations and to other local diffuse particle sources (e.g. unpaved footpaths) resulting from motor traffic are estimated to be in magnitudes of 0.1–1.6 $\mu g\,m^{-3}$. Simulation results do not indicate that local traffic emissions cause

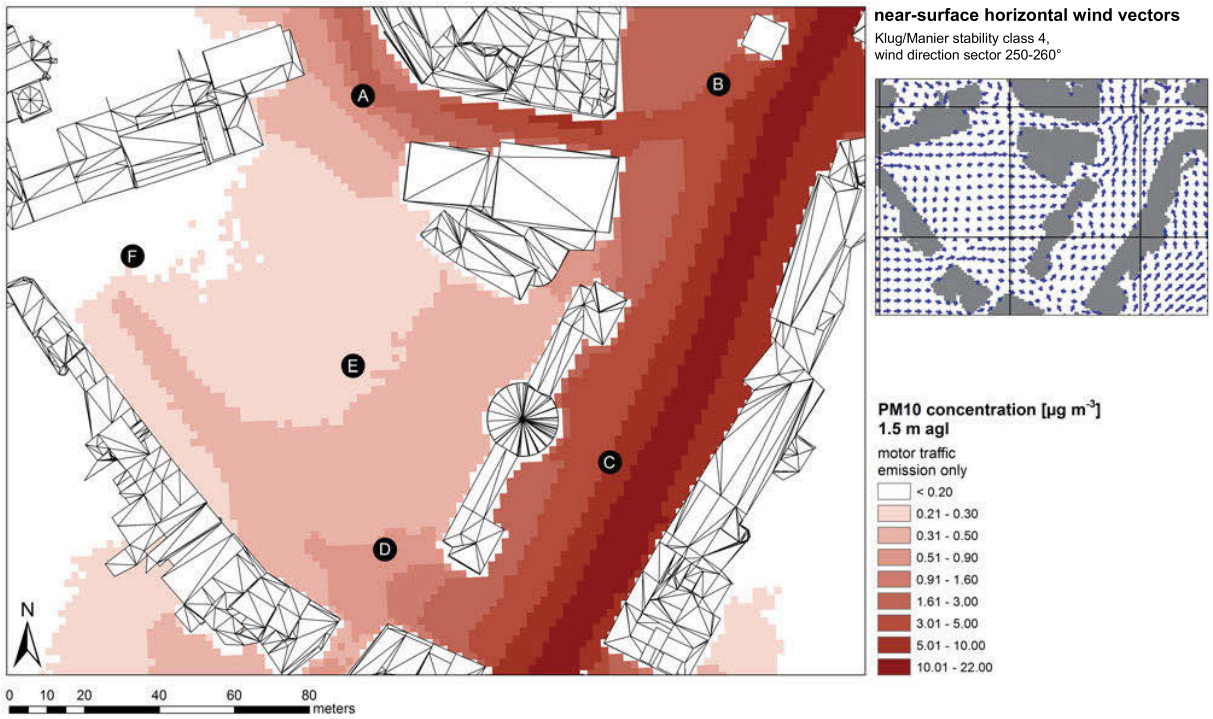

Figure 8: Contour plot of the simulated distribution of average PM_{10} concentrations induced by motor traffic only [µg m^{-3}] at 1.5 m agl for the research site "Elisenbrunnen", Aachen, for different chosen weekdays in February, May and September 2014, 10:00–17:00, during cyclonic weather conditions including depicted measurement locations A–F (black dots). Upper right plot shows near-surface horizontal wind vectors (blue arrows) representative for mean inflow boundary conditions (Klug/Manier stability class 4, wind direction sector 250–260°).

Table 1: Mean PM_{10} remainder (ΔPM_{10}) for monitoring locations A–F calculating the difference between arithmetic mean $PM_{(0.25;10)}$ values of the semi-parallel measurements and the sum of arithmetic mean PM_{10} data out of the simulation and the arithmetic mean background PM_{10} concentration recorded at the rural background air quality monitoring station "Burtscheid" (AABU).

	monitoring location					
	A	B	C	D	E	F
Mean $PM_{(0.25;10)}$ measured	17.0	14.4	15.3	19.6	24.9	29.4
Mean PM_{10} simulated	0.5	2.7	4.3	0.6	0.2	0.2
Mean rural background PM_{10} (AABU)			11.4			
Δ PM_{10}	5.0	0.2	−0.4	7.6	13.3	17.9

elevated $PM_{(0.25;10)}$ concentrations inside the green area. In fact, simulation results illustrate the exact opposite when it comes to the comparison with spatial patterns of measured $PM_{(0.25;10)}$ and $PM_{(1;10)}$ concentrations (cf. Fig. 6 and Fig. 7). As expected, under southwest inflow situations particles tend to accumulate in the alleyway ("Ursulinerstr.") and street canyons ("Friedrich-Wilhelm-Platz"), where dilution of aerosols is difficult, as well as in areas downwind from emission sources where particles get dammed up at obstacles. Simulated traffic induced average PM_{10} concentrations with a distinctive gradient for the monitoring sites A–F complete the picture. Highest mean values were simulated for sites B and C with declining concentrations at locations A and D, whereas monitoring sites inside the green area with maximum distance to the traffic lines (E, F) show minimum average PM_{10} concentrations (Fig. 8).

Approximations of PM_{10} remainders (ΔPM_{10}) indicate that local diffuse particle sources and urban background transport contribute to local PM_{10} concentrations inside the green area of up to 17.9 µg m^{-3}, whereas the impact on measurement locations in vicinity to the main roads (measurement locations B and C) was calculated to be close to zero (Table 1). From this analysis we may conclude that resuspension of PM from unpaved grounds within the green park area would have been a major contribution to the elevated measured $PM_{(0.25;10)}$ and $PM_{(1;10)}$ levels at sites E and F and possibly also at site A and D within limits of specified uncertainties (cf. 2.5.2).

3.3 Urban park user perception of air quality

A first analysis addressed seasonal effects on physical influences like particulate matter and on perception

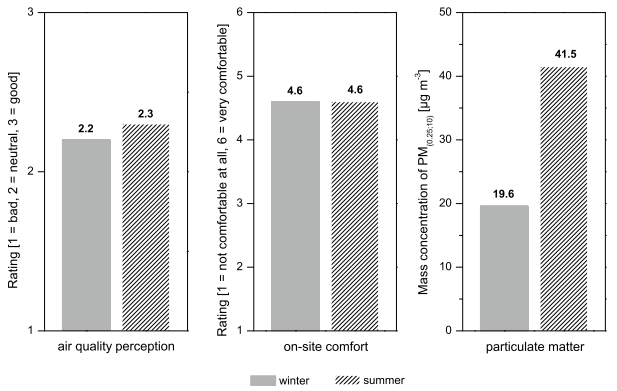

Figure 9: Bar diagram of arithmetic mean ratings of air quality perception on a 3-point Likert scale (1 = bad, 2 = neutral, 3 = good) [left illustration], of on-site comfort on a 6-point Likert scale (1 = not comfortable at all, 6 = very comfortable) [middle illustration] and arithmetic mean $PM_{(0.25;10)}$ concentrations ($\mu g\,m^{-3}$) of time series measurements [right illustration]. Grey bars show data from the winter campaign (February 2014) whereas black striped bars display data from the summer campaign (July 2014).

of air quality. The independent-samples t-test unveiled a significant difference in measurements of $PM_{(0.25;10)}$ time series ($t(212) = -10.3$, $p <= 0.001$) in February 2014 (arithmetic mean = $19.6\,\mu g\,m^{-3}$, standard deviation (SD) = $7.5\,\mu g\,m^{-3}$) and in July 2014 (arithmetic mean = $41.5\,\mu g\,m^{-3}$, SD = $26.6\,\mu g\,m^{-3}$). These findings indicate higher PM stressors during the summer campaign than during measurements in February in Aachen. The significant difference between particulate matter concentration in winter and summer could be proved. Contrary to the significant differences between summertime and the winter campaign in Aachen regarding mean concentration of $PM_{(0.25;10)}$, the perception of air quality was assessed comparably. Results of air quality perception ratings show similar mean values in winter and summer, reaching mean values of 2.2 and 2.3 on a Likert scale ranging from 1.0 (= bad) to 3.0 (= good). In both seasons pedestrians' evaluation patterns were comparably similar, with the same SD of 0.6. Thus, we can conclude that there are no seasonal differences regarding the rating of pedestrians of PM levels even though in fact marked differences between summer and winter campaigns are obvious from measured data (Fig. 9). A detailed look at physically measured $PM_{(0.25;10)}$ data set against survey results regarding the perception of air quality add to the picture (Fig. 10). In fact, park users described perceived air quality as both good, neutral and bad under almost all measured $PM_{(0.25;10)}$ concentrations (ranging from 11.3 to $36.2\,\mu g\,m^{-3}$ during the winter campaign and 17.0 to $129.9\,\mu g\,m^{-3}$ during the summer campaign). That applies for both investigated seasons (albeit we worked with a refined Likert scale range from 1.0 = very bad air quality to 6.0 = very good air quality during the summer campaign). Consequently, no significant correlation was found between measured $PM_{(0.25;10)}$ and perceived air quality for both campaigns during the winter season and the summer season (winter: r 0.13; summer: r −0.20).

Beyond the results of non-sensitivity to perception of PM within air quality, a further analysis focused on the question whether there is a relationship between PM (as a physical stressor) and/or the perception of on-site (climate) comfort. For on-site comfort, a 6-point Likert scale was used to question how comfortable the current site was for the interviewee (1 = not comfortable at all, 6 = very comfortable). The descriptive outcomes reveal a similar rating of on-site comfort of 4.6 (arithmetic mean) on the Likert scale both for winter- and summertime surveys (Fig. 9). As can be seen, the perception of on-site comfort did not coincide with the seasonal differences of mean $PM_{(0.25;10)}$ data. Hence, the exposure resulting from high overall mean $PM_{(0.25;10)}$ concentration during summer was not perceived within this evaluation.

However, there is a significant correlation between on-site (climate) comfort values and perception data of air quality ($r = 0.29$; $p <= 0.000$), showing that participants' evaluations coincide: the higher (i.e. more comfortable) the perceived air quality was, the higher was the perceived on-site comfort even though both measurements did not relate to the measured $PM_{(0.25;10)}$ concentration in both seasons.

4 Conclusions

This study showed the heterogeneous and complex mass concentration distribution of aerosols at very small scales similar to earlier studies (Birmili et al., 2013a, Merbitz et al., 2012c). The combination of experiments and the use of a micro-scale particle dispersion model allowed for an understanding of spatial gradients and the identification of different particle sources in the urban roughness layer of roughly an area of 400 m by 400 m in the inner city of Aachen. Even though traffic is assumed to be the most important particle source across urban agglomerations, $PM_{(0.25;10)}$ and $PM_{(1;10)}$ metrics showed unexpected distribution patterns with highest mean concentrations inside a park several tens of meters away from trafficked roads. Semi-parallel particle measurements of $PM_{(0.25;1)}$, however, revealed an extensively equal distribution pattern in the whole area under study with only slightly increased mean concentrations close to the traffic lines. AUSTAL2000 simulation results of only traffic induced emissions of PM_{10} showed a different distribution pattern compared to $PM_{(0.25;10)}$ and $PM_{(1;10)}$ measurements. The simulation, conducted with similar meteorological inflow boundary conditions observed during semi-parallel measurements, unveiled a major impact of road traffic on the aerosol concentration in the area under study similar in magnitude to related findings in other studies (Merbitz et al. 2012b). Mean PM_{10} concentrations were simulated to be highest near to traffic lines. When moving away from traffic sources mean PM_{10} concentrations seemed to rapidly decrease.

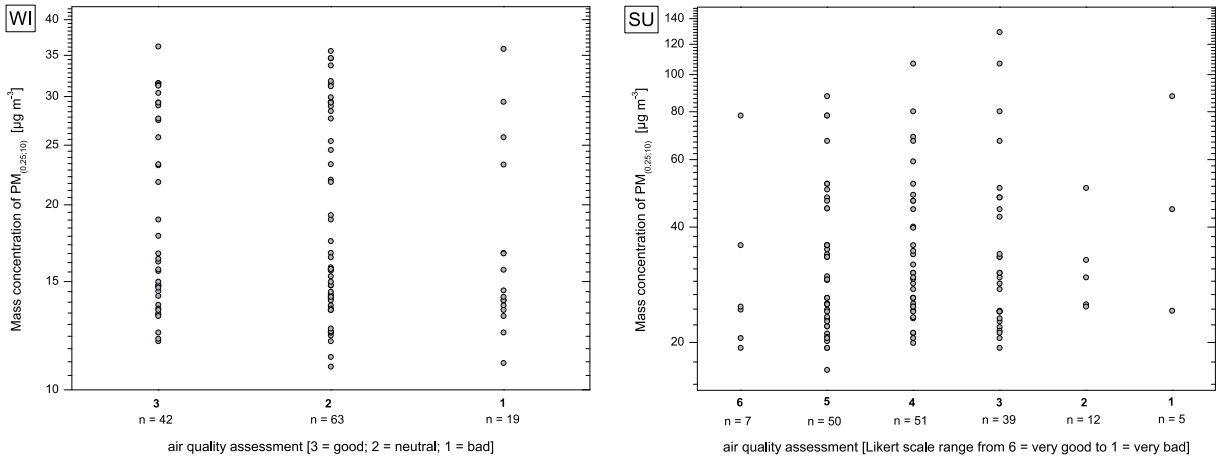

Figure 10: Scatter plot diagrams of measured $PM_{(0.25;10)}$ concentrations in $\mu g\,m^{-3}$ vs. air quality assessments on a 3-point Likert scale (3 = good, 2 = neutral, 1 = bad) during the winter campaign (left illustration "WI") and vs. air quality assessments on a 6-point Likert scale (from 6 = very good to 1 = very bad,) during the summer campaign (right illustration "SU").

The direct influence of local traffic PM_{10} emissions on the park area tended to be negligible. Both the analysis of experimental data alone and the comparison to simulation results of only traffic induced PM emissions provides strong evidence for the hypothesis that surfaces of dried-out grass and unsurfaced footpaths in the park provided a big source of coarse airborne particles ($PM_{(1;10)}$) and give a plausible explanation for the unexpected spatial distribution patterns of $PM_{(0.25;10)}$ and $PM_{(1;10)}$ metrics. During the measurement campaign in February, May and September 2014 the contribution of diffuse resuspension particle sources to measured mean mass concentration of $PM_{(0.25;10)}$ was estimated to be between 13.3 and 17.9 $\mu g\,m^{-3}$ inside the park area.

Reflection on our results raises two questions: a) Can fixed site aerosol instrumentation provide representative statements for an entire city area regarding the urban space user's exposure to particles, in particular when the city area as a general rule contains e.g. heterogeneous subsurfaces und numerous different particle sources? b) Is PM_{10} as a single metric a good measure for air quality regulation regarding aerosols inside cities since different particle size fractions with different impacts on the human body (Kreyling et al., 2006) can be distributed in various ways (Ning and Sioutas, 2010)?

In terms of human perception, mass concentrations of $PM_{(0.25;10)}$ were not reliably assessed, neither in relation to seasons, nor in relation to air quality and on-site comfort. The low standard deviations suggest a rather comparable perception among urban park users, not taking into consideration the high age range (10–95 years) or gender. In marked contrast to findings from Nikolopoulou et al. (2011), who claimed a significant positive correlation between PM concentrations and perception of air quality during a similar study in similar PM concentration magnitudes, we can conclude that perception of air quality was imprecise and unrelated to the real exposure, regardless of age and gender. Nevertheless, data revealed a close relationship between the awareness of air quality and on-site comfort, thus corroborating the sensitivity of pedestrians to perception of urban stressors. Due to an undersized sample this study lacks a deeper investigation into what actually formed the park users' opinion on air quality and on-site comfort, which is probably influenced more by factors like sense of place (Brody et al., 2004) or acoustic occurrences than by actual air quality conditions. The fact that exposure to airborne particles is indeed dangerous and has insidious adverse effects on human health although it is obviously not perceivable in investigated concentration magnitudes makes it even more important to reduce PM concentrations.

5 Acknowledgments

This project is part of the interdisciplinary Project House HumTec (Human Technology Center) at RWTH Aachen University. The financial support from the German federal and state governments through the German Research Foundation (Deutsche Forschungsgemeinschaft, DFG) is gratefully acknowledged. We would like to thank the scientific editor and two anonymous reviewers for very helpful comments on this manuscript. Thanks to students I. Zirwes and M. Moers who helped enthusiastically with field experiments and traffic counts. We acknowledge S. Wilhelm from the Northrine-Westfalian State Office for Nature, Environment, and Consumer Protection (LANUV) for providing PM_{10} data from monitoring stations in Aachen. U. Janicke kindly helped with issues regarding AUSTAL2000.

References

Badland, H.M., M.J. Duncan, 2009: Perceptions of air pollution during the work-related commute by adults in Queensland, Australia. – Atmos. Env. **43**, 5791–5795. DOI: 10.1016/j.atmosenv.2009.07.050.

Bekö, G., B.U. Kjeldsen, Y. Olsen, J. Schipperijn, A. Wierzbicka, D.G. Karottki, J. Toftum, S. Loft, G. Clausen, 2015: Contribution of various microenvironments to the daily personal exposure to ultrafine particles: Personal monitoring coupled with GPS tracking. – Atmos. Env. **110**, 122–129. DOI:10.1016/j.atmosenv.2015.03.053.

Birmili, W., J. Rehn, A. Vogel, C. Boehlke, K. Weber, F. Rasch, 2013a: Micro-scale variability of urban particle number and mass concentrations in Leipzig, Germany. – Meteorol. Z. **22**, 155–165. DOI:10.1127/0941-2948/2013/0394.

Birmili, W., L. Tomsche, A. Sonntag, C. Opelt, K. Weinhold, S. Nordmann, W. Schmidt, 2013b: Variability of aerosol particles in the urban atmosphere of Dresden (Germany): Effects of spatial scale and particle size. – Meteorol. Z. **22**, 195–211. DOI:10.1127/0941-2948/2013/0395.

Brody, S.D., B.M. Peck, W.E. Highfield, 2004: Examining Localized Patterns of Air Quality Perception in Texas: A Spatial and Statistical Analysis. – Risk Analysis **24**, 1561–1574. DOI: 10.1111/j.0272-4332.2004.00550.x.

Broich, A.V., L.E. Gerharz, O. Klemm, 2012: Personal monitoring of exposure to particulate matter with a high temporal resolution. – Environ. Sci. Pollut. Res. **19**, 2959–2972. DOI: 10.1007/s11356-012-0806-3.

Brook, R.D., S. Rajagopalan, C.A. Pope, J.R. Brook, A. Bhatnagar, A.V. Diez-Roux, F. Holguin, Y. Hong, R.V. Luepker, M.A. Mittleman, A. Peters, D. Siscovick, S.C. Smith, L. Whitsel, J.D. Kaufman, on behalf of the American Heart Association Council on Epidemiology and Prevention, Council on the Kidney in Cardiovascular Disease, and Council on Nutrition, Physical Activity and Metabolism, 2010: Particulate Matter Air Pollution and Cardiovascular Disease: An Update to the Scientific Statement From the American Heart Association. – Circulation **121**, 2331–2378. DOI:10.1161/CIR.0b013e3181dbece1.

Chen, L., E. Ng, 2012: Outdoor thermal comfort and outdoor activities: A review of research in the past decade. – Cities **29**, 118–125. DOI:10.1016/j.cities.2011.08.006.

Chow, J.C., J.G. Watson, J.L. Mauderly, D.L. Costa, R.E. Wyzga, S. Vedal, G.M. Hidy, S.L. Altshuler, D. Marrack, J.M. Heuss, G.T. Wolff, C.A. Pope, D.W. Dockery, 2006: Health Effects of Fine Particulate Air Pollution: Lines that Connect. – J. Air Waste Manag. Assoc. **56**, 1368–1380. DOI:10.1080/10473289.2006.10464545.

Dons, E., L. Int Panis, M. Van Poppel, J. Theunis, H. Willems, R. Torfs, G. Wets, 2011: Impact of time–activity patterns on personal exposure to black carbon. – Atmos. Env. **45**, 3594–3602. DOI: 10.1016/j.atmosenv.2011.03.064.

Gabriel, K.M.A., W.R. Endlicher, 2011: Urban and rural mortality rates during heat waves in Berlin and Brandenburg, Germany. – Environ. Pollut. **159**, 2044–2050. DOI: 10.1016/j.envpol.2011.01.016.

German Federal Ministry for Environment, Nature Conservation and Nuclear Safety (BMU), 2002: First General Administrative Regulation for the Federal Emission Control Law / Instructions for Pollution Control. – TA Luft (in German); Gemeinsames Ministerialblatt **24**, 511–605.

Johansson, E., S. Thorsson, R. Emmanuel, E. Krüger, 2014: Instruments and methods in outdoor thermal comfort studies – The need for standardization. – Urban Climate **10**, 346–366. DOI:10.1016/j.uclim.2013.12.002.

Keller, M., P. de Hahn, W. Knörr, S. Hausberger, H. Steven, 2004: Handbook Emission Factors for Road Transport (in German). – UBA Berlin, BUWAL Bern, UBA Wien, Bern, Heidelberg, Graz, Essen. 127 pp.

Kozawa, K.H., A.M. Winer, S.A. Fruin, 2012: Ultrafine particle size distributions near freeways: Effects of differing wind directions on exposure. – Atmos. Env. **63**, 250–260. DOI: 10.1016/j.atmosenv.2012.09.045.

Kreyling, W.G., M. Semmler-Behnke, W. Möller, 2006: Ultrafine Particle–Lung Interactions: Does Size Matter? – J. Aerosol Med. **19**, 74–83. DOI:10.1089/jam.2006.19.74.

Laden, F., J. Schwartz, F.E. Speizer, D.W. Dockery, 2006: Reduction in Fine Particulate Air Pollution and Mortality: Extended Follow-up of the Harvard Six Cities Study. – American Journal of Respiratory and Critical Care Medicine **173**, 667–672. DOI:10.1164/rccm.200503-443OC.

Lohmeyer, A., M. Stockhauser, A. Moldenhauer, E. Nitzsche, I. Düring, 2004: Calculation of traffic induced particle emissions due to blown up dust and abrasions for the land register of the State of Saxony. Workpackages 1 and 2 (in German). – Sächsisches Landesamt für Umwelt und Geologie, Dresden.

Maras, I., M. Buttstädt, J. Hahmann, H. Hofmeister, C. Schneider, 2014: Investigating public places and impacts of heat stress in the city of Aachen, Germany. – Die Erde **44**, 290–303. DOI:10.12854/erde-144-20.

Maras, I., T. Schmidt, B. Paas, M. Ziefle, C. Schneider, 2016: The impact of biometeorological factors on perceived thermal comfort at urban public places. – Meteorol. Z., **25**, DOI:10.1127/metz/2016/0705

Merbitz, H., M. Buttstädt, S. Michael, W. Dott, C. Schneider, 2012a: GIS-based identification of spatial variables enhancing heat and poor air quality in urban areas. – Appl. Geogr. **33**, 94–106. DOI:10.1016/j.apgeog.2011.06.008.

Merbitz, H., F. Detalle, G. Ketzler, C. Schneider, F. Lenartz, 2012b: Small scale particulate matter measurements and dispersion modelling in the inner city of Liège, Belgium. – Int. J. Env. Pol. **50**, 234. DOI: 10.1504/IJEP.2012.051196.

Merbitz, H., S. Fritz, C. Schneider, 2012c: Mobile measurements and regression modeling of the spatial particulate matter variability in an urban area. – Sci. Total Environ. **438**, 389–403. DOI:10.1016/j.scitotenv.2012.08.049.

Mishra, V.K., P. Kumar, M. Van Poppel, N. Bleux, E. Frijns, M. Reggente, P. Berghmans, L. Int Panis, R. Samson, 2012: Wintertime spatio-temporal variation of ultrafine particles in a Belgian city. – Sci. Total Environ. **431**, 307–313. DOI:10.1016/j.scitotenv.2012.05.054.

Nikolopoulou, M., J. Kleissl, P.F. Linden, S. Lykoudis, 2011: Pedestrians' perception of environmental stimuli through field surveys: Focus on particulate pollution. – Sci. Total Environ. **409**, 2493–2502. DOI: 10.1016/j.scitotenv.2011.02.002.

Ning, Z., C. Sioutas, 2010: Atmospheric Processes Influencing Aerosols Generated by Combustion and the Inference of Their Impact on Public Exposure: A Review. – Aerosol Air Quality Res. **10**, 43–58. DOI:10.4209/aaqr.2009.05.0036.

Padró-Martínez, L.T., A.P. Patton, J.B. Trull, W. Zamore, D. Brugge, J.L. Durant, 2012: Mobile monitoring of particle number concentration and other traffic-related air pollutants in a near-highway neighborhood over the course of a year. – Atmos. Env. **61**, 253–264. DOI: 10.1016/j.atmosenv.2012.06.088.

Pope, C.A., R.T. Burnett, M.J. Thun, E.E. Calle, D. Krewski, K. Ito, G.D. Thurston, 2002: Lung cancer, cardiopulmonary mortality, and long-term exposure to fine particulate air pollution. – JAMA **287**, 1132–1141.

Quiros, D.C., Q. Zhang, W. Choi, M. He, S.E. Paulson, A.M. Winer, R. Wang, Y. Zhu, 2013: Air quality impacts of a scheduled 36-h closure of a major highway. – Atmos. Env. **67**, 404–414. DOI:10.1016/j.atmosenv.2012.10.020.

Raimbault, M., D. Dubois, 2005: Urban soundscapes: Experiences and knowledge. – Cities **22**, 339–350. DOI: 10.1016/j.cities.2005.05.003.

Schmidt, T., I. Maras, B. Paas, J. Stienen, M. Ziefle, 2015: Psychophysical observations on human perceptions of climatological stress factors in urban environments. – In: Proceedings 19th Triennial Congress of the IEA **9**, 14.

Schneider, C., G. Ketzler, 2015: Klimamessstation Aachen-Hörn. - Monatsberichte Februar, Mai, September / 2014, RWTH Aachen, Geographisches Institut, Lehr- und Forschungsgebiet Physische Geographie und Klimatologie.

Seinfeld, J.H., S.N. Pandis, 2006: Atmospheric chemistry and physics: from air pollution to climate change. 2nd ed. – J. Wiley, Hoboken, New Jersey, 1203 pp.

Shirom, A., S. Melamed, M. Nir-Dotan, 2000: The relationships among objective and subjective environmental stress levels and serum uric acid: The moderating effect of perceived control. – J. Occupational Health Psychology **5**, 374–385. DOI:10.1037/1076-8998.5.3.374.

Spinazzè, A., A. Cattaneo, D.R. Scocca, M. Bonzini, D.M. Cavallo, 2015: Multi-metric measurement of personal exposure to ultrafine particles in selected urban microenvironments. – Atmos. Env. **110**, 8–17. DOI: 10.1016/j.atmosenv.2015.03.034.

Steinle, S., S. Reis, C.E. Sabel, 2013: Quantifying human exposure to air pollution – Moving from static monitoring to spatio-temporally resolved personal exposure assessment. – Sci. Total Env. **443**, 184–193. DOI: 10.1016/j.scitotenv.2012.10.098.

United Nations, Population Division, Department of Economic and Social Affairs, 2014: World urbanization prospects: the 2014 revision. – United Nations, New York, 27 pp.

Venn, A.J., S.A. Lewis, M. Cooper, R. Hubbard, J. Britton, 2001: Living Near a Main Road and the Risk of Wheezing Illness in Children. – Amer. J. Respiratory Critical Care Medicine **164**, 2177–2180. DOI:10.1164/ajrccm.164.12.2106126.

Von Klot, S., 2005: Ambient Air Pollution Is Associated With Increased Risk of Hospital Cardiac Readmissions of Myocardial Infarction Survivors in Five European Cities. – Circulation **112**, 3073–3079. DOI: 10.1161/CIRCULATIONAHA.105.548743.

WHO, 2013: Health risks of air pollution in Europe – HRAPIE project. – Online available at http://www.euro.who.int/__data/assets/pdf_file/0017/234026/e96933.pdf?ua=1 (Accessed March 18, 2015).

Yang, W., J. Kang, 2005: Acoustic comfort evaluation in urban open public spaces. – Appl. Acoust. **66**, 211–229. DOI: 10.1016/j.apacoust.2004.07.011.

Journal paper II

A comparison of model performance between ENVI-met and Austal2000 for particulate matter

DOI:10.1016/j.atmosenv.2016.09.031

Atmospheric Environment 145 (2016) 392–404

Contents lists available at ScienceDirect

Atmospheric Environment

journal homepage: www.elsevier.com/locate/atmosenv

A comparison of model performance between ENVI-met and Austal2000 for particulate matter

Bastian Paas [a, b, c, *], Christoph Schneider [b]

[a] Department of Geography, RWTH Aachen University, Wüllnerstaße 5b, D-52062 Aachen, Germany
[b] Department of Geography, Humboldt-Universität zu Berlin, Unter den Linden 6, D-10099 Berlin, Germany
[c] Project House HumTec, RWTH Aachen University, Theaterplatz 14, D-52062 Aachen, Germany

HIGHLIGHTS

- A performance analysis of 2 dispersion models Austal2000 & ENVI-met is presented.
- All models used had the tendency to underpredict observed PM concentrations.
- Predictions of both models gained precision in the high-end concentration range.
- Austal2000's predictions were closer to field observations than those of ENVI-met.
- For best results the models used should be initiated with local atmospheric data.

ARTICLE INFO

Article history:
Received 13 July 2016
Received in revised form
12 September 2016
Accepted 14 September 2016
Available online 14 September 2016

Keywords:
ENVI-Met
Austal2000
Micro-scale simulations
Particle dispersion
Model performance
Particulate matter

ABSTRACT

This study evaluates the performance of the German dispersion model Austal2000 according to the technical instructions on air quality control (TA Luft), a Lagrangian model, in four real-world particulate matter test cases against ENVI-met, a microclimate model featuring a pollutant dispersion module that bases on the Eularian approach. The four test cases include different traffic induced area sources of PM_{10}, complex terrain with varying ground surfaces and different urban obstacles i.e. buildings. A comparison is made between the calculated concentrations of both models. Furthermore, predictions are compared with field data. Particle measurements are conducted with an optical particle counter. For evaluation, quantile-quantile plots as well as further performance measures i.e. the fractional bias and the robust highest concentration that focuses on the important high-end concentrations are applied. Both models underpredicted observed $PM_{(0.25;10)}$ concentrations for all test cases. All datasets show that predictions of both simulation tools were closer to field observations in the high-end concentration range. Model calculation results show mostly better agreement to observations under neutral stability classes of the atmosphere. With the exception of ENVI-met in one test case predictions of simulation runs of both models lead to results closer to observations when initiated with local meteorological measurement data, where wind speed as one of the key drivers of dispersion models was lower. In almost all of the test cases, Austal2000's predictions were closer to the field observations than those of ENVI-met. The latter model undercut predicted PM_{10} concentrations of Austal2000 by the factor of around two. This evaluation indicates that Austal2000 is the stronger model compared with ENVI-met considering the distribution of PM_{10} in complex and urban terrain.

1. Introduction

Results of epidemiological studies suggest that exposure to particulate matter (PM) could have significant impacts on health (Pope et al., 2002; WHO, 2013). It is estimated that in European cities life expectancy at age 30 is reduced by up to 22 months solely due to the fact that outdoor particle concentrations exceed the World Health Organization (WHO) air quality guidelines (Pascal et al., 2013). Especially in cities numerous different particle sources can be found (Belis et al., 2013). Still, road traffic seems to have the greatest impact on particle concentrations in the urban roughness layer when the direct influence of industrial emissions is low (Morawska et al., 1999). Throughout the world air pollution dispersion modelling is an important tool in urban air quality

* Corresponding author. Department of Geography, Wüllnerstaße 5b, RWTH Aachen University, Germany.
E-mail address: bastian.paas@geo.rwth-aachen.de (B. Paas).

http://dx.doi.org/10.1016/j.atmosenv.2016.09.031
1352-2310/

regulation and planning. Models simulate the dispersion of air pollutants and are cost- and time-effective integrative options to field measurements. Furthermore, highly resolved information can be gathered in space and time rather than derived from point measurements that are only representative for the location where the measurements were taken (Broich et al., 2012). However, models have to be properly evaluated before their results can be used with confidence (Chang and Hanna, 2004). When model predictions are not reliable and accurate, misinterpretation of simulation results is likely. This is especially true when the physical processes on which the model physics rely are not thoroughly understood by the user. Decisions based on underestimated simulation results can yield implementations that are unhealthy for the population. Decisions based on overestimated model results can lead to excessive restrictions and evitable costs (Langner and Klemm, 2011).

In this study we compare the performance of two models, namely the dispersion model Austal2000 and the microclimate model ENVI-met. Both models are applicable for dispersion simulation at micro-scales and able to handle complex terrain. They are both freely available. ENVI-met is published under the creative common license for non-commercial use. The German reference dispersion model Austal2000 was developed by Janicke consulting engineers (Janicke consulting GbR, Überlingen, Germany) for the German Federal Environmental Agency (Umweltbundesamt). Austal2000 is a reference implementation of the specifications given in appendix 3 of the technical instructions on air quality control (TA Luft; BMU, 2002). ENVI-met was developed by M. Bruse (ENVI-met GmbH, Essen, Germany) as a holistic microclimate model and also features a module for dispersion simulation (Bruse and Fleer, 1998). ENVI-met has the distinction of being an easy-to-use tool with a graphical user interface and a user-friendly editor for users who do not necessarily need to understand the complex physics ENVI-met relies on to operate the model. Therefore, the model qualifies particularly for areas of application like architecture as well as urban and environmental planning. This study gives an overview of the performance of ENVI-met in comparison to Austal2000 by comparing data sets of four actual test cases focusing on the distribution of particles with an aerodynamic diameter (DAE) smaller than 10 μm (PM_{10}). The four test cases include investigations in two different areas under study i.e. two inner-city park areas as structural elements of typical mid-sized German cities. In each of the two study areas two test cases were set up with model runs initiated with either inflow boundary conditions (IBC) defined by meteorological observations from weather stations further away from the areas under study (1800–2500 m beeline) or IBCs defined by local measurements. A comparison is made between the predicted concentrations of each model using scatter plots. Simulation data is furthermore compared to measurements that were performed with an optical particle counter (OPC) using Q-Q plots as suggested by Chambers (1983) and Venkatram et al. (2001). As recommended in the literature (Patel and Kumar, 1998) and applied in recent air quality model performance studies (Langner and Klemm, 2011), additional performance measures were calculated to evaluate the capability of the two models compared to observations. Fractional bias (FB) is used as a performance measure that enables an assessment of discrepancy between the measurement-based and the simulation-based sample (Perry et al., 2005). Additionally, the robust highest concentration (RHC) is calculated as it reflects the high end of the concentration ranges (Hanna, 1988). The reason for that is that higher concentrations are usually of particular interest when it comes to air quality regulation and health-damaging exposure of pollutants.

2. The modelling software used

2.1. Austal2000

Austal2000 is based on the Lagrangian approach and is designed for long-term sources and continuous buoyant plumes. The model is capable of calculating the dispersion of multiple point, line and area sources of odorous substances and pollutants (e.g. SO_2, NO, NO_2, NH_3, PM) and includes dry deposition algorithms. In Germany, Austal2000 is widely used for short-range transport of particles and gases in both applied studies (Merbitz et al., 2012; Schiavon et al., 2015; Dias et al., 2016; Paas et al., 2016; Pepe et al., 2016) and in model performance research (Langner and Klemm, 2011; Letzel et al., 2012). As a steady-state Lagrangian dispersion model, Austal2000 simulates the dispersion of pollutants by utilizing a random walk process. Wind vectors determine the direction and velocity of dispersion. A Markov process is used to randomly vary the turbulence vector. The intensity of turbulence determines the variety of the random element. The aerosol concentration is calculated by quantifying the particle number in a given grid cell (Janicke, 2011). Meteorological input parameters (all from ground-based measurements) that have to be provided by the user are: wind direction (wd), wind speed (ws), roughness length (z_0), measurement height of the wind component measurements, and the stability classes according to Klug-Manier. The Klug-Manier classes represent the German standard stability classification for the atmosphere and are based on the Monin-Obukhov length theory. Klug-Manier classes are comparable to the Pasquill stability classes (Foken, 2008) that are widely-used in the United States (Mohan and Siddiqui, 1998). Provision of roughness length values by the user is not a requirement since Austal2000 is able to calculate z_0 for selected locations using an internal database. A prerequisite, however, is that the coordinates of the study location are known. For cases with obstacles (e.g. buildings) and complex terrain input data actuate the preceded and implemented model TALdia to calculate a wind field library. The software code as a standalone software without a graphical user interface as well as a detailed program documentation is freely available from the developer's webpage (Janicke, 2011). The Austal2000 simulations of PM_{10} distribution were performed with version 2.6.11. Georeferencing of CAD data was conducted using the ESRI software ArcGIS, version 10.2.2. Displaying of the results was realized using the OriginLab software Origin Pro, version 8.

2.2. ENVI-met

ENVI-met is a prognostic three-dimensional microclimate model that is designed to simulate the surface-plant-air interactions in urban environments with a typical resolution down to 0.5 m in space and 1–5 s in time (Bruse and Fleer, 1998). In the research community ENVI-met is widely used in the context of human bio-meteorology and thermal comfort studies (Ali-Toudert and Mayer, 2006; Ng et al., 2012; Ambrosini et al., 2014; Jänicke et al., 2015; Maras et al., 2016). However, the model also features a pollution dispersion module accordingly to simulate numerous point, line and area sources of substances, e.g. NO, NO_2, O_3 and PM which becomes more and more popular (Nikolova et al., 2011; Wania et al., 2012; Hofman and Samson, 2014; Morakinyo and Lam, 2016). It includes particle sedimentation depending on size and mass and deposition at surfaces. A simple upstream advection approach is used to calculate the pollutant dispersion. ENVI-met is based on a three-dimensional computational fluid dynamics (CFD) model. For each spatial grid cell and time step, the CFD model solves the Reynolds-averaged non-hydrostatic Navier-Stokes equations. Turbulence is calculated using the 1.5th order closure

κ-ε model. Two prognostic equations are used to solve the variables κ and ε which determine the kinetic energy in the turbulence and the turbulent dissipation respectively. In consequence, these two equations represent the turbulent properties of the flow (Jones and Launder, 1972). For initialization of meteorological input parameters, i.e. wd, ws (measured in 10 m agl), z_0, relative humidity (rh), air temperature (T_a), specific humidity (sh) and cloud coverage (optional) have to be provided by the user. For sh information from upper air soundings have to be used (values from 2500 m agl have to be provided) whereas all other parameters can be obtained from ground based measurements. The software package is split into both an expert version which is only accessible by the consulting company of the developer and a freely available basic version with limited features for non-commercial use published under the creative common license. The ENVI-met simulations of PM_{10} distribution were performed using the free version V4 Preview III. Georeferencing of CAD data was conducted using the ESRI software ArcGIS, version 10.2.2. Displaying and analyzing of the results were realized using the visualizing tool Leonardo which is part of the ENVI-met software package.

3. Experimental design

3.1. Areas under study

Two research sites were chosen for this study. They are located in the cities of Aachen and Münster respectively (see Fig. 1). Both research sites were characterized as inner-city park areas that are remote from industrial areas. The areas under study are featuring “complex terrain”. In this study “complex terrain” is referred to the complex urban geometry of street canyons and squares that are characterized by numerous obstacles like houses with varying height, varying ground levels as well as major traffic lines that cut through the green areas (see Fig. 2). Aachen and Münster are both representative mid-sized German cities with a population of around 250,000 inhabitants located in the West of Germany. However, they are characterized by different topographies. The research site in Aachen spans an area of around 180 m by 180 m, is surrounded by dense perimeter development and features three main traffic lines. The open space in the city of Münster is characterized by an area with wider extent compared to the research site in the city of Aachen with a dimension of 250 m by 350 m. Four main traffic lines are cutting though the area under study. The site contains two lakes. The bigger lake “Aasee” is situated to the west of the research site. A small lake named “Kanonengraben” is located in the southeast of the area under study. The green area is surrounded by isolated freestanding buildings.

3.2. Model domains

Referring to the best practice guidelines given by Franke et al. (2007) and the practical work of Vos et al. (2013) who performed ENVI-met pollutant dispersion simulations as well, for all simulations presented in this study, the computational domains have been chosen sufficiently large in order to keep the influence of the domain boundaries on the solution to a minimum. A distance of 8 H from the buildings that surround the research sites (park areas) to the computational domain boundaries (where H represents the building height) was kept. The computational domain of the area under study in Aachen was modeled as an area as large as 420 m by 420 m with a spatial resolution of 2 m in the case of Austal2000. For ENVI-met a core model domain with a horizontal extent of 250 m by 250 m with a spatial resolution of 2 m was set up. Additionally, 10 nesting grids were used as a surrounding with increasing grid size towards the boundaries of the domain to keep clear distance of 132 m to the core domain. An overall computational domain with a horizontal extent of 514 m by 514 m was used (see Fig. 1). In the area under study in Aachen the maximum building-height-to-street-width (aspect) ratio H/W is 1.5. The obstacles vary in height from 5 m to a maximum building height of 40 m whereas the maximum altitude difference of the terrain surface is 8 m. The computational area representing the research site in Münster was modeled as an area as large as 420 m by 420 m with a spatial resolution of 2 m in the case of Austal2000. For ENVI-met a domain with an extent in the X-Y-plane of 380 m by 256 m with a spatial resolution of 2 m was developed as the core model. In addition, 10 nesting grids were used as a surrounding with increasing grid size towards the boundaries of the computational domain to keep clear distance of 132 m to the core domain. An overall computational domain with an extent in X-Y-direction of 644 m by 520 m was used with ENVI-met for the Münster test cases (see Fig. 1). The maximum H/W in the area under investigation in Münster is 1.0. The obstacles vary in height from 1 m to a maximum building height of 19 m whereas the maximum altitude difference of the terrain surface is 8 m.

3.3. Emission input data

Emissions for all used test cases and simulation tools were calculated by multiplying emission factors (μg vehicle^{-1} m^{-1}) referring to the guidelines published by Keller and de Hahn (2004) and Lohmeyer et al. (2004) with prevailing traffic intensity (vehicles s^{-1}). The used emission factors included both the amount of combustion processes and blown up dust as well as tire and break abrasions. Traffic intensity was defined by averaged traffic counts including a separation of different vehicle classes (trucks > 7.5 t, busses, cars). Traffic counts were manually performed in parallel to the particle concentration measurements (see Sect. 3.5) individually for each trafficked street leading to the investigation areas (“Ursulinerstr.”, “Hartmannstr.”, “Friedrich-Wilhelm-Platz” in Aachen; “Weselerstr.”, “Aegidistr.”, “Adenauerallee”, “Bismarck-allee” in Münster). The traffic data were averaged over 1 h periods. In principle, traffic emissions are represented as line sources. In order to account for a more realistic spatial positioning, the sources are spread out over the entire width of the traffic lanes. Emissions were implemented as area sources in 0.5 m agl in both models. For the calculations conducted with Austal2000 for each simulation run one billion particles were emitted in the computational domain.

3.4. Meteorological input data

Meteorological input parameters are required as inflow boundary conditions that actuate the dispersion models (see 2.1 & 2.2). For two test cases time-series data (1-h averages) from continuously operated weather stations were used as input parameters. The weather stations were located in suburban areas of Aachen and Münster. For one test case in Aachen entry criteria for the modelling tools were set with meteorological data from the permanent weather station “Aachen-Hörn” (6° 03′ 40″ E, 50° 46′ 44″ N), located 1800 m away from the area under study in the city center of Aachen. The wind sensor to determine wd and ws (Wind Monitor 05103, R.M. Young Company, Traverse City, Michigan, USA) was installed on top of a roof (6.5 m above the rooftop) in 29 m agl. The shielded temperature and humidity sensor (CS215, Campbell Scientific, Inc., Logan, Utah, USA) was mounted on a mast in 2 m agl (Schneider and Ketzler, 2016). Input data for one test case in Münster were obtained from the climatology working group of the University of Münster which operates the permanent weather station “ILÖK” 2100 m away from the investigation area (7° 35′ 45″

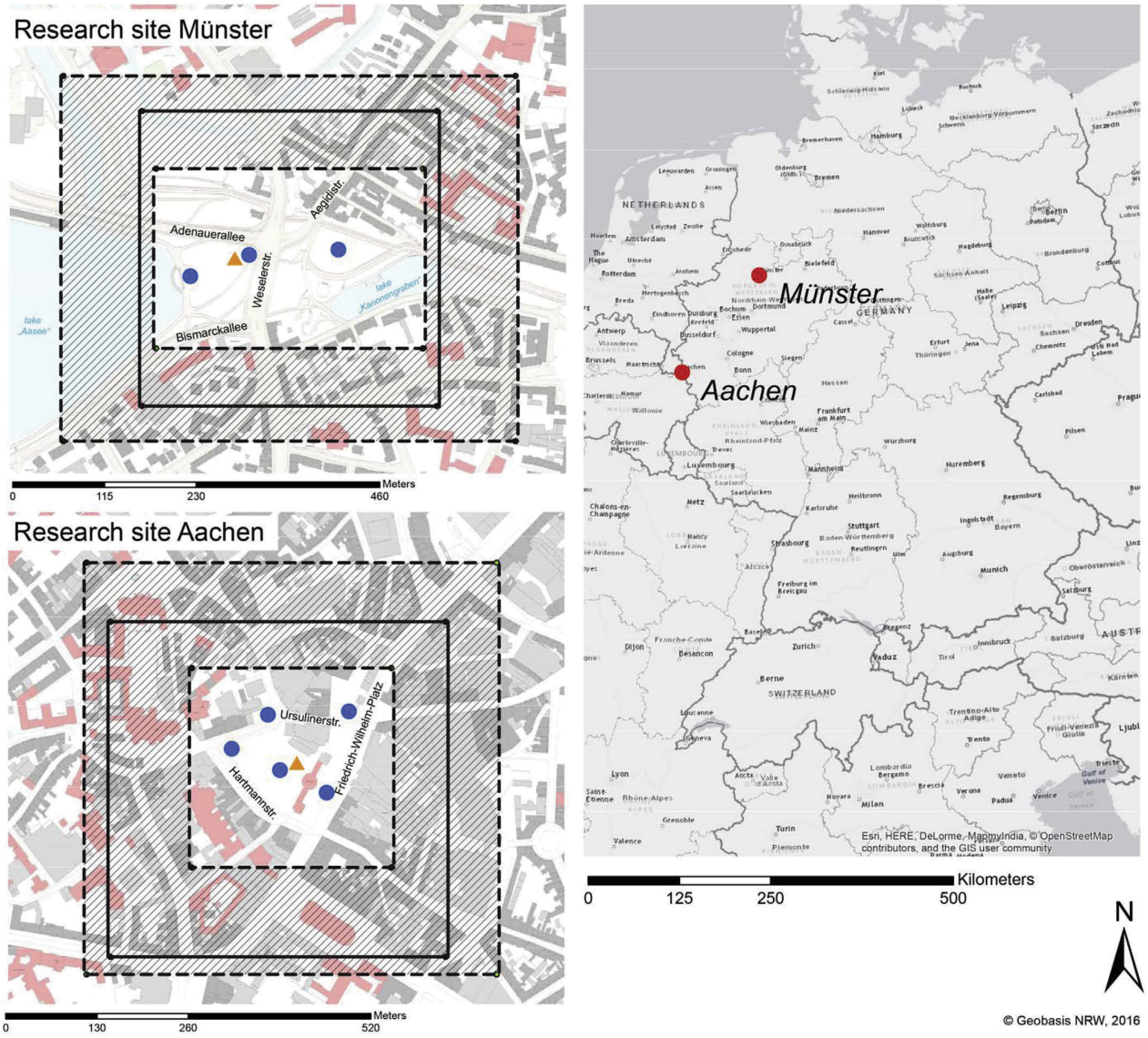

Fig. 1. The location of the two areas under study in Germany (right) with close-ups of the research sites in Münster (upper left illustration) and in Aachen (lower left illustration) including the receptor points where measurements of PM concentrations were carried out (blue dots), the measurement locations where meteorological input data for both models were taken (orange triangles) and markings of the computational domain sizes of the two models used (black continuous frame: Austal2000; black dashed frames: ENVI-met with the hatched area representing the nesting grid area). (For interpretation of the references to colour in this figure legend, the reader is referred to the web version of this article.)

E, 51° 58′ 9″ N). Sensors to determine wd and ws (WindSonic Anemometer RS-232, Gill Instruments Limited, Lymington, Hampshire, UK) as well as the shielded temperature and humidity sensor (41382VC, R.M. Young Company, Traverse City, Michigan, USA) were mounted on a permanent mast on top of a roof (10 m above the rooftop) in 34 m agl. Time-series data (1-h averages) of local meteorological measurements that were performed inside the research sites in Aachen and Münster were used for the initialization of two further test cases. For these cases high frequency measurements of the wind vector were carried out in the middle of the research sites (see Fig. 1) with a three-dimensional sonic anemometer (USA-1, METEK Meteorologische Messtechnik GmbH, Elmshorn, Germany). In Aachen the anemometer was mounted on top of a street lamp in 3.4 m agl. During the field campaign in Münster the anemometer was mounted on top of a tripod in 2.67 m agl. However, concerning wind data, ENVI-met requires information from 10 m agl (see Sect. 2.2). Accordingly, ws was recalculated where needed by extrapolating anemometer data to 10 m agl, assuming a logarithmic wind profile under neutral stratification (z_0 = 0.8; Kármán's constant = 0.4). Measurements of rh and T_a took place with a shielded resistance probe (41382VC, R.M. Young Company, Traverse City, Michigan, USA) in 2 m agl, using the same mounting location as the anemometer. Austal2000 requires input concerning the stratification of the atmosphere (see Sect. 2.1). Klug-Manier stability classes were calculated using wind speed data (10 m agl) and information on cloud cover according to the guideline given in the technical instructions on air quality control (TA Luft; BMU, 1986).

Fig. 2. Photographs of the areas under study showing the street canyon situations in Aachen (a)) and Münster (b)) as well as the inner green area characteristics in Aachen (c)) and Münster (d)).

3.5. Particle concentration measurements

Local aerosol measurements were carried out using a single OPC (Model EDM 107G, Grimm GmbH, Ainring, Germany) to determine mass concentration of suspended particles. The OPC integrates the approaches of light scattering technology with single particle counting. The frequency of scattered light pulse signals translates into the number of contained particles of the air sample. The scattering intensities are used to detect the particle sizes. Particles are classified into a size distribution in a range between 0.25 and 32 μm DAE containing 31 different size channels. Internally, the particle number size distribution is converted into mass concentrations for an indicated time interval. The sensor operates at a volumetric flow rate of 1.2 L min^{-1} and a time resolution of 6 s (Grimm and Eatough, 2009). Particles were sampled at the mean respiratory height of 1.6 m agl and stored as 1-h arithmetic means of mass concentrations with a DAE between 0.25 μm and 10 μm ($PM_{(0.25;10)}$). The sensor used had been factory calibrated on a regular basis (VDE standard 0701-0702) within the calibration validity period and was calibrated last on 13/01/2015. Prior to calibration, the latest inspection showed a deviation of −0.6 μg m^{-3} (−4.2%) for $PM_{(0.25;10)}$ of the OPC to the factory's reference unit 107 S/N.

Five evenly distributed receptor points were selected inside the area under study in Aachen, where measurements with the OPC were carried out (see Fig. 1). In Aachen, data were collected as one-day time series during overall 9 selected days. In February 2014 measurements were carried out at all five receptor points; each day at a different receptor point. In July 2014 measurements took place at four receptor points; each day at a different measurement location resulting in a sample of 46 data points of full-hour averages in total from both measurement campaigns in Aachen. Three evenly distributed receptor points were selected inside the research site in Münster (see Fig. 1). Particle concentration measurements in Münster were carried out as one-day time series during overall six selected days. During February 2015 data were collected at all three measurement locations, each day at a different receptor point. Throughout three selected days in July and August 2015 particle measurements were repeated analogously to the winter campaign. The overall sample consists of 33 full-hour averages from both measurement campaigns in Münster. The general weather situations for the measurement campaigns were chosen to be equal for both periods, including radiation weather conditions with only partly clouded skies and no precipitation. The inflow and prevailing wind during the field experiments varied. Data collection in all cases took place between 10:00 h and 17:00 h local time on weekdays to avoid the typical peaks during early morning and evening rush hours. Always before being compared to simulation results, measurement raw data of $PM_{(0.25;10)}$ (1-h averages) were further processed. The background concentration (PM_{10}; 1-h averages) was deducted from raw particle measurement data obtained from the OPC using measurement data from government air quality sites Aachen-Burtscheid (AABU) and Münster-Geist (MSGE), operated by the North Rhine-Westphalian State Office for Nature, Environment, and Consumer Protection (LANUV). It is known that calculations with particle measurement data from different sensor types i.e. the OPC used and different sensors operated at the government sites (AABU: Nephelometer; MSGE: Tapered-element oscillating microbalance) should be treated with caution and deterioration might be accepted when it comes to data quality (Wiedensohler et al., 2012). However, data of the used OPC seemed to be in line with compared measurement data from the government site AABU, showing good agreement and only a slight overestimation (Paas et al., 2016). Hereinafter, only adjusted particle measurement data is shown where background concentration was subtracted from raw $PM_{(0.25;10)}$ measurement values.

3.6. Test cases

Overall, four test cases were set up for this study. Two test cases were set up with the same model domain and emission input for the research site in the city of Aachen. Two test cases were set up equally for the research site in the city of Münster. All simulations were performed analogously to the periods of particle concentration measurements (see Sect. 3.5). Only the meteorological IBCs varied among the different test cases for each research site. For the first test case of the research site in the city of Aachen meteorological data from the distant weather station “Aachen-Hörn” initiated the model runs (test case AA1). In this case the wind was predominantly coming from southwest (see Fig. 3), with wind speeds between 4 m s^{-1} and 7 m s^{-1} being most common (in 10 m agl). Local measurement data with wind mainly from south and predominant wind speeds between 1 m s^{-1} and 3 m s^{-1} (in 10 m

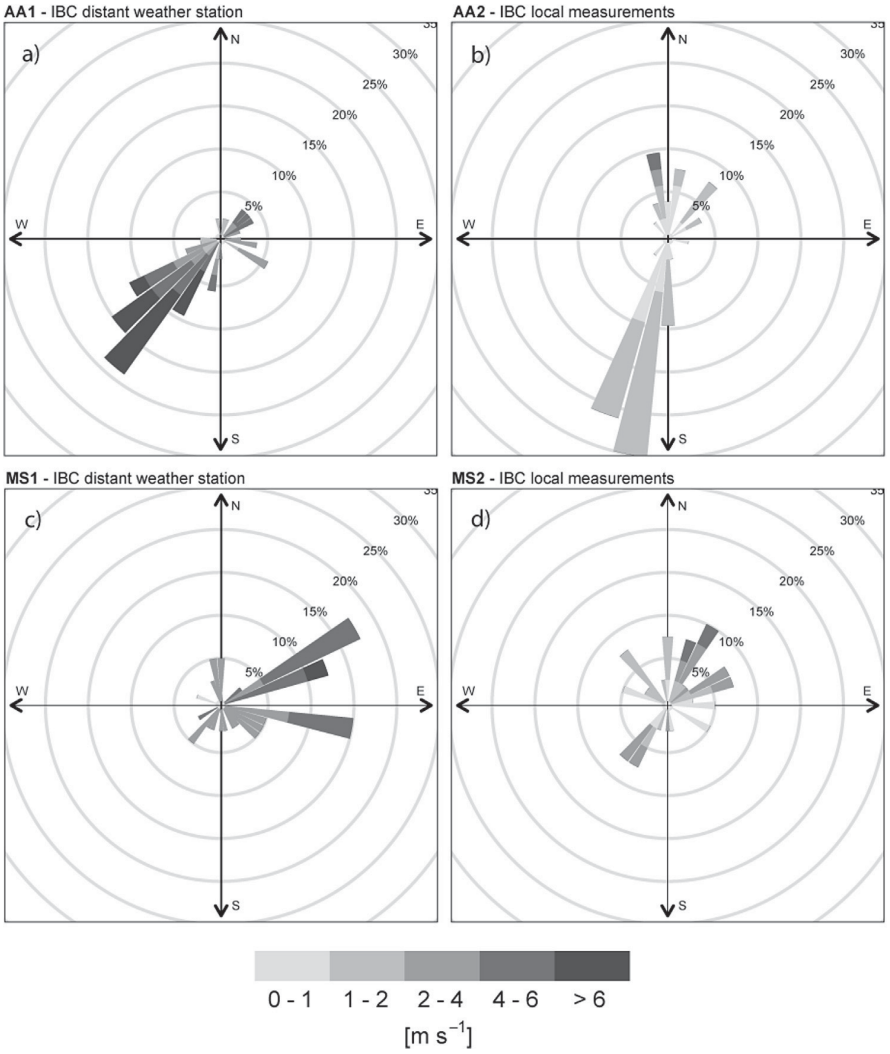

Fig. 3. Wind rose plot showing wind vector measurement data (normalized, 10 m agl) during the investigation periods for a) the Aachen-testcase AA1, b) the Aachen-testcase AA2, c) the Münster-testcase MS1 and d) the Münster-testcase MS2.

Table 1
Summary of the four test cases that were conducted in this study.

Emitted substance	City	General setting	Study periods	IBC data	Test case
PM_{10}	Aachen	Inner city park area, complex terrain, varying ground surface, dense perimeter development, 3 area sources (traffic lines)	9 selected weekdays in February, July 2014	Distant weather station "Aachen-Hörn"	AA1
				Local measurements in the area under study	AA2
	Münster	Inner city park area, open space, varying ground surface, surface water, isolated freestanding buildings, 4 area sources (traffic lines)	6 selected weekdays in February, July, August 2015	Distant weather station "ILÖK"	MS1
				Local measurements in the area under study	MS2

agl) were used as IBCs for the second test case of the research site in the city of Aachen (test case AA2). For the first test case of the research site in the city of Münster meteorological data from the distant weather station "ILÖK" initiated the model runs (test case MS1). In this case the wind was predominantly coming from easterly directions, with an average wind speed of 4 m s^{-1} during the period of investigation. Local measurement data with varying wind directions but mostly coming from northeast and wind speeds between 2 m s^{-1} and 5 m s^{-1} being most common (10 m agl) were used as IBCs for the second test case of the research site in the city of Münster (test case MS2). A short summary of the four different test cases is given in Table 1.

4. Methods of performance analysis

Data sets of both models are inter-compared by utilizing scatter plot diagrams to find out if and how well ENVI-met predicts PM_{10} concentration close to the German reference model Austal2000. Furthermore, predicted values of each model are compared to observations. Quantile-quantile (Q-Q) plots are useful visualization tools for the assessment of concentration distributions (Chambers, 1983) and are especially recommended for the evaluation of regulatory models (Venkatram et al., 2001). Q-Q plots are created by ranking the simulated and measured concentrations and then pairing them by rank. Perfect rank correlation results in a plot with data points forming a 1:1 line. A good model will produce results in this plot similar to the slope of this line. The upper end of ground-level concentrations of pollutants is of particular concern in air quality regulation and urban planning (Cox and Tikvart, 1990). Again, good model predictions concerning the important high end concentrations will result in Q-Q plots, where in the upper concentration end the data points are close to the 1:1 line (Perry et al., 2005).

Merely comparing measurement data to simulation results side by side does not necessarily provide an entire assessment of which model best represents actual measured pollutant concentrations. Therefore, it is necessary to analyze model data by utilizing additional "performance measures to determine whether one model is significantly better than another" (Patel and Kumar, 1998).

The FB can be used as the fundamental measure of discrepancy between the measurement-based and simulation-based sample (Cox and Tikvart, 1990). The FB is a dimensionless and normalized measure which varies between −2 and +2 for extreme over- or under-prediction of the model. The value of zero represents a perfect model. The formula is given by Hanna, 1988 (Eq. (1))

$$FB = \frac{2\left(\overline{C}_O - \overline{C}_p\right)}{\left(\overline{C}_O + \overline{C}_p\right)} \tag{1}$$

where C_O and C_p are the observed and predicted concentrations respectively.

Due to the highlighted importance of the upper end of concentrations, this study uses the RHC as an additional indicator that refers to the peak concentrations of air pollutants. The RHC was chosen as a preferred statistic over actual maxima because it mitigates the undesirable influence of unusual events in virtue of a smoothed estimate of the high-end concentrations. A good model will provide RHCs of predicted data close to RHCs calculated from observation data. The formula is given by Perry et al., 2005 (Eq. (2))

$$RHC = x^{\{n\}} + \left(x - x^{\{n\}}\right)\ln\left(\frac{3n-1}{2}\right) \tag{2}$$

where n is the number of values used to characterize the upper end of the concentration distribution, x is the average of the $n-1$ largest concentration values, and $x^{\{n\}}$ is the nth largest concentration value. Cox and Tikvart (1990) suggest selecting $n = 26$ but mention that it can be lower in cases where the sample is not adequate (with fewer concentrations exceeding the threshold value where the threshold value is defined as a concentration near background) but

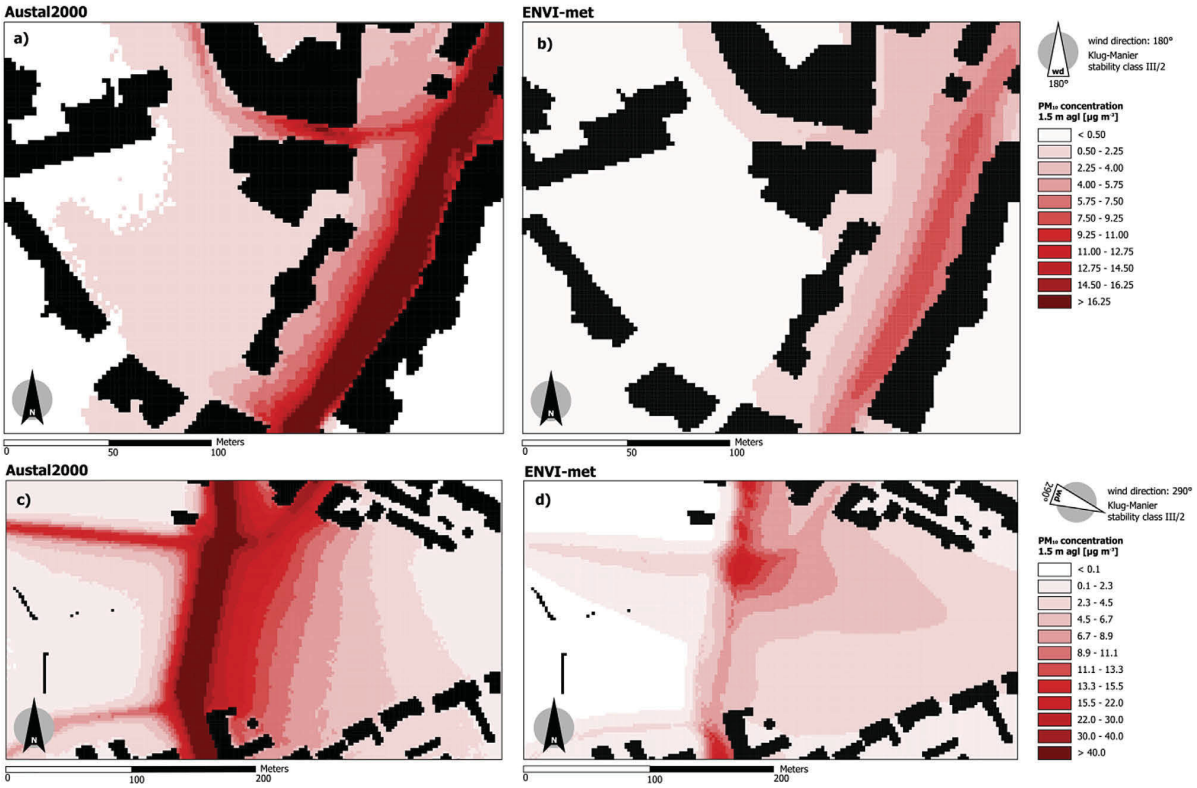

Fig. 4. Predicted traffic-induced PM_{10} concentration distribution of selected situations in 1.5 m agl of (a) Austal2000 and (b) ENVI-met for the Aachen test case (AA2) with inflow boundary conditions (IBC) defined by local meteorological measurements (1-h average; prevailing wind direction = 180°; Klug-Manier stability class III/2) and of (c) Austal2000 and (d) ENVI-met for the Münster test case (MS2) with inflow boundary conditions (IBC) defined by local meteorological measurements (1-h average; prevailing wind direction = 290°; Klug-Manier stability class III/2).

with $n > 3$ at the minimum. We used $n = 16$ in the Aachen test case samples (AA1, AA2) and $n = 10$ in the Münster test case samples (MS1, MS2) of this study representing in each test case the fraction of measurement values exceeding the annual mean value of the PM_{10} background concentration in the city of Aachen (15 μg m^{-3}) and Münster (19 μg m^{-3}), respectively (LANUV, 2015). All calculations were based on 1-h averages since the 1-h averaging time is recommended as the basic element for evaluation (Fox, 1981). Data processing took place with the R software package using version 3.0.2.

5. Results

The overall dispersion results show similarities to some degree in both models. Fig. 4 shows 1-h averages of Austal2000 and ENVI-met PM_{10} predictions of depicted model runs which were initiated with local measurement data for the Aachen test case AA2.

The highest PM_{10} concentrations were predicted for locations in close vicinity to traffic lines particularly at the main road "Friedrich-Wilhelm-Platz" (cf. Fig. 1). Corresponding simulated PM_{10} concentrations seem to decline rapidly further from the traffic lines in both models. Input data of the wind vector are the key meteorological driver for the used models and make for higher PM_{10} concentrations in the north of the model area of the test case AA2. Under IBCs with winds from the south, Austal2000 predicted a situation where particles tend to accumulate in e.g. the narrow alleyway ("Ursulinerstr.") as well as in areas downwind from emission sources where particles get dammed up at obstacles. In comparison, ENVI-met results unveil more smoothly dispersed PM_{10} concentrations which are rapidly declining further from the sources. Dispersion results of both models calculated for the MS2 test case where urban obstacles are present to a lesser extent show a more even distribution of the PM_{10} concentration. Particles seem to be transported with the wind away from the traffic lines in both models. The distribution appears to be furthermore influenced by the ground surface structure especially in the east of the model areas for the MS2 test case. However, the two models calculated different spatial distributions of PM_{10} concentrations east of the

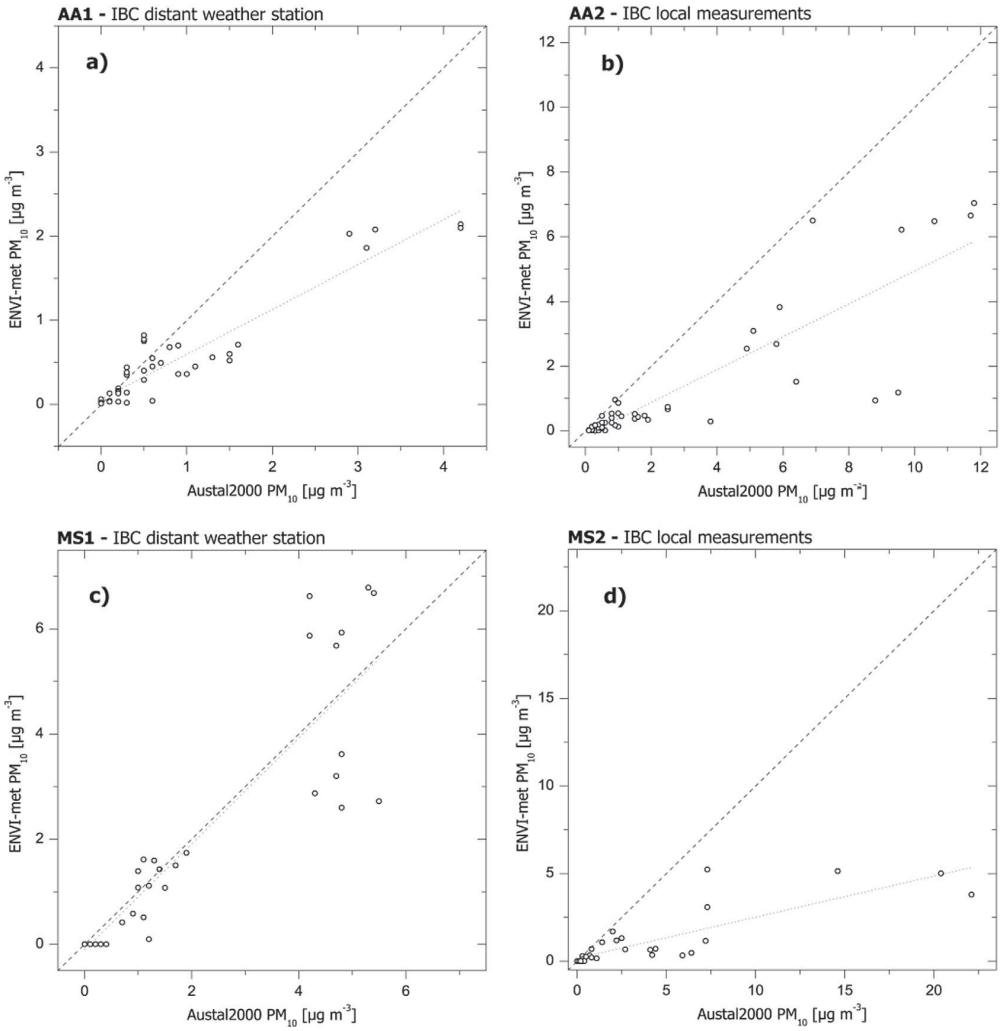

Fig. 5. Scatter plot for predicted PM_{10} concentrations of all the receptor points of (a) the AA1 test case (IBC: data from the distant weather station; R^2: 0.75; slope: 0.51), the AA2 test case (IBC: data from local measurements; R2: 0.89; slope: 0.53), the MS1 test case (IBC: data from the distant weather station; R^2: 0.79; slope: 1.01) and the MS2 test case (IBC: data from local measurements; R2: 0.89; slope: 0.53). The dashed line illustrates a 1:1 reproduction of ENVI-met predictions over Austal2000. The dotted line represents the linear regression of the samples.

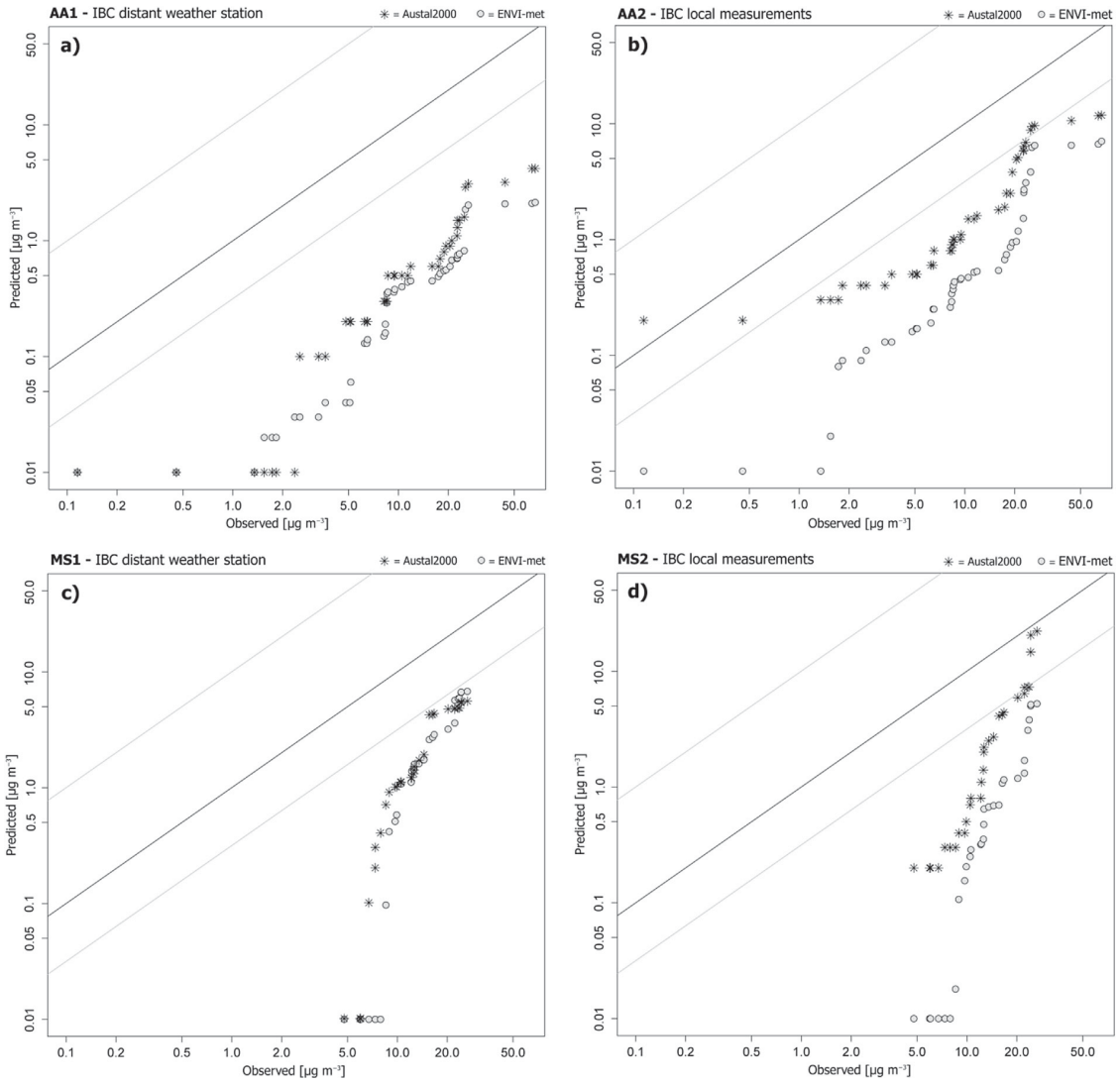

Fig. 6. Q-Q plot for predicted PM_{10} concentrations of all the receptor points of (a) the AA1 test case (IBC: data from the distant weather station), of (b) the AA2 test case (IBC: data from local measurements), of (c) the MS1 test case (IBC: data from the distant weather station) and of (d) the MS2 test case (IBC: data from local measurements) as 1-hr averages. Black stars represent predicted PM_{10} concentrations of Austal2000. Grey circles show predicted PM_{10} concentration of ENVI-met. The black line indicates the 1:1 rank correlation of the distributions. The grey lines depict the factor of two over and under estimates.

"Weselerstr.". Compared to Austal2000 the predicted PM_{10} concentrations of ENVI-met are mostly two times lower throughout the whole areas under study in both test cases.

The direct comparison of ENVI-met predictions over Austal2000 simulation results at the receptor points adds to the picture (see Fig. 5). Although PM_{10} concentration values of ENVI-met show a very good agreement to Austal2000 results in all test cases (R^2: 0.68–0.89), the slopes of the linear regression lines (AA1: 0.53, AA2: 0.51, MS1: 1.01, MS2: 0.23) indicate an underestimation of predicted PM_{10} concentrations by the factor of two on average in the case of ENVI-met in comparison to Austal2000.

Q-Q plots for all four test cases using all measurement data of all receptor points are presented in Fig. 6. Both models almost constantly underpredicted the observed $PM_{(0.25;10)}$ concentrations. Corresponding to the findings in Fig. 5 this is especially true for ENVI-met simulation results. ENVI-met even undercuts the predicted PM_{10} concentrations of Austal2000 almost always and in particular in the low concentration range.

Concerning test case AA1 that contains simulations that were initiated with data from the distant weather station both models strongly underpredicted observations. Under IBCs defined by local measurements (AA2) both models gained precision. Austal2000 still underpredicted measurement data; however, the model only underpredicted observations by the factor of around two in the entire range of concentrations. Initiated with local measurement data in test case AA2, ENVI-met produced somewhat better simulation results as well and especially in the mid and high-end concentration ranges. In the upper concentration range ENVI-met results are closer to the simulation results of Austal2000. However, predicted concentrations of ENVI-met fell apart in the lower concentration range, where the underprediction is several times higher in comparison to Austal2000. Comparing the Q-Q plots of test cases

Table 2
FB for all four test cases segregated in atmospheric stability classes after Klug-Manier.

Atmospheric stability (Klug-Manier)	AA1		AA2		MS1		MS2	
	Austal 2000	ENVI-met	Austal 2000	ENVI-met	Austal 2000	ENVI-met	Austal 2000	ENVI-met
III/1 (neutral)	1.58	1.75	–	–	1.32	1.20	0.58	1.62
III/2 (neutral)	1.85	1.90	0.91	1.28	1.56	1.46	0.98	1.64
IV (unstable)	1.93	1.95	–	–	1.17	1.45	1.16	1.38
V (very unstable)	–	–	1.68	1.93	1.42	1.55	1.47	1.86
Total	1.81	1.88	1.41	1.71	1.44	1.46	1.12	1.71

MS1 and MS2 it becomes obvious that the distinction between the results of the two test cases is less clear. For test case MS1 where the models were operated with IBCs from the distant weather station "ILÖK" results of both models are comparable in the entire concentration range. In the upper concentration range both models calculated lower concentrations of PM_{10} in comparison to measurement data with a factor of around two underprediction. Their calculations for lower concentrations differ seriously from the measurement values with underprediction by several orders of magnitude. Under IBCs defined by local measurements (MS2) only Austal2000 reached results closer to observations. While overall still underpredicting, Austal2000 calculated values very close to measurement data.

Looking at the FBs given in Table 2, ENVI-met, over the entire investigation period in all test cases, strongly underpredicted the actual $PM_{(0.25;10)}$ concentration (FB: 1.46–1.88). Austal2000's underprediction was overall less strong with FBs between 1.12 and 1.81. Both models performed better under neutral stratification conditions of the atmosphere (Klug-Manier stability classes III/1 and III/2) most of the time. When initiated with local meteorological input data (test case MS2) a best FB value of 0.58 in the case of Austal2000 was calculated for neutral stratification of the atmosphere (Klug-Manier stability class III/1). ENVI-met performed best in the test case MS1 for the Klug-Manier stability class III/1 with a calculated FB of 1.20. The comparison of the FBs of both the Aachen and Münster test cases emphasizes that i.e. Austal2000 gained precision by using IBCs as model input parameters from local meteorological measurements. That counts for ENVI-met in the Aachen test cases as well, whereas in the Münster test cases the calculated FBs are even higher for the MS2 test case when ENVI-met was initiated with local measurement data.

The analysis of the calculated RHCs (Table 3) confirms the former findings for the high-end concentration range as well. Both models continued to underpredict the observed concentrations over the entire study period. RHCs for measurement data were calculated to be 73.6 μg m^{-3} for the Aachen test cases (AA1, AA2) and 33.1 μg m^{-3} for the Münster test cases (MS1, MS2), respectively. For observations the standard deviations of the highest concentration values (SD_{HC}) representing the same sample size of the RHCs (see Sect. 4) are ±25.6 μg m^{-3} for the Aachen test cases (AA1, AA2) and ±2.8 μg m^{-3} for the Münster test cases (MS1, MS2). In particular during the AA1 test case the RHC that was calculated from observations was seriously underpredicted by both models (Austal2000 RHC: 4.8 μg m^{-3}; ENVI-met RHC: 2.5 μg m^{-3}).

When considering RHCs it becomes evident that both models produced results closer to observations during the Münster test cases with underprediction of both models to a lesser extent. In particular Austal2000 simulated results in the important high-end concentration range with a RHC of 21.4 μg m^{-3} (SD_{HC}: ±6.7 μg m^{-3}) very close to the RHC derived from observations.

Table 3
RHC and SD_{HC} (in brackets) in μg m^{-3} of observed and predicted PM_{10} concentrations for all four test cases.

	AA1	AA2	MS1	MS2
Observed	73.6 (±25.8)		33.1 (±2.8)	
Austal2000	4.8 (±1.2)	18.0 (±3.2)	6.1 (±0.4)	21.4 (±6.7)
ENVI-met	2.5 (±0.7)	9.3 (±2.5)	9.5 (±1.6)	5.2 (±1.7)

6. Discussion

The evaluation of pollutant dispersion model performance is of broad relevance since dispersion models are used intensively for both scientific applications, to better understand the spatial distribution of e.g. pollutants like PM in the atmosphere, as well as for urban air quality regulation and planning. This is especially true for the models Austal2000 and ENVI-met who are both freely available. However, up to now ENVI-met results of pollutant dispersion were exclusively compared to observations in a study concerning ultrafine particles (Nikolova et al., 2011) or in research using the approach of biomagnetic monitoring with the help of the total deposited mass of PM (Hofman and Samson, 2014). Until recently, ENVI-met has never been compared to a different model under similar inflow boundary conditions regarding the dispersion of ground level airborne particles. Austal2000's performance regarding the distribution of pollutants in complex terrain was exclusively evaluated in studies concerning NO_X or benzene (Schiavon et al., 2015). When considering PM the performance was assessed in research conducted with meso-scale computational domains that were not able to resolve complex urban areas at the spatial resolution of individual street canyons (Dias et al., 2016; Pepe et al., 2016). The results of this study provide model users of both the scientific community and users of applied studies advice what level of performance can be expected under different initial conditions from the simulation tools ENVI-met and Austal2000 in real-world applications. The outcomes refer to investigations of the atmospheric composition concerning PM_{10} on the micro-scale with the help of performance measures as recommended in the literature. Still, the results of the given test cases lack numerous aspects of real-world conditions. The findings of this study fall short in statements regarding e.g. the simulation of PM_{10} distribution during night-time (including periods of e.g. low turbulence characteristics), the prediction of PM_{10} dispersion in highly polluted areas (considering higher emission rates e.g. during rush hours) or the distribution of other pollutants like SO_2, NO, NO_2 or NH_3. Both models Austal2000 and ENVI-met underpredicted observed PM_{10} concentrations in all test cases and especially in the low end concentration range. Schiavon et al. (2015) found a tendency of underprediction (35% in comparison to observations) using Austal2000 as well, though related to the annual mean concentration of NO_X. However, before judging the performance of a model it has to be taken into account that in any case individual model prediction certainly differs from corresponding observation data because simulation tools cannot include all the variables that affect observations at a specific time and location (Venkatram, 2008). Numerous sources of error are included in pollutant dispersion modelling in general. Observation data for instance include

background concentration from long distance transport. Simulation results feature only the increase of concentrations as a function of local source emissions (Langner and Klemm, 2011). However, uncertainty might be also accepted when it comes to modelling of particle sources since it can be challenging to obtain correct emission rates of an area source (Faulkner et al., 2007). In this study, dynamic processes of the modeled area sources i.e. traffic flows were simplified with emission rates that were calculated only by taking averaged traffic volumes and emission factors into account (see Sect. 3.3). Furthermore, not all processes that effect the microscale dispersion of particles can be flawlessly included into the used models. Sources of error could be the neglecting of e.g. the influence of obstacles like trees or shrubs on the wind- and turbulence field (Gromke and Blocken, 2015), the deposition effect of vegetation elements on local airborne particles (Hofman and Samson, 2014) or the local release of particles out of undefined sources. The Aachen test cases showed predictions of both models with an overall wider variation from observations in comparison to the calculations of the Münster test cases. It seems possible that local diffuse particle sources contributed to measurement data due to particle release of dried-out grass and unsurfaced footpaths (Birmili et al., 2013; Paas et al., 2016). Therefore, in the test cases AA1 and AA2, particle measurement data were still biased and overrated after processing (deduction of background concentration) and not only influenced by motor traffic. Beyond, air quality modelers have not yet agreed upon the magnitude of standards for judging model performance (Yassin, 2013). Chang and Hanna (2004) suggested considering a model as acceptable if most of its predictions are within a factor of two of the observations. Furthermore, performance tested under similar initial conditions alone is barely sufficient to judge the overall capability of a model. ENVI-met rather than Austal2000 is e.g. able to integrate vegetation elements (shrubs or trees) into the dispersion calculations (Wania et al., 2012; Morakinyo and Lam, 2016). This feature could come in handy for urban planners and landscape architects who are aiming at studies concerning the effects of vegetation as design elements in urban environments on airborne pollutants like PM.

Under all of the tested conditions the comparison of model predictions to observations shows that both models gained accuracy when the simulation runs were initiated with IBCs of local atmospheric measurements except for ENVI-met in the test case MS2. With locally measured wind speeds two times lower in comparison to measurement data of the distant weather station (cf. Fig. 3), higher predicted PM_{10} concentration are to be expected, since the wind vector is the key driver as an initial condition of the dispersion models used. Dilution of pollutants i.e. the horizontal air mass exchange is reduced during conditions with lower horizontal wind speeds. The coherence between reduced wind speed and concentration increase of pollutants was confirmed by Gromke et al., 2008 and Wania et al., 2012 by conducting wind tunnel experiments and CFD simulations. It can be stated that the slight change in wind direction due to missing or different urban obstacles in IBC data derived from the database of the distant weather station had an impact on the inferior predictions of test cases AA1 and MS1 as well. Perry et al. (2005) verified that uncertainty in wind direction alone may cause disappointing results from what otherwise may be well-performing dispersion models. Further improvements of overall predictions could be obtained with the help of inflow boundary conditions derived from different wind field models i.e. MISKAM in the case of Austal2000 as confirmed by Letzel et al. (2012). The calculated FBs emphasize that both models strongly underpredicted the observed $PM_{(0.25;\ 10)}$ concentrations. The overall best performance is reached by Austal2000 in test case MS2 with a total FB of 1.12. As opposed to this, Dias et al. (2016) found Austal2000 to agree well with observations in their study with an overall FB of −0.04. However, it becomes apparent that both models gained precision when predicting PM_{10} concentration under neutral stratification regimes of the atmosphere (cf. Table 2). Results of both models show most of the time poor performance under unstable and very unstable stratification regimes (Klug-Manier stability classes IV and V) in all test cases (FB: 1.16–1.95). It seems possible that both models had difficulties to calculate an accurate mixing of the atmosphere under unstable und very unstable conditions with possibly an over estimation of the dilution rate regarding PM_{10} concentrations. On the contrary, Pepe et al., 2016 derived good results with Austal2000 simulating NO_X concentrations during daytime under increasing height of the mixing layer. It turned out that ENVI-met overall performed inferior to Austal2000 when it comes to predictions of traffic-induced near-surface concentrations of PM_{10}. Presumably as a result of the Lagrangian method, where particles follow trajectories of the wind vector, the dispersion simulation results of Austal2000 seem to be more sophisticated especially when the environment of the computational domain is more complex. An attempt to explain the poor performance of ENVI-met is that the model bases on a simpler Eularian approach that does not mimic the random walk of particles.

7. Conclusions and outlook

In this study a performance analysis with the help of different statistical performance measures of the dispersion models Austal2000 and ENVI-met on the basis of four real-world particulate matter test cases is presented. Results highlight that both models considerably underpredicted observed $PM_{(0.25;10)}$ concentrations for all test cases. Overall, the performance of both models can be rated as nearly acceptable only under specific circumstances. The analysis of all datasets shows that predictions of both simulation tools were closer to field observations in the high-end concentration range that is important for regulatory purposes. It turned out that both models had difficulties to calculate accurate predictions under unstable and very unstable atmospheric stability classes. Predictions of simulation runs of both models that were initiated with in-situ data of local atmospheric measurements lead to results closer to observation data (except for ENVI-met in the Münster test cases). In test case MS2 Austal2000 achieved the overall best results with an underprediction of the RHC of about 30% in comparison to observed $PM_{(0.25;10)}$ concentrations and a total FB of 1.12. Given the specific conditions and scope of the investigation, a model user has to evaluate whether he/she can obtain preferably meteorological data of local measurements close to or inside the area under study as input parameters to operate the dispersion models Austal2000 or ENVI-met successfully with best possible results.

In almost all of the test cases, Austal2000's predictions are closer to field observations than those of ENVI-met. The spatial analysis emphasizes that the distribution simulation of Austal2000 is more sophisticated especially but not limited to cases with complex terrain. In this study Austal2000 performed the task of dispersion simulation of traffic induced PM_{10} emissions in complex terrain reasonably well when initiated with IBCs out of local meteorological measurements with the tendency of underprediction. ENVI-met underestimated data of particle measurements more intensively in comparison to Austal2000 almost always and over the entire concentration range. Overall, the simulation results of ENVI-met undercut predicted PM_{10} concentration of Austal2000 by the factor of around two. Generally speaking, this analysis indicates that Austal2000 is the stronger model compared with ENVI-met considering the distribution of PM_{10} in complex and urban terrain.

Dispersion modelling is a valuable tool for air quality regulators and planners and delivers spatial predictions of environmental

impacts in the atmosphere. This is especially true in the case of the modelling tools Austal2000 and ENVI-met which are both freely available. However, output data of Austal2000 and in particular of ENVI-met must, as in any other case of predictive models, be interpreted with caution and should wherever possible be backed up with at least a minimal amount of observational data.

Acknowledgements

This study has been carried out within the project Urban Future Outline (UFO) as part of the interdisciplinary Project House HumTec (Human Technology Center) at RWTH Aachen University funded by the Excellence Initiative of the German federal and state governments. We thank O. Klemm from the University of Münster for providing measurement data of the weather station „ILÖK“ and S. Wilhelm from the North Rhine-Westphalian State Office for Nature, Environment, and Consumer Protection for providing PM_{10} measurement data of the government air quality network. This study would not have been possible without the data. We thank all students who helped enthusiastically with field experiments and traffic counts. We acknowledge D. Both for language editing of the manuscript. We would like to thank the scientific editor and two anonymous reviewers for very helpful comments on this manuscript.

References

Ali-Toudert, F., Mayer, H., 2006. Numerical study on the effects of aspect ratio and orientation of an urban street canyon on outdoor thermal comfort in hot and dry climate. Build. Environ. 41, 94–108. http://dx.doi.org/10.1016/j.buildenv.2005.01.013.

Ambrosini, D., Galli, G., Mancini, B., Nardi, I., Sfarra, S., 2014. Evaluating mitigation effects of urban heat Islands in a historical small center with the ENVI-met® climate model. Sustainability 6, 7013–7029. http://dx.doi.org/10.3390/su6107013.

Belis, C.A., Karagulian, F., Larsen, B.R., Hopke, P.K., 2013. Critical review and meta-analysis of ambient particulate matter source apportionment using receptor models in Europe. Atmos. Environ. 69, 94–108. http://dx.doi.org/10.1016/j.atmosenv.2012.11.009.

Birmili, W., Rehn, J., Vogel, A., Boehlke, C., Weber, K., Rasch, F., 2013. Micro-scale variability of urban particle number and mass concentrations in Leipzig, Germany. Meteorol. Z. 22, 155–165. http://dx.doi.org/10.1127/0941-2948/2013/0394.

German Federal Ministry for Environment, Nature Conservation and Nuclear Safety (BMU), 1986. Technical Instructions on Air Quality Control (TA Luft) (No. Appendix C). Berlin.

German Federal Ministry for Environment, Nature Conservation and Nuclear Safety (BMU), 2002. Technical Instructions on Air Quality Control (TA Luft) (No. Appendix 3). Berlin.

Broich, A.V., Gerharz, L.E., Klemm, O., 2012. Personal monitoring of exposure to particulate matter with a high temporal resolution. Environ. Sci. Pollut. Res. 19, 2959–2972. http://dx.doi.org/10.1007/s11356-012-0806-3.

Bruse, M., Fleer, H., 1998. Simulating surface–plant–air interactions inside urban environments with a three dimensional numerical model. Environ. Model. Softw. 13, 373–384. http://dx.doi.org/10.1016/S1364-8152(98)00042-5.

Chambers, J.M. (Ed.), 1983. Graphical Methods for Data Analysis, The Wadsworth Statistics/probability Series. Wadsworth International Group ; Duxbury Press, Belmont, Calif. : Boston.

Chang, J.C., Hanna, S.R., 2004. Air quality model performance evaluation. Meteorol. Atmos. Phys. 87 http://dx.doi.org/10.1007/s00703-003-0070-7.

Cox, W.M., Tikvart, J.A., 1990. A statistical procedure for determining the best performing air quality simulation model. Atmos. Environ. Part A. General Top. 24, 2387–2395. http://dx.doi.org/10.1016/0960-1686(90)90331-G.

Dias, D., Tchepel, O., Antunes, A.P., 2016. Integrated modelling approach for the evaluation of low emission zones. J. Environ. Manag. 177, 253–263. http://dx.doi.org/10.1016/j.jenvman.2016.04.031.

Faulkner, W.B., Powell, J.J., Shaw, B.W., Lacey, R.E., 2007. Comparison of dispersion models for ammonia emissions from a ground-level area source. Trans. ASAE 50, 2189–2197.

Foken, T., 2008. Micrometeorology. Springer, Berlin.

Fox, D.G., 1981. Judging air quality model performance. Bull. Am. Meteorol. Soc. 62, 599–609. http://dx.doi.org/10.1175/1520-0477(1981)062<0599:JAQMP>2.0.CO;2.

Franke, J., Hellsten, A., Schlunzen, H., Carissimo, B., 2007. Best Practice Guideline for the CFD Simulation of Flows in the Urban Environment, in: Cost Action 732: Quality Assurance and Improvement of Microscale Meteorological Models. Brussels.

Grimm, H., Eatough, D.J., 2009. Aerosol measurement: the use of optical light scattering for the determination of particulate size distribution, and particulate mass, including the semi-volatile fraction. J. Air & Waste Manag. Assoc. 59, 101–107. http://dx.doi.org/10.3155/1047-3289.59.1.101.

Gromke, C., Blocken, B., 2015. Influence of avenue-trees on air quality at the urban neighborhood scale. Part II: traffic pollutant concentrations at pedestrian level. Environ. Pollut. 196, 176–184. http://dx.doi.org/10.1016/j.envpol.2014.10.015.

Gromke, C., Buccolieri, R., Di Sabatino, S., Ruck, B., 2008. Dispersion study in a street canyon with tree planting by means of wind tunnel and numerical investigations – evaluation of CFD data with experimental data. Atmos. Environ. 42, 8640–8650. http://dx.doi.org/10.1016/j.atmosenv.2008.08.019.

Hanna, S.R., 1988. Air quality model evaluation and uncertainty. JAPCA 38, 406–412. http://dx.doi.org/10.1080/08940630.1988.10466390.

Hofman, J., Samson, R., 2014. Biomagnetic monitoring as a validation tool for local air quality models: a case study for an urban street canyon. Environ. Int. 70, 50–61. http://dx.doi.org/10.1016/j.envint.2014.05.007.

Janicke, 2011. Austal2000-Program Documentation of Version 2.4. Janicke Consulting, Dunum, Germany.

Jänicke, B., Meier, F., Hoelscher, M.-T., Scherer, D., 2015. Evaluating the effects of façade greening on human bioclimate in a complex urban environment. Adv. Meteorol. 2015, 1–15. http://dx.doi.org/10.1155/2015/747259.

Jones, W., Launder, B., 1972. The prediction of laminarization with a two-equation model of turbulence. Int. J. Heat Mass Transf. 15, 301–314. http://dx.doi.org/10.1016/0017-9310(72)90076-2.

Keller, M., de Hahn (Eds.), 2004. Handbuch Emissionsfaktoren des Straßenverkehrs HBEFA 2.1. INFRAS, UBA Berlin. BUWAL Bern, UBA Wien.

Langner, C., Klemm, O., 2011. A comparison of model performance between AERMOD and AUSTAL2000. J. Air Waste Manag.. Assoc. 61, 640–646. http://dx.doi.org/10.3155/1047-3289.61.6.640.

LANUV, 2015. Bericht über die Luftqualität im Jahre 2014. LANUV–Fachbericht 60. Recklinghausen.

Letzel, M., Fallsak, T., Angel, D., 2012. Improvement of AUSTAL2000 results due to flow and turbulence input from MISKAM. Gefahrst. - Reinhalt. Luft 72, 329–334.

Lohmeyer, A., Stockhauser, M., Moldenhauer, A., Nitzsche, E., Düring, I., 2004. Berechnung der KFZ-bedingten Feinstaubemissionen infolge Aufwirbelung und Abrieb für die Emissionskataster Sachsen (No. Arbeitspakete 1 und 2). Dresden.

Maras, I., Schmidt, T., Paas, B., Ziefle, M., Schneider, C., 2016. The impact of human-biometeorological factors on perceived thermal comfort in urban public places. Meteorol. Z. http://dx.doi.org/10.1127/metz/2016/0705.

Merbitz, H., Detalle, F., Ketzler, G., Schneider, C., Lenartz, F., 2012. Small scale particulate matter measurements and dispersion modelling in the inner city of Liège, Belg. Int. J. Environ. Pol.. 50, 234. doi:10.1504/IJEP.2012.051196

Mohan, M., Siddiqui, T.A., 1998. Analysis of various schemes for the estimation of atmospheric stability classification. Atmos. Environ. 32 http://dx.doi.org/10.1016/S1352-2310(98) 00109–5.

Morakinyo, T.E., Lam, Y.F., 2016. Simulation study of dispersion and removal of particulate matter from traffic by road-side vegetation barrier. Environ. Sci. Pollut. Res. 23, 6709–6722. http://dx.doi.org/10.1007/s11356-015-5839-y.

Morawska, L., Thomas, S., Gilbert, D., Greenaway, C., Rijnders, E., 1999. A study of the horizontal and vertical profile of submicrometer particles in relation to a busy road. Atmos. Environ. 33, 1261–1274. http://dx.doi.org/10.1016/S1352-2310(98)00266-0.

Ng, E., Chen, L., Wang, Y., Yuan, C., 2012. A study on the cooling effects of greening in a high-density city: an experience from Hong Kong. Build. Environ. 47, 256–271. http://dx.doi.org/10.1016/j.buildenv.2011.07.014.

Nikolova, I., Janssen, S., Vos, P., Vrancken, K., Mishra, V., Berghmans, P., 2011. Dispersion modelling of traffic induced ultrafine particles in a street canyon in Antwerp, Belgium and comparison with observations. Sci. Total Environ. 412–413, 336–343. http://dx.doi.org/10.1016/j.scitotenv.2011.09.081.

Paas, B., Schmidt, T., Markova, S., Maras, I., Ziefle, M., Schneider, C., 2016. Small-scale variability of particulate matter and perception of air quality in an inner-city recreational area in Aachen. Germany. Meteorol. Z. 25, 305–317. http://dx.doi.org/10.1127/metz/2016/0704.

Pascal, M., Corso, M., Chanel, O., Declercq, C., Badaloni, C., Cesaroni, G., Henschel, S., Meister, K., Haluza, D., Martin-Olmedo, P., Medina, S., 2013. Assessing the public health impacts of urban air pollution in 25 European cities: results of the Aphekom project. Sci. Total Environ. 449, 390–400. http://dx.doi.org/10.1016/j.scitotenv.2013.01.077.

Patel, V.C., Kumar, A., 1998. Evaluation of three air dispersion models: ISCST2, ISCLT2, and Screen2 for mercury emissions in an urban area. Environ. Monit. Assess. 53, 259–277. http://dx.doi.org/10.1023/A:1005810619145.

Pepe, N., Pirovano, G., Lonati, G., Balzarini, A., Toppetti, A., Riva, G.M., Bedogni, M., 2016. Development and application of a high resolution hybrid modelling system for the evaluation of urban air quality. Atmos. Environ. 141, 297–311. http://dx.doi.org/10.1016/j.atmosenv.2016.06.071.

Perry, S.G., Cimorelli, A.J., Paine, R.J., Brode, R.W., Weil, J.C., Venkatram, A., Wilson, R.B., Lee, R.F., Peters, W.D., 2005. AERMOD: a dispersion model for industrial source applications. Part II: model performance against 17 field study databases. J. Appl. Meteorol. 44, 694–708. http://dx.doi.org/10.1175/JAM2228.1.

Pope, C.A., Burnett, R.T., Thun, M.J., Calle, E.E., Krewski, D., Ito, K., Thurston, G.D., 2002. Lung cancer, cardiopulmonary mortality, and long-term exposure to fine particulate air pollution. JAMA 287, 1132–1141.

Schiavon, M., Redivo, M., Antonacci, G., Rada, E.C., Ragazzi, M., Zardi, D., Giovannini, L., 2015. Assessing the air quality impact of nitrogen oxides and

benzene from road traffic and domestic heating and the associated cancer risk in an urban area of Verona (Italy). Atmos. Environ. 120, 234–243. http://dx.doi.org/10.1016/j.atmosenv.2015.08.054.

Schneider, C., Ketzler, G., 2016. Klimamessstation Aachen-Hörn - Monatsberichte Februar, Mai, September/2014, RWTH Aachen. Geogr. Inst. Lehr Forschungsgebiet Phys. Geogr. Klimatol. issn: 1861–4000.

Venkatram, A., 2008. Computing and displaying model performance statistics. Atmos. Environ. 42, 6862–6868. http://dx.doi.org/10.1016/j.atmosenv.2008.04.043.

Venkatram, A., Brode, R., Cimorelli, A., Lee, R., Paine, R., Perry, S., Peters, W., Weil, J., Wilson, R., 2001. A complex terrain dispersion model for regulatory applications. Atmos. Environ. 35, 4211–4221. http://dx.doi.org/10.1016/S1352-2310(01)00186-8.

Vos, P.E.J., Maiheu, B., Vankerkom, J., Janssen, S., 2013. Improving local air quality in cities: to tree or not to tree? Environ. Pollut. 183, 113–122. http://dx.doi.org/10.1016/j.envpol.2012.10.021.

Wania, A., Bruse, M., Blond, N., Weber, C., 2012. Analysing the influence of different street vegetation on traffic-induced particle dispersion using microscale simulations. J. Environ. Manag. 94, 91–101. http://dx.doi.org/10.1016/j.jenvman.2011.06.036.

WHO, 2013. Health Risks of Air Pollution in Europe – HRAPIE Project [WWW Document]. http://www.euro.who.int/__data/assets/pdf_file/0017/234026/e96933.pdf?ua=1 (accessed 3.18.15).

Wiedensohler, A., Birmili, W., Nowak, A., Sonntag, A., Weinhold, K., Merkel, M., Wehner, B., Tuch, T., Pfeifer, S., Fiebig, M., Fjäraa, A.M., Asmi, E., Sellegri, K., Depuy, R., Venzac, H., Villani, P., Laj, P., Aalto, P., Ogren, J.A., Swietlicki, E., Williams, P., Roldin, P., Quincey, P., Hüglin, C., Fierz-Schmidhauser, R., Gysel, M., Weingartner, E., Riccobono, F., Santos, S., Grüning, C., Faloon, K., Beddows, D., Harrison, R., Monahan, C., Jennings, S.G., O'Dowd, C.D., Marinoni, A., Horn, H.-G., Keck, L., Jiang, J., Scheckman, J., McMurry, P.H., Deng, Z., Zhao, C.S., Moerman, M., Henzing, B., de Leeuw, G., Löschau, G., Bastian, S., 2012. Mobility particle size spectrometers: harmonization of technical standards and data structure to facilitate high quality long-term observations of atmospheric particle number size distributions. Atmos. Meas. Tech. 5, 657–685. http://dx.doi.org/10.5194/amt-5-657-2012.

Yassin, M.F., 2013. Numerical modeling on air quality in an urban environment with changes of the aspect ratio and wind direction. Environ. Sci. Pollut. Res. 20, 3975–3988. http://dx.doi.org/10.1007/s11356-012-1270-9.

Journal paper III

Modeling of urban near-road atmospheric PM concentrations using an artificial neural network approach with acoustic sound input

DOI:10.3390/environments4020026

environments

MDPI

Article

Modelling of Urban Near-Road Atmospheric PM Concentrations Using an Artificial Neural Network Approach with Acoustic Data Input

Bastian Paas [1,2,3,*], Jonas Stienen [3,4], Michael Vorländer [3,4] and Christoph Schneider [2]

1 Department of Geography, RWTH Aachen University, Wüllnerstaße 5b, D-52062 Aachen, Germany
2 Department of Geography, Humboldt-Universität zu Berlin, Unter den Linden 6, D-10099 Berlin, Germany; c.schneider@geo.hu-berlin.de
3 Project house HumTec, RWTH Aachen University, Theaterplatz 14, D-52062 Aachen, Germany
4 Institute of Technical Acoustics, RWTH Aachen University, Kopernikusstraße 5, D-52074 Aachen, Germany; jst@akustik.rwth-aachen.de (J.S.); mvo@akustik.rwth-aachen.de (M.V.)
* Correspondence: bastian.paas@geo.rwth-aachen.de; Tel.: +49-241-809-6459

Academic Editor: Zhongchao Tan
Received: 23 February 2017; Accepted: 23 March 2017; Published: 26 March 2017

Abstract: Air quality assessment is an important task for local authorities due to several adverse health effects that are associated with exposure to e.g., urban particle concentrations throughout the world. Based on the consumption of costs and time related to the experimental works required for standardized measurements of particle concentration in the atmosphere, other methods such as modelling arise as integrative options, on condition that model performance reaches certain quality standards. This study presents an Artificial Neural Network (ANN) approach to predict atmospheric concentrations of particle mass considering particles with an aerodynamic diameter of 0.25–1 µm ($PM_{(0.25–1)}$), 0.25–2.5 µm ($PM_{(0.25–2.5)}$), 0.25–10 µm ($PM_{(0.25–10)}$) as well as particle number concentrations of particles with an aerodynamic diameter of 0.25–2.5 µm ($PNC_{(0.25–2.5)}$). ANN model input variables were defined using data of local sound measurements, concentrations of background particle transport and standard meteorological data. A methodology including input variable selection, data splitting and an evaluation of their performance is proposed. The ANN models were developed and tested by the use of a data set that was collected in a street canyon. The ANN models were applied furthermore to a research site featuring an inner-city park to test the ability of the approach to gather spatial information of aerosol concentrations. It was observed that ANN model predictions of $PM_{(0.25–10)}$ and $PNC_{(0.25–2.5)}$ within the street canyon case as well as predictions of $PM_{(0.25–2.5)}$, $PM_{(0.25–10)}$ and $PNC_{(0.25–2.5)}$ within the case study of the park area show good agreement to observations and meet quality standards proposed by the European Commission regarding mean value prediction. Results indicate that the ANN models proposed can be a fairly accurate tool for assessment in predicting particle concentrations not only in time but also in space.

Keywords: ANN; neural networks; machine learning; particulate matter; prediction; motor traffic; acoustics; sound

1. Introduction

Exposure to both particles and noise is associated with an enhanced risk of various adverse health effects [1,2]. Inside urban areas various particle sources can be found [3]. Still, motor traffic is the major source for increased intra-urban levels of particulate matter (PM) inside cities considering low industrial activity [4–6]. Furthermore, PM concentrations are highly influenced by background particle transport besides the interference with motor traffic [7]. High noise levels in urban areas are often

attributable to local road traffic as well. In Europe, high levels of both noise and particle concentrations mostly occur within street canyons [8].

Numerous studies have evaluated the relation between particle concentrations and noise levels in cities near road arterials assuming that both can be allocated to the same motor traffic emitter. Generally speaking, a relation could be proved between particle concentrations and noise levels; however, the statistical correlation between both is complex and different for various metrics [9]. Recent studies highlight that the correlation between equivalent sound pressure levels (A-weighted or non-weighted) and aerosol concentrations is generally higher for either small particle fractions like PM_1 [10] or ultrafine particle metrics like the particle number concentration (PNC), respectively [7,11–14]. The correlation tends to increase with decreasing particle sizes [13]. The relation to noise is less strong for coarse particle fractions like PM_{10} [15] or $PM_{2.5}$ [12,14]. The metric of A-weighted equivalent sound pressure levels (SPL_{eq}(A)) is of particular interest when it comes to the investigation of stressors for humans since SPL_{eq}(A) is a reference metric that emphasizes the human perception of noise integrated over the entire frequency spectrum. It is, therefore, highly popular in studies where noise levels have been compared to particle concentrations [13]. The metric of SPL_{eq}(A), however, accentuates by definition frequency ranges around 1 KHz but plays down lower frequency ranges, where most of the sonic energy transport can be expected from motor traffic-induced sounds [16]. Additionally, besides motor traffic sound that can be assigned to sources of particle emissions, many supplementary sources of sound can be found. Until now, only very occasionally optimization of the acoustic data towards an exhausting representative of motor traffic sounds out of the unweighted noise spectrum has been come into focus when evaluated against concentrations of pollutants like PM [13].

Monitoring of particle concentrations with reference methods is an important task due to the surveillance of air quality standards. However, reference sensors are expensive and therefore in Europe mostly very limited measurements are taken inside urban areas. As a result, spatially resolving information on the local urban concentration of e.g., PM is scarce. Recently developed economic micro-sensors have until now not been able to mitigate the poor availability of information in the dimension of space since this generation of micro-sensor platforms still shows mostly poor performance in particular for PM [17].

Modelling approaches can help to address these shortcomings as alternative or supplementary options to instrumental monitoring. Many different approaches have been developed over time. Deterministic models up to full numerical solutions describing the physical phenomena that determine the transportation of pollutants in the atmosphere are powerful approaches to predict concentrations and the distribution of pollutants in time and space [18,19]. Deterministic models were found to be valid methods; but still, there is room for improvement with regard to their performance. Dispersion models can show unacceptable uncertainties despite of the integration of complex physical relationships and vast computational effort that is needed to derive the results (e.g., [20]). Furthermore, for practical applications often crucial input parameters such as local meteorological data and emission rates of pollutants to initiate deterministic models do not exist in reasonable quality or are available only to a limited extent in dimensions of both space and time.

Statistical modelling, as an alternative modelling approach, can be considered an objective estimation technique in the sense that the method is based on statistical data analysis establishing empirical relationships between ambient pollutant concentrations and influencing variables like e.g., meteorological parameters [21,22] or land use patterns [23,24]. The problem is that many common solutions like regression modelling are not applicable for non-linear problems often found in the real world (environmental or ecological contexts). The relationship between e.g., meteorology and pollutant concentrations, in particular, is complex and potentially multi-scale in nature [25]. The same holds true for the conjunction between sound and pollution levels [13]. Beyond, particle concentrations are more prone to changes introduced by micrometeorology; whereas the influence of meteorology on sound propagation is less strong [7,13]. These settings make the complex nature of the problem highly suitable for an artificial neural network (ANN) approach [26]. The ability of ANNs to learn underlying

data generating processes without the requirement of prior knowledge of the nature of relationships between variables, given sufficient data samples, has led to popular usage for e.g., the prediction and forecasting in environmental studies, among others [25,27]. ANNs are powerful tools that were successfully developed and tested also for prediction within the field of air quality [26]. ANNs were applied and refined over time for e.g., the prediction of hourly concentrations of NO_x and NO_2 in urban air [28], daily average PM_{10} concentrations one day in advance [29], hourly concentrations of CO, NO_2, PM_{10} and O_3 using traffic counts as a major input parameter [30] and ambient air levels of arsenic, nickel, cadmium and lead [22].

In this study, an artificial neural network approach is presented using available meteorological data and inexpensive sound measures as input variables as a cost-effective integrative option to predict aerosol concentrations in urban areas on a basis of 10-min averages where permanent sensor operation is not possible or feasible. The term "prediction" is used hereinafter as a synonym for "now-casting" instead of forecasting establishing the relationship between observed independent variables (e.g., meteorological or acoustical variables) and an observed dependent variable (particle concentrations). Particular concern is put on the selection of input variables, i.e., on the sound data processing in order to determine the sound metric with the maximum predictive information to represent the motor traffic-induced particle emission input of the developed ANN models. The models were developed, validated and tested in a case study environment of a street canyon in direct vicinity to a road arterial ("Aachen-Karlsgraben" test case). In a second step, the validated ANN models were applied and tested by the use of a data set collected within a second research site representing an open green area ("Münster-Aasee" test case). Here the approach was to test for the first time the ability of the ANN approach to gather spatial information on particle concentrations apart from direct vicinity to traffic lanes.

2. Materials and Methods

2.1. Research Sites

2.1.1. Aachen-Karlsgraben

The development and the validation of the proposed ANN model approach took place with a dataset that was collected in a typical street canyon, at the most inner circular road named "Karlsgraben" that surrounds the historic district in the West of the city of Aachen, Germany (see Figure 1). Buildings that enclose the street canyon are containing 4–5 floors and major parts of the buildings are of residential use. Only very occasional business is characterizing the research site containing an electronic hardware store as well as two restaurants. The two restaurants feature enclosed dining areas with the kitchens lying backwards of the houses so that in consequence exhaust air containing particles due to cooking, etc. are emitted to the backyard and not into the street canyon under investigation. Both are located on the other side of the road, 30 m beeline from the installed measurement equipment. The building-height(h)-to-street-width(w) aspect ratio of the street canyon h/w is ~1. The "Karlsgraben" road is a loop arterial oriented to North-South direction in the area under study with two traffic lanes (2-way) and an average traffic volume of approximately 501 vehicles per hour daytime, composed of 93% passenger cars, 2% busses (diesel), 4% delivery vehicles and 1% mostly diesel-powered heavy duty vehicles (manually counted for seven randomly picked hours at different times of day during the period of investigation). Besides the larger traffic share of busses at the study site, the composition of traffic there is similar to the average traffic composition in the state North Rhine Westphalia (NRW). According to the German Federal Office for Motor Traffic (Kraftfahrtbundesamt), the overall vehicle fleet composition in 2012 in the state NRW, where the city of Aachen belongs to, was 94% passenger cars (about 30% diesel), 4% delivery vehicles, 2% heavy duty vehicles, and 0.1% busses [31].

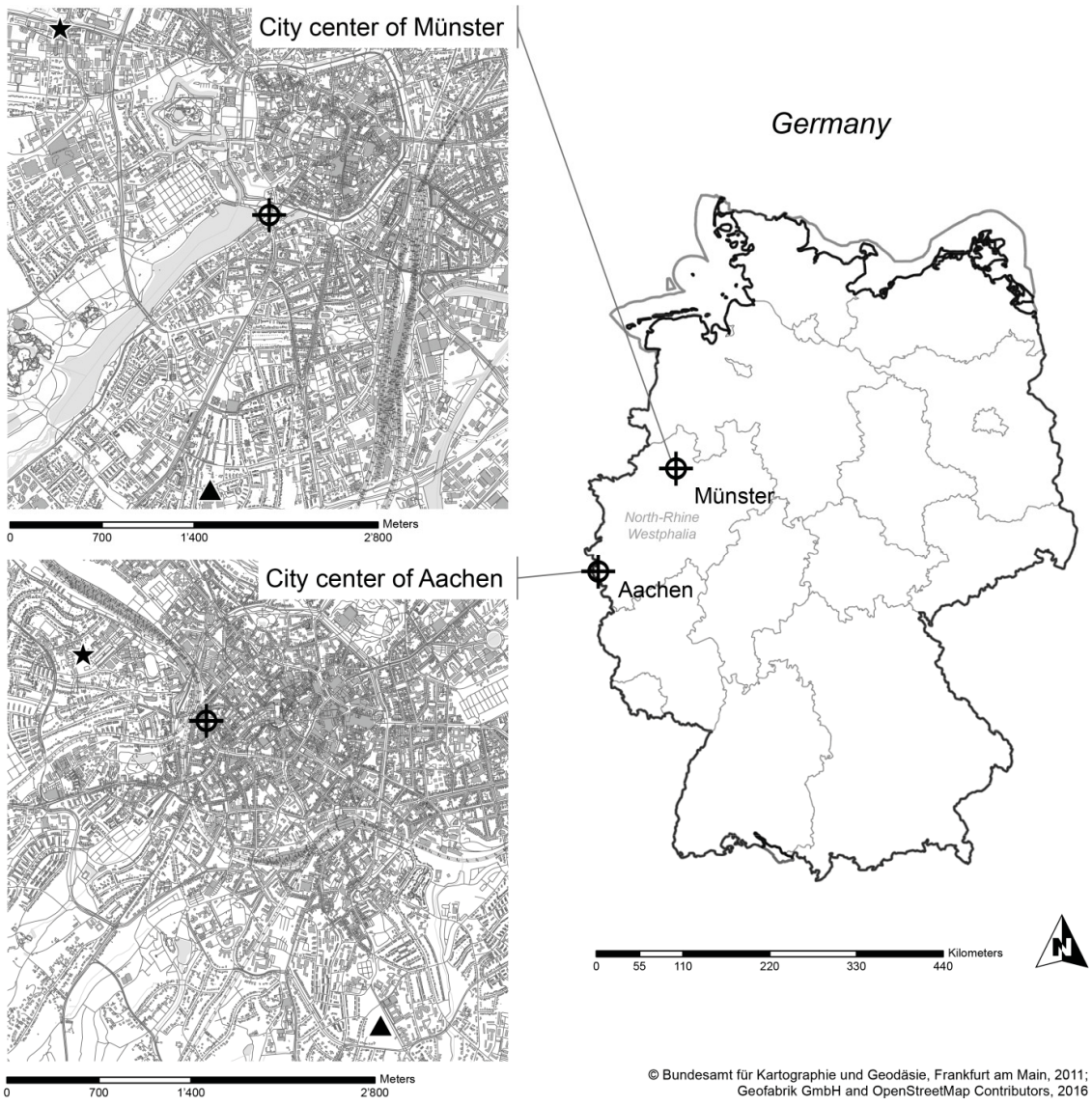

Figure 1. The location of the two areas under study in Germany (right illustration) with close-ups of the city centers of Münster (upper left illustration) and Aachen (lower left illustration) including depictions of the research sites (crosshair cursors), government air quality monitoring stations (triangles) and weather stations (stars).

The stretch of road under study covers a range of 200 m and is located between two intersections that are controlled with traffic lights. The "Karlsgraben" road features a speed limit of 50 km·h^{-1}; however, because most of the motor traffic is between accelerating and slowing down due to the traffic lights up front and at the end of the stretch of road under study, the average speed of motor traffic was estimated to be ~30 km·h^{-1} (mostly fluent) in front of the data collecting sensors. Field data collection for the "Aachen-Karlsgraben" campaign took place halfway between two traffic lights eastward next to the traffic lane (1 m off-street) curbside of "Karlsgraben" road (see Figure 2).

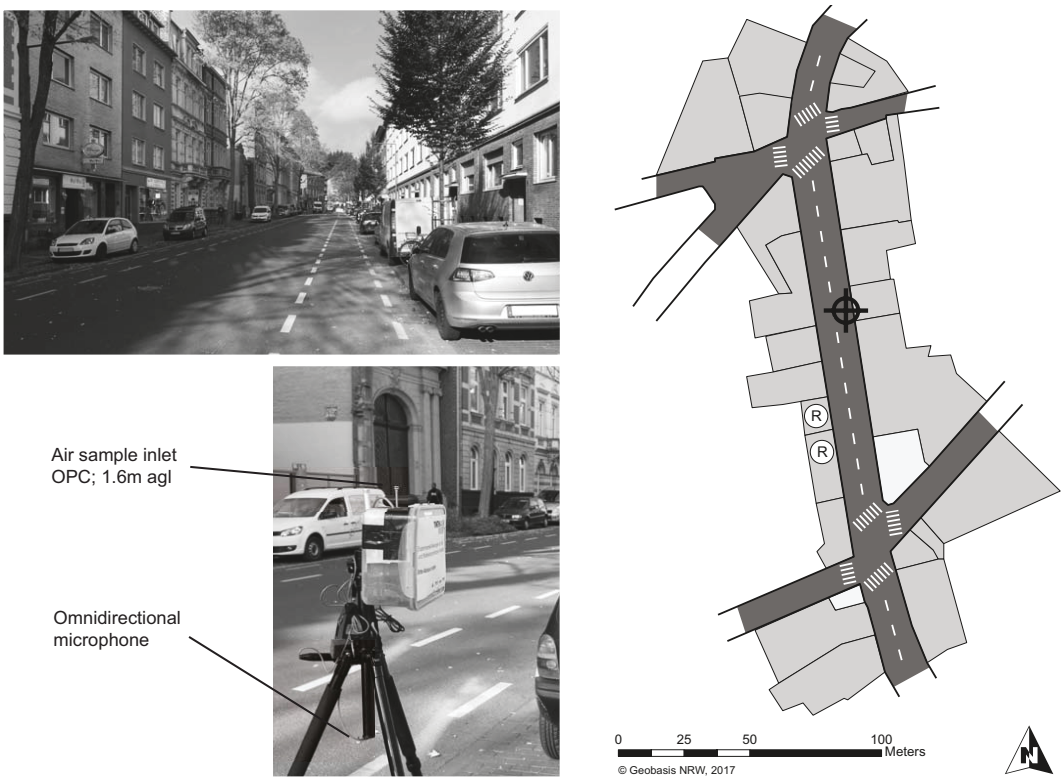

Figure 2. Scheme of the "Aachen-Karlsgraben" research site (right illustration) including depictions of the measurement location (crosshair cursor) and locations of two restaurants (marked with "R") as well as images of both the street canyon of "Karlsgraben" road (upper left image) and the installed on-location measurement equipment (lower left image).

2.1.2. Münster-Aasee

An open space in the city of Münster, NRW, Germany was used as a test case for the development of the ANN models to examine the performance beyond the bounds of an isolated street canyon. The area under study in Münster is characterized by an inner-city park area with a dimension of 250 m by 350 m. The area under study is featuring "complex terrain". In this study, "complex terrain" is referred to the complex urban geometry that is characterized by numerous obstacles like houses and vegetation elements with varying height as well as varying ground levels. The site is remote from industrial areas and contains two lakes. The green area is surrounded by isolated freestanding buildings. Four roads are cutting though the park area in Münster where measurements of sound and particle concentrations were taken. One major traffic arterial, "Weselerstrasse", is oriented from North-East to South-West and contains four traffic lanes (2-way) and an average traffic volume of 2175 vehicles per hour daytime. Field data collection for the "Münster-Aasee" campaign took place at three different locations. One measurement location was in vicinity to the main traffic arterial "Weselerstrasse" (westward, 10 m off-street), where one-third of the data set was collected. Two further locations where data collection took place were located 100 m beeline from "Weselerstrasse" inside the green area eastwards and westwards, respectively. At both measurement locations inside the green area one-third of the complete data set was collected each. Further details of information on the topography of the research site "Münster-Aasee" and the respective collection of data can also be found in [20].

2.2. Artificial Neural Network Approach

Artificial neural network models are universal approximators with the ability to generalize through learning non-linear relationships between provided variables of input(s) and output(s) [32]. The objective of all ANN prediction models is to find an unknown functional relationship $f(X, W)$ which links the input vectors in X to the output vectors in Y [25]. All ANN models are basing on the following form described with the equation (Equation (1)) given by [33]:

$$Y = f(X, W) + \varepsilon \quad (1)$$

where W is the vector of model parameters (connection weights) and ε represents the vector of model errors. Thus, in order to develop the ANN model, the vector of model inputs (X), the form of the functional relationship ($f(X, W)$), which is governed by the network architecture and the model structure (e.g., the number of hidden layers, number of neurons and type of transfer function) and the vector of model parameters (W), which includes the connection and bias weights, have to be defined [33]. The development of the ANN models for the different test cases in this study followed the guidelines and recommendations on ANN model development published in the reviews from [25,27,33] where applicable. Developing of the ANN model in this study was realized using "neuralnet 1.33" with the R software package, version 3.3.1 [34].

2.2.1. Model Architecture—Multi-Layer Perceptron

A Multi-Layer Perceptron (MLP) was selected as the basis of the ANN models in this study to predict mass concentrations of particles with an aerodynamic diameter (DAE) between 0.25 µm and 1 µm ($PM_{(0.25–1)}$), between 0.25 µm and 2.5 µm ($PM_{(0.25–2.5)}$), between 0.25 µm and 10 µm ($PM_{(0.25–10)}$) as well as particle number concentrations with a DAE between 0.25 µm and 2.5 µm ($PNC_{(0.25–2.5)}$). The MLP is the most commonly used ANN model architecture [33,35] and has been found to perform well for applications like the prediction of air pollutant concentrations [26,30]. MLPs typically contain three types of layers of neurons: the input layer, the hidden layer(s), and the output layer [33]. As feed-forward networks, MLPs propagate information only in one direction, i.e., from the input layer to the output layer. In this study, an MLP containing three single layers (one input layer, one hidden layer, one output layer) was used for all ANN models developed (see Figure 3). The number of input neurons (IL_n) is determined by the selected number of input variables. The output layer (OL) in each ANN model is restricted to a single output neuron, i.e., the variable that will be predicted (in this study either $PM_{(0.25–1)}$, $PM_{(0.25–2.5)}$, $PM_{(0.25–10)}$ or $PNC_{(0.25–2.5)}$). The number of neurons in the hidden layer (HL_n) has to be determined in the model structure selection process. The neurons of the MLP are inter-connected by weights and output signals which are a function of the sum of the inputs to the neuron modified by a transfer function [25]. Both linear and non-linear transfer functions can be used at hidden and output layers [27]. Various types of functions are possible. However, ANN models where inputs are summed and processed by a non-linear function have the ability to represent any smooth measurable function between the input and output vectors, and are therefore highly suitable to capture complexity and non-linear relationships inherent in the systems being modeled [33]. The suitable set of weights is found through training (finding the weight with the smallest error) of the ANN model with a subset of the sample that represents the input and output vectors [36]. Different training algorithms can be applied to minimize the error function.

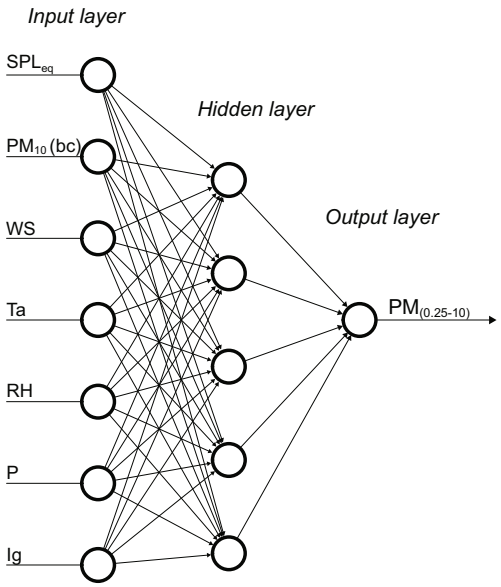

Figure 3. Architecture of the proposed Multi-Layer Perceptron (MLP) to predict $PM_{(0.25–10)}$ concentrations including one hidden layer.

2.2.2. Input Variable Selection

Input variable selection is one of the most important steps in ANN model development [33]. An appropriate set of ANN model inputs "is considered to be the smallest set of input variables required to adequately describe the observed behavior of the system" [37]. Hence, the input selection process was divided in two different actions to determine an appropriate set of inputs. In a first step, input significance is justified using an ad hoc approach where potential input variables (i.e., candidates) were determined basing on a priori knowledge considering the nature of the problem and available data. When it comes to the prediction of local aerosol concentrations as part of the urban roughness layer two main aspects need to be considered: sources of particles and characteristics of particle dispersion [30]. Motor traffic emissions regarding both the amount of combustion processes and blown up dust as well as tire and break abrasions are identified to be the major source of particles near urban arterials [4,6,38]. Vehicular emissions are related to the volume of traffic, vehicle type and speed [30], which, in turn, are assumed to be attributable to traffic sound. A linear and well established correlation between traffic counts and sound levels could be proved [13,39]. Therefore, time integrals of equivalent sound pressure levels were considered as input variable candidates representing the source of particles inside the ANN model. Overall, 24 candidates of different sound metrics were considered (for details, see below Section 2.3.2). Local concentrations of particles are furthermore influenced by the source of background particle transport [7]. In consequence, a second input variable serving as another representative of particle sources inside urban areas was defined using 24-h moving averages of the PM_{10} background concentration (PM_{10} (bc)) obtained from suburban government stations. Considering the variation of pollutant transportation, i.e., the particle dispersion, it is assumed that meteorological conditions are the major factors influencing these dynamics [13]. Variables of atmospheric air temperature (Ta) and pressure (P), relative humidity (RH), wind speed (WS), wind direction (WD) and global radiation (Ig) are directly or indirectly associated with variations of particle transportation [30,40,41] and were consequently considered as meteorological input variable candidates in the development of the ANN models. As an addition, all of the considered meteorological variable candidates are routine metrics that are available at almost every meteorological station and available at low additional costs. Precipitation is also proved to have a major impact on both particle concentrations due to wash-out effects [42] and sound emissions of motor traffic mainly due to shifted tire sound characteristics [43]. However, precipitation was deliberately left out of consideration in this

study to keep the nature of the problem for the development process of the ANN model as simple as possible.

Input variables need to be determined based on both the significance and independence of inputs [27]. Consequently, an analysis of Partial Mutual Information (PMI) was applied to proof relevance and independency of the proposed initial candidate set of acoustical and meteorological variables determined during the ad hoc selection step. The PMI algorithm was selected over other commonly used methods such as generalized linear models (GLMs), as it is proved to be a superior approach in particular to examine non-linear dependences [44]. More information on the mathematical basis of the PMI analysis can be found in [37,45]. The goal was to sample out a set of variables with maximum predictive power and minimum redundancy since redundant information in the model input stage can cause various problems; one of the most important being the likelihood of overfitting as a result of confusion during the training process of the ANN model [33,36]. The final input selection using PMI was justified using the Akaike Information Criterion (AIC), which is a measure of the trade-off between ANN model complexity and the information within the candidate set of inputs, as a function of the number of input candidates. The AIC is the recommended criterion within the use of PMI for samples where the distribution of data may be unknown and the assumption of Gaussian distribution may not hold [37]. Variable candidates have been selected in an iterative process up until a minimum AIC was reached for a given set of variable candidates which represents the optimum number of inputs to be selected [37]. For reasons of comparison all ANN models have been developed additionally without using acoustic data input. Calculated AICs for individual input variable selection steps as well as the input variables defined for the optimum model architecture of each ANN model are presented below in Section 2.2.4.

2.2.3. Data Splitting

The valid data set, including the selected input (see Section 2.2.2) and output variables, were divided into training, validation and testing subsets, in order that cross-validation could be used to avoid overfitting of the MLP and to ensure best possible generalization of the ANN model on unknown input data. The sample was divided into data subsets with a split-sample-ratio of 70% training data to 20% validation data to 10% test data. One popular approach to split the sample in different subsets is to assign data points according to the random principle. While this may be an adequate method for large sample sizes there is a chance that the data in one of the subsets may be biased towards extreme or uncommon events [25]. In this study, a method based on stratified sampling of the Self-Organizing Map (SOM) was used to split the data set into subsamples ensuring that the statistical properties of the subsets are similar [46]. In principle, a SOM clusters the available data by delineation of sub-domains within a dataset for which data within the same sub-domain are similar, but distinct from data in other sub-domains. Stratified random·sampling is applied to allocate data samples from each SOM cluster to the subsets of training, validation and testing. As a result, it is made certain that patterns from all identified sub-domains of the multivariate input-output space are represented in each subset [46]. The training set consists of data vectors used for training the network, i.e., fitting the weights of the neurons of each layer for the desired output. The subset of validation data was used to tune the ANN model structure. The test set was used to assess the performance of the developed ANN model after training on unseen input data. SOM-based stratified data splitting (SBSS) was performed following the recommendations of [46] regarding the settings of the SOM. The adjustment of the SOM map units is one of the most influential parameters and depends on the SOM grid size (SOM_{gs}) which should be determined by the sample size of the data set (s_n), where SOM_{gs} should be equal to $\sim s_n^{0.54}$. The length of the SOM map should be 1.6 times the SOM_{gs}, whereas the width should be equal to the SOM_{gs}, resulting in a SOM map size used in this study of a ratio of 5.8 by 3.6 within the "Aachen-Karlsgraben" test case and a ratio of 4.3 by 2.7 within the "Münster-Aasee" test case representing the length and width respectively. Proportional random sampling has been applied to the sample. SOM parameters that have been used for implementing SBSS are presented in Table 1.

Table 1. Self-Organizing Map (SOM) parameters for implementing SOM-based stratified data splitting (SBSS). "Münster-Aasee" test case settings are given in brackets if distinct from "Aachen-Karlsgraben" test case settings.

Parameter	Ordering	Tuning
Initial learning rate	0.9	0.1
Initial neighborhood size	3.6 (2.7)	1
Epochs	2	20

In Figure 4 data histograms for both test cases and all ANN models of the trained SOMs and data sets of input variables are shown illustrating how input data vectors are clustered by the SOM. The data histogram visualization shows how many vectors were assigned to each cluster. More detailed mathematical descriptions regarding SOM-based stratified sampling can be found in [46].

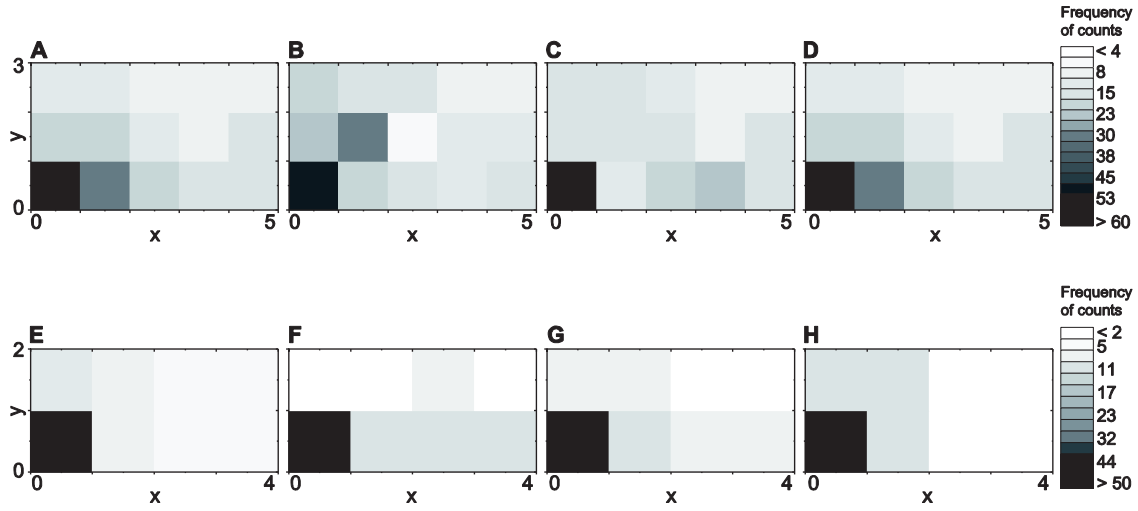

Figure 4. Self-Organizing Map (SOM) data histograms of Artificial Neural Network (ANN) models that include acoustic data input within the "Aachen-Karlsgraben" test case concerning outputs of $PM_{(0.25–1)}$ (**A**), $PM_{(0.25–2.5)}$ (**B**), $PM_{(0.25–10)}$ (**C**) and $PNC_{(0.25–2.5)}$ (**D**) and within the "Münster-Aasee" test case concerning outputs of $PM_{(0.25–1)}$ (**E**), $PM_{(0.25–2.5)}$ (**F**), $PM_{(0.25–10)}$ (**G**) and $PNC_{(0.25–2.5)}$ (**H**), respectively. The frequencies of counts of input vectors in each SOM cluster are marked with grey-scale codes ("Aachen-Karlsgraben: upper legend; "Münster-Aasee": lower legend).

2.2.4. Model Structure Selection

Together with the ANN model architecture, the model structure defines the functional relationship $f(X, W)$ between model inputs and outputs (Section 2.1, Equation (1)). Model structure selection includes the determination of the optimum number of neurons in the hidden layer and how they process incoming signals by the use of suitable transfer functions [46]. In general, an optimum ANN model structure minimizes the uncertainty of the network and maximizes model parsimony considering network size [27]. The model structure can be determined by the use of a stepwise iterative process which is the most-used systematical application to find out the optimal number of neurons in the hidden layer [33]. In a first model structure selection step, a constructive algorithm was applied in the ANN model development process. The iterative procedure started by using the defined IL_n-HL_n-OL architecture of the ANN model (Section 2.2.1; Section 2.2.2), combined with the simplest ANN model structure possible (HL_n = 1). The network structure was gradually made more complex by adding neurons in the hidden layer, one at a time, until there was no significant improvement in model performance. Since it is recommended that the ratio of the number of data points used for training to the number of the network weight and biases should be always greater

than 2.0 [47] the network size was kept reasonable in size according to the sizes of the data samples (see below Section 2.3). The ANN model structure was tested on the basis of the Root Mean Squared Error (RMSE) of the network (see below, Section 2.5). The second part of this optimization process is the determination of the best suitable transfer function. Two different non-linear variants of functions were considered in the development process of the ANN model, i.e., hyperbolic tangent and the logistic sigmoidal. The obtained RMSEs for different ANN model structures created during the refinement process, considering both different number of neurons in the hidden layer and two different transfer functions, are presented in Figure 5. It turned out that the best performing final ANN model to predict $PM_{(0.25–10)}$-concentrations was operated by using a logistic sigmoidal transfer function. The best performing ANN models to predict concentrations of $PM_{(0.25–1)}$, $PM_{(0.25–2.5)}$ and $PNC_{(0.25–2.5)}$ were using a hyperbolic tangent transfer function. The optimum HL_n to predict concentrations of $PM_{(0.25–1)}$ was found to be six. The best performing ANN model to predict concentrations of $PM_{(0.25–2.5)}$ contained four hidden neurons. The optimum HL_n of the ANN models to predict concentrations of $PM_{(0.25–10)}$ and $PNC_{(0.25–2.5)}$ were detected to be five (see Figure 5). The ANN models using only input data of meteorology and background particle transport developed for comparison passed the same procedure of model structure selection as described above. A summary of the finalized ANN model architecture used to predict concentrations of $PM_{(0.25–1)}$, $PM_{(0.25–2.5)}$, $PM_{(0.25–10)}$ and $PNC_{(0.25–2.5)}$, including the determined number of neurons in the input layer, their respective input variables as well as the HL_n and the best performing transfer functions, is presented in Table 2.

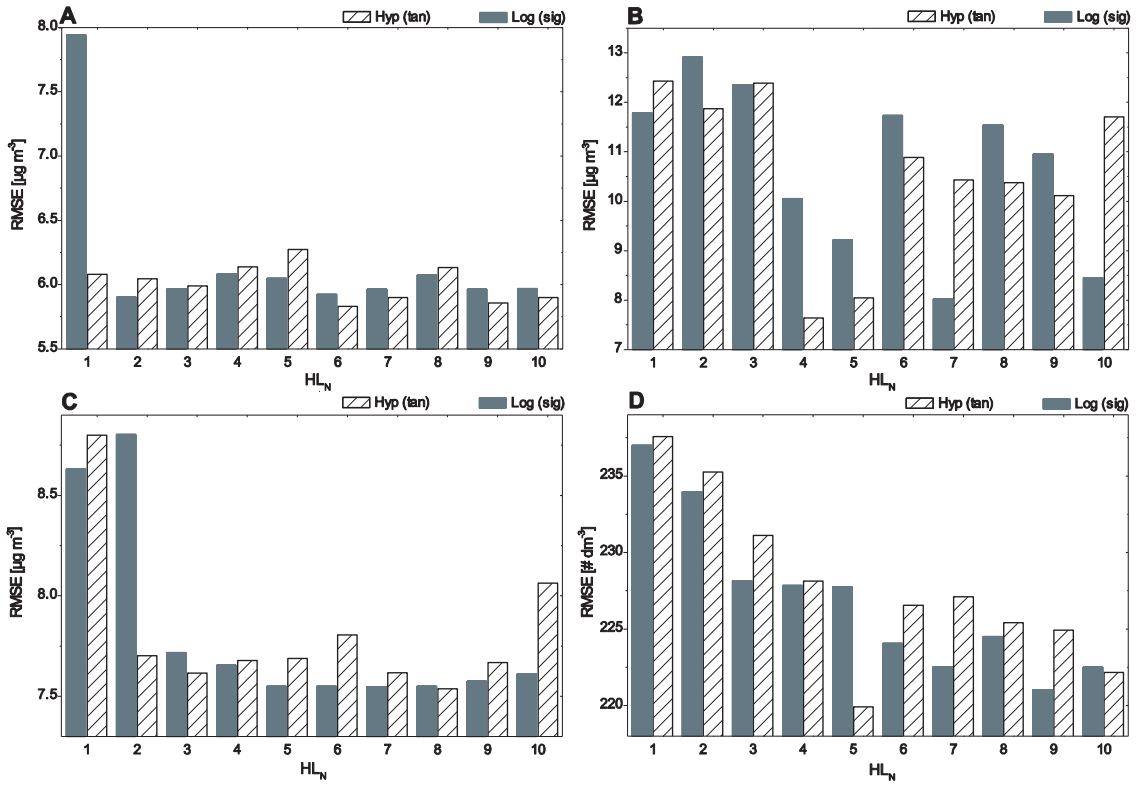

Figure 5. Results of the optimization procedure of the Multi-Layer Perceptron (MLP) structure considering the number of neurons in the hidden layer (HL_n) and two different transfer functions (Logarithmic sigmoidal: grey bars; Hyperbolic tangent: hatched black bars) using a constructive algorithm for the Artificial Neural Network (ANN) models that include acoustic data input to predict concentrations of $PM_{(0.25–1)}$ (**A**), $PM_{(0.25–2.5)}$ (**B**), $PM_{(0.25–10)}$ (**C**) and $PNC_{(0.25–2.5)}$ (**D**).

Table 2. Summary of the finalized Artificial Neural Network (ANN) model architecture including number of neurons in the input layer (IL_n) input variable candidates (IVC) and respective Akaike Information Criterion (AIC) values given in square brackets, number of neurons in the hidden layer (HL_n), determined transfer functions and the dedicated output layer (OL). Numbers in parentheses indicate settings used for the alternative models using input variables excluding acoustic data. Determined input variables for the final ANN models are indicated in bold letters.

IL_n	**5 (4)**	**6 (5)**	**6 (5)**	**7 (6)**
IVC [AIC]	**PM_{10} (bc)**	**PM_{10} (bc)**	**PM_{10} (bc)**	**PM_{10} (bc)**
	Ta [−428]	**RH [−242]**	**RH [−171]**	**RH [−241]**
	P [−843]	**Ta [−274]**	**Ta [−235]**	**Ta [−283]**
	Ig [−868]	**Ig [−358]**	**WS [−251]**	**Ig [−365]**
	WS [−866]	**P [−366]**	**P [−270]**	**WS [−423]**
	WD [−832]	WS [−346]	WD [−246]	P [−430]
	RH [−810]	WD[−388]	Ig [−210]	WD [−421]
	SPLeq [−6]	**SPLeq [−8]**	**SPLeq [−10]**	**SPLeq [−9]**
	SPLeq15Hz(A) [−1]	SPLeq15Hz [−2]	SPLeq15Hz [−1]	SPLeq15Hz(A) [−4]
	SPLeq16kHz [23]	SPLeq34Hz [10]	SPLeq15Hz(A) [2]	SPLeq15Hz(A) [5]
	SPLeq63Hz(A) [51]	SPLeq34Hz(A) [14]	SPLeq63Hz(A) [27]	SPLeq34Hz [8]
	SPLeq15Hz [55]	SPLeq15Hz(A) [18]	SPLeq125Hz(A) [55]	SPLeq34Hz(A) [10]
	SPLeq34Hz(A) [70]	SPLeq16kHz [45]	SPLeq34Hz [70]	SPLeq250Hz(A) [14]
	SPLeq16kHz(A) [78]	SPLeq250Hz(A) [61]	SPLeq16kHz(A) [127]	SPLeq250Hz [19]
	SPLeq125Hz(A) [112]	SPLeq250Hz [66]	SPLeq8kHz [154]	SPLeq16kHz(A) [57]
	SPLeq8kHz [137]	SPLeq16kHz(A) [83]	SPLeq250Hz(A) [168]	SPLeq16kHz [73]
	SPLeq250Hz(A) [154]	SPLeq63Hz(A) [117]	SPLeq34Hz(A) [176]	SPLeq63Hz(A) [105]
	SPLeq63Hz [165]	SPLeq125Hz(A) [147]	SPLeq16kHz [189]	SPLeq125Hz(A) [133]
	SPLeq34Hz [174]	SPLeq8kHz [171]	SPLeq63Hz [201]	SPLeq63Hz [146]
	SPLeq125Hz [189]	SPLeq63Hz [183]	SPLeq8kHz(A) [207]	SPLeq125Hz [161]
	SPLeq250Hz [194]	SPLeq125Hz [199]	SPLeq125Hz [225]	SPLeq8kHz [184]
	SPLeq8kHz(A) [200]	SPLeq8kHz(A) [205]	SPLeq250Hz [229]	SPLeq8kHz(A) [189]
	SPLeq500Hz(A) [207]	SPLeq500Hz [212]	SPLeq4kHz(A) [241]	SPLeq500Hz [195]
	SPLeq4kHz [219]	SPLeq4kHz(A) [224]	SPLeq500Hz [247]	SPLeq4kHz [208]
	SPLeq1kHz [221]	SPLeq1kHz [225]	SPLeq500Hz(A) [250]	SPLeq1kHz [210]
	SPLeq4kHz(A) [226]	SPLeq4kHz [230]	SPLeq4kHz [253]	SPLeq4kHz(A) [215]
	SPLeq500Hz [230]	SPLeq500Hz(A) [233]	SPLeq2kHz(A) [257]	SPLeq500Hz(A) [218]
	SPLeq(A) [240]	SPLeq(A) [243]	SPLeq(A) [260]	SPLeq(A) [233]
HL_n	**6 (7)**	**4 (3)**	**5 (4)**	**5 (4)**
Transfer function	Hyp-Tan (Hyp-Tan)	Hyp-Tan (Hyp-Tan)	Log-Sig (Log-Sig)	Hyp-Tan (Hyp-Tan)
OL	$PM_{(0.25–1)}$	$PM_{(0.25–2.5)}$	$PM_{(0.25–10)}$	$PNC_{(0.25–2.5)}$

2.2.5. Model Calibration—Backpropagation Algorithm

The process of finding a set of connection weights between neurons that results in an ANN model with a given functional form to best represent the desired input/output relationship is called "training" [33]. The back-propagation (BP) algorithm, a first-order local search procedure, is the most used algorithm for training an MLP [25]. The learning process basically consists of two iterative steps: forward computing of data and backward propagation of error signals [30]. Developed by [48], BP uses a gradient descent algorithm in which the network weights are moved along the negative of the gradient of the performance function [36].Usually, the BP algorithm is implemented following the steps hereinafter: (I) Initialization of network weights starting with small random values; (II) Propagation of an input vector from the training subset of data through the network to obtain an output; (III) Calculation of an error signal; (IV) Back-propagation of the error signal through the network; (V) Weight-adjustment at each neuron to minimize the overall error; (VI) Repetition of steps II–V with the next input vector, until the overall error is satisfactorily small [25]. Training was stopped when the performance of the MLP on the test sample reached a maximum, which, in turn, was assumed

to represent the global minimum of the error surface. Details of the mathematical formulation of the BP algorithm can be found in [49].

2.3. Field Data—Collection and Pre-Processing

All simultaneously conducted measurements in Aachen, including the collection of aerosol data, acoustics and meteorology were taken at different days of week and different times of day for the reason that the dataset represents a best possible spectrum of both noise levels and particle concentration levels representative for the area under study during daytime at business days. Data collection at the "Aachen-Karlsgraben" research site took place at 27 October 2016, 28 October 2016, 3 November 2016, 4 November 2016 and 30 November 2016 at different times of day between 04:30 a.m. at the earliest and 08:00 p.m. at the latest resulting in a sample of overall 293 10-min averages of all variables. Outliers (e.g., due to sounds resulting from ambulance or police sirens) as well as the first and last ten minutes of data recordings were manually deducted from the raw data set. The pre-processed sample used for the development of the ANN models consists of 275 10-min averages of all variables. Meteorological prerequisite conditions for the Aachen campaign were chosen to avoid rainy periods and atmospheric conditions concerning both well-marked dilution of pollutants as well as conditions where resuspension of particles due to gusting wind is likely, i.e., data collection took place during low wind speed conditions and an upstream wind vector perpendicular to the street canyon under study. The measurements in Münster took place at three different weekdays in February as well as three different weekdays in July 2015 between 10:00 a.m. and 05:00 p.m. local time resulting in a pre-processed sample of overall 97 10-min averages of all variables to evaluate the performance of the developed ANN models under different initial conditions beyond an isolated street canyon.

2.3.1. Particles

Local aerosol measurements were carried out using an optical particle counter (OPC), Model EDM 107G (Grimm GmbH, Ainring, Germany) to determine different metrics regarding the concentration of airborne particles. The OPC bases on the approach of single particle counting by the use of light scattering technique. The number of contained particles of the air sample is derived from the frequency of scattered light pulse signals. Particle sizes are obtained from the amplitude of the backscatter signal. The OPC classifies detected particles into a size distribution in a range between 0.25 and 32 µm DAE containing 31 different size channels. Internally, the particle number size distribution is converted into mass concentrations for an indicated average time interval. The sensor operates at a volumetric flow rate of 1.2 L min^{-1} and a time resolution of 6 s [50]. The OPC used had been factory calibrated on a regular basis (VDE standard 0701-0702) within the calibration validity period and was calibrated last on 13 January 2015. In all cases particles were sampled at the mean respiratory height of 1.6 m agl and stored as 10-min arithmetic means of $PM_{(0.25–1)}$, $PM_{(0.25–2.5)}$), $PM_{(0.25–10)}$ and $PNC_{(0.25–2.5)}$. Data of PM_{10} (bc) were obtained as 24-h moving averages from government air quality sites Aachen-Burtscheid (AABU) and Münster-Geist (MSGE), operated by the North Rhine-Westphalian State Office for Nature, Environment, and Consumer Protection (LANUV) assuming that both government stations represent the urban background particle concentration which can be expected at the research sites even though both government stations are around 2.5 km beeline from respective areas under investigation.

2.3.2. Acoustics

Time series of physical sound pressure values were captured with a mobile recorder (Type H6, Zoom Corporation, Tokyo, Japan) at 44.1 kHz sampling rate with 24 Bit resolution using an omnidirectional microphone (KE-4 electret-microphone, Sennheiser Electronic GmbH & Co. KG, Wedemark, Germany). The calibration process has been performed in a post-processing step by comparing a Root Mean Square (RMS) 1 kHz pure-tone signal at 94 dB re 20 µPa from a portable sound source (Type 4231 Sound Calibrator, Brüel & Kjær Sound & Vibration Measurement A/S, Nærum, Denmark), which has been captured for each measurement time-series individually (once

per day). The measurements were carried out with the microphone installed on a tripod 1.2 m agl at the same location where data of particle concentrations were taken (Section 2.3.1). From·sound pressure time series, 10-min averages of equivalent sound pressure levels as integrals over the entire captured bandwidth of frequencies between 0 Hz and 22 kHz (SPL_{eq}) were determined. Furthermore, 10-min averages of sound pressure levels representing single octave bands of 15 Hz, 34 Hz, 63 Hz, 125 Hz, 250 Hz, 500 Hz, 1 kHz, 2 kHz, 4 kHz, 8 kHz and 16 kHz were calculated. Similarly, equivalent A-weighted sound pressure levels as described by ISO standard 226:2003 were computed as 10-min averages [16] again either as integrals over the captured bandwidth of frequencies between 0 Hz and 22 kHz ($SPL_{eq}(A)$) or as metrics of single octave bands as mentioned before. Descriptive statistics concerning the observed aerosol concentrations and acoustic data of both campaigns are summarized in Table 3. Mean values of observed sound levels reflect average values that are published by the state government of NRW for the areas under study. Furthermore, it is stated that at both research sites of the "Aachen-Karlsgraben" and the "Münster-Aasee" campaigns motor traffic is the major source of sound [51].

Table 3. Descriptive statistics concerning arithmetic mean values (AM) and standard deviations (SD) of observed particle concentrations as well as mean values (L_{eq}) and 10/90% percentiles (L_{10}/L_{90}) of acoustic data of the "Aachen-Karlsgraben" and "Münster-Aasee" test cases.

Variable	$PM_{(0.25–1)}$	$PM_{(0.25–2.5)}$ ($\mu g \cdot m^{-3}$)	$PM_{(0.25–10)}$	$PNC_{(0.25–2.5)}$ ($\#\cdot dm^{-3}$)	SPL (dB)
"Aachen-Karlsgraben"	AM: 15.9 SD: 4.2	AM: 19.4 SD: 5.3	AM: 30.4 SD: 8.9	AM: 545 SD: 217	L_{eq}: 74.1 L_{10}: 79.7 L_{90}: 63.4
"Münster-Aasee"	AM: 16.3 SD: 10.2	AM: 18.4 SD: 9.9	AM: 28.7 SD: 9.1	AM: 545 SD: 460	L_{eq}: 69.5 L_{10}: 75.2 L_{90}: 62.0

2.3.3. Meteorology

Meteorological input variables in this study consist of data from nearby weather stations, whose values are monitored in real time by the RWTH Aachen University (6°03′40″ E, 50°46′44″ N; 1500 m beeline from the area under study of "Aachen-Karlsgraben") and the University of Münster (7°35′45″ E, 51°58′9″ N; 2100 m beeline from the area under study of "Münster-Aasee"), respectively. Meteorological data of local authorities have been chosen in order that they are available at no/low additional costs. Since many cities operate meteorological monitoring stations this approach ensures a low-cost possibility for future applications of the model. In Aachen the wind sensor to determine WD and WS (Wind Monitor 05103, R.M. Young Company, Traverse City, MI, USA) is installed on top of a roof (6.5 m above the rooftop) in 29 m agl. The shielded temperature and humidity sensor (CS215, Campbell Scientific, Inc., Logan, UT, USA) is mounted on a mast in 2 m agl. [52]. During the time of data collection during the campaign in Aachen 2016 the wind was coming from·south-westerly directions (185°–270°), with an average wind speed of 3.2 $m \cdot s^{-1}$ (in 29 m agl). At the weather station in Münster sensors to determine WD and WS (WindSonic Anemometer RS-232, Gill Instruments Limited, Lymington, Hampshire, UK) as well as the shielded temperature and humidity sensor (41382VC, R.M. Young Company, Traverse City, MI, USA) are mounted on a permanent mast on top of a roof (10 m above the rooftop) in 34 m agl. During the Münster campaign in February 2015 the wind was predominantly coming from easterly directions, with an average wind speed of 4 $m \cdot s^{-1}$. Varying wind directions but wind mostly coming from northeast and wind speeds between 2 $m \cdot s^{-1}$ and 5 $m \cdot s^{-1}$ being most common were observed during the campaign in July 2015. Conditions were dry with no precipitation during the periods of data collection in Münster.

2.4. Field Data—Post-Processing

Before computing, data of both input and output variables were normalized. In this study, data of all variables used were normalized into the range [0, 1] with:

$$X_{norm} = \frac{(X_i - X_{min})}{(X_{max} - X_{min})} \quad (2)$$

where X_{norm} is the normalized value, X_i is the original value, and X_{min} and X_{max} are the minimum and maximum values out of the sample of X_i. This was due to eliminate the influence of different dimensions of data and to avoid overflows of the ANN model during calculations as a result of very large or small weights towards a maximization of model parsimony considering computational effort [28]. After the computation, output values were transformed back to real prediction data.

2.5. Performance Measures

In order to evaluate the performance of the ANN models, several statistical performance indicators were used, namely the RMSE, the Mean Bias (MB), the Centralized Mean Squared Error (CRMSE) the Model Efficiency score (MEF) and the Fractional Bias (FB). The RMSE (Equation (3)) was mainly used in the development process of the ANN model and represents residual errors, which gives a global perspective of the differences between the observed and predicted values [53]:

$$RMSE = \frac{1}{n}\sqrt{\sum_{i=1}^{n}(C_{P_i} - C_{O_i})^2} \quad (3)$$

where C_O and C_p are the observed and predicted concentrations, respectively. A graphical approach (target diagram) was used as an additional measure providing an exhaustive indication of model response [54]. The methodology of the target diagram bases on the main principle of [55] and was modified by the Joint Research Centre (JRC) of the European Commission within the framework of the Forum for Air Quality Modelling in Europe (FAIRMODE) to develop a harmonized methodology to evaluate model results based on a consensus set of statistical indicators. The methodology of the target diagram has been introduced by [56] within the DELTA tool. The target diagram reports the MB and CRMSE, both normalized by the standard deviation of the observations (σ_O), on the abscissa and ordinate, respectively [54]. The MB is given by Equation (4):

$$MB = \frac{1}{n}\sum_{i=1}^{n}(C_{P_i} - C_{O_i}) = \overline{C_P} - \overline{C_O} \quad (4)$$

The *CRMSE* is described by Equation (5):

$$CRMSE = \frac{1}{n}\sqrt{\sum_{i=1}^{n}\left[(C_{P_i} - \overline{C_P}) - (C_{O_i} - \overline{C_O})\right]^2} \quad (5)$$

The target diagram includes a boundary circle of unit radius that defines the acceptable limit value of the *MEF* [22]:

$$MEF = 1 - \left(\frac{RMSE}{\sigma_O}\right)^2 \quad (6)$$

For an acceptable model, the target value of model results must be plotted inside the boundary circle (radius = 1) of the target diagram, so that the calculated MEF becomes >0 [22]. Moreover, when the requirements of an acceptable model are fulfilled considering MEF, it is automatically guaranteed that predictions and observations are positively correlated. Generally, the closer the reached performance score is to the origin of the target diagram, the better is the model performance [54]. The FB was used as an additional basic measure of model performance. The FB represents a fundamental indicator

of discrepancy between the samples of prediction and observation values, respectively [57]. The FB is dimensionless and normalized. Values of the FB range between −2 and +2 for extreme over- or under-prediction of the model, where a value of zero represents a perfect model. The formula is given by Hanna, 1988 (Equation (7)):

$$FB = \frac{2(\overline{C}_O - \overline{C}_p)}{(\overline{C}_O + \overline{C}_p)} \quad (7)$$

3. Results

Four ANN models to predict concentrations of $PM_{(0.25–1)}$, $PM_{(0.25–2.5)}$, $PM_{(0.25–10)}$ and $PNC_{(0.25–2.5)}$ using input data of SPL_{eq}, PM_{10} (bc) as well as meteorological conditions were developed and validated with a data set collected during the campaign "Aachen-Karlsgraben". Similarly four ANN models were developed excluding input data of acoustic sound for comparison reasons. After individual training of the networks by the use of training data sets taken from the measurement campaigns "Aachen-Karlsgraben" and "Münster-Aasee", respectively, their predictive performance using unseen test input data concerning 10-min averages were evaluated. For that purpose, ANN model results were compared to observations. The ANN model predictions of the "Aachen-Karlsgraben" test case reveal mixed results in this regard. In Figure 6 10-min averages of predicted $PM_{(0.25–1)}$, $PM_{(0.25–2.5)}$, $PM_{(0.25–10)}$ and $PNC_{(0.25–2.5)}$ concentrations over respective observations are presented. It can be seen that all predictions are positively related to observations (slope: 0.02–0.24). However, predictions of $PM_{(0.25–1)}$ and $PM_{(0.25–2.5)}$ did not coincide to observations (R^2: 0.05–0.13). The model to predict concentrations of $PM_{(0.25–2.5)}$ seems to be almost completely insensitive to model inputs with very little variation within the prediction sample. The relation of model predictions to observations regarding $PM_{(0.25–10)}$ and $PNC_{(0.25–2.5)}$ within the "Aachen-Karlsgraben" test case is moderate (R^2: 0.28–0.48). In comparison, the ANN models using inputs without acoustic data failed to predict concentrations of $PM_{(0.25–1)}$ (R^2: 0.16, slope: 0.01) and $PM_{(0.25–10)}$ (R^2: 0.14, slope: 0.02). In these cases the models were completely insensitive to inputs. Observations concerning the metric of $PNC_{(0.25–2.5)}$ were reproduced similarly to results of the ANN model that incorporated the acoustic data input. Depiction B of Figure 6 unveils a better performance for $PM_{(0.25–2.5)}$ of the ANN model that excluded acoustic data input with a good reproduction of observations (R^2: 0.35, slope: 0.81) albeit noticeable scatter within the prediction sample. Figure 7 shows 10-min averages of predicted $PM_{(0.25–1)}$, $PM_{(0.25–2.5)}$, $PM_{(0.25–10)}$ and $PNC_{(0.25–2.5)}$ concentrations compared to observations calculated with the ANN models using unseen input data of the "Münster-Aasee" test data sets. It becomes obvious that both ANN models with and without the use of acoustic input data were again not able to reproduce measurement data of $PM_{(0.25–1)}$ (slope: 0.03–0.11). The models were completely insensitive to the inputs indicated by constant predictions values over the entire range of observations with almost no variation in the prediction sample. Concerning $PM_{(0.25–10)}$ within the "Münster-Aasee" test case it turned out that the ANN model that used additional acoustic data inputs calculated decent predictions (R^2: 0.78, slope: 0.43) whereas the ANN model that excluded acoustic data input was again insensitive to input variables (R^2: 0.69, slope: 0.03). Results of predicted concentrations of $PM_{(0.25–2.5)}$ and $PNC_{(0.25–2.5)}$ of both types of ANN models show a very good agreement to observations over the entire concentration range (R^2: 0.65–0.9; slope: 0.62–1.04). The addition of acoustic data to the set of input variables turned out to improve the accuracy of model predictions calculating concentrations of both $PM_{(0.25–10)}$ and $PNC_{(0.25–2.5)}$ within the "Münster-Aasee" test cases.

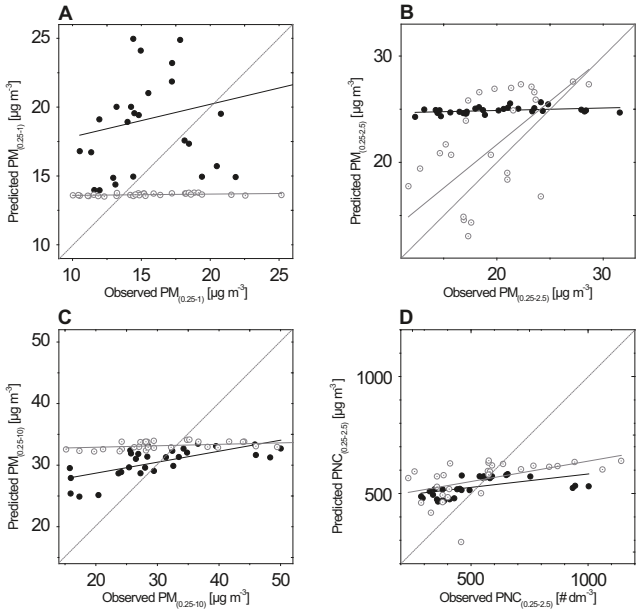

Figure 6. Scatter plot diagram showing Artificial Neural Network (ANN) model predictions of (**A**) $PM_{(0.25–1)}$, (**B**) $PM_{(0.25–2.5)}$, (**C**) $PM_{(0.25–10)}$ and (**D**) $PNC_{(0.25–2.5)}$ over respective observations for the "Aachen-Karlsgraben" test case. The dashed line illustrates a 1:1 reproduction of ANN models predictions over observations. The thin solid lines indicate linear regression results between the samples of ANN model predictions and observations. Black marks depict results of ANN models using additional acoustic data inputs whereas grey marks indicate results of ANN models using inputs without acoustic data.

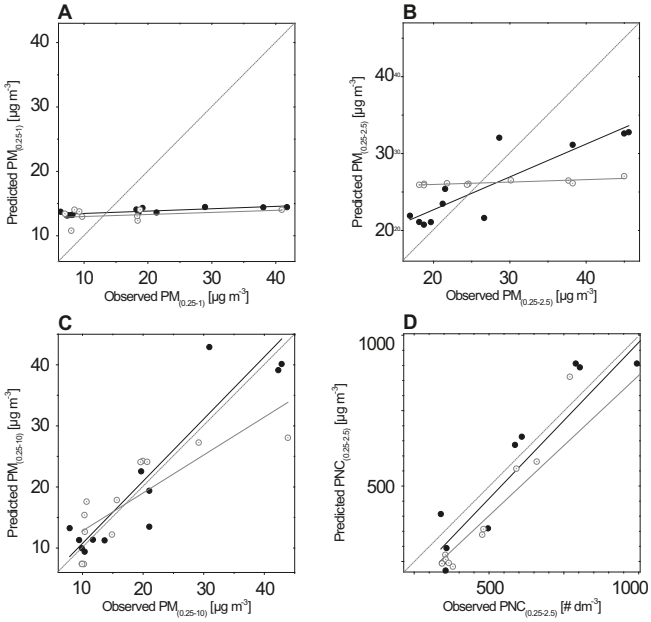

Figure 7. Scatter plot diagram showing Artificial Neural Network (ANN) model predictions of (**A**) $PM_{(0.25–1)}$, (**B**) $PM_{(0.25–2.5)}$, (**C**) $PM_{(0.25–10)}$ and (**D**) $PNC_{(0.25–2.5)}$ over respective observations for the "Münster-Aasee" test case. The dashed line illustrates a 1:1 reproduction of ANN models predictions over observations. The thin solid lines indicate linear regression results between the samples of ANN model predictions and observations. Black marks depict results of ANN models using additional acoustic data inputs whereas grey marks indicate results of ANN models using inputs without acoustic data.

Performance measures as well as statistics concerning the test samples of measurement data are summarized in Table 4. From the perspective of mean value reproduction that is indicated by the FB observations were reproduced well with ANN models using acoustic data input that showed also good response to the inputs (cf. Figures 6 and 7) with predictions close to $\overline{C_O}$ (FB: −0.02–0.13). Results of ANN models using acoustic data that proved to be insensitive to the inputs unveiled also increased FBs with either tendencies of over prediction in the case of $PM_{(0.25–1)}$ and $PM_{(0.25–2.5)}$ within the "Aachen-Karlsgraben" test environment (FB: −0.17–−0.22) or under prediction in the case of $PM_{(0.25–1)}$ within the "Münster-Aasee" test environment (FB: 0.30). The comparison of standard deviations of observations (SD) and predictions (SD'), respectively, add to the picture that ANN models used to predict concentrations of $PM_{(0.25–1)}$ were completely insensitive to input parameters.

Table 4. Artificial Neural Network (ANN) model performance measures and test set statistics including coefficients of determination between the observation and prediction sample (R^2) as well as the respective slopes of the regression lines, mean particle concentration values, standard deviations of the observations (SD) and standard deviations of predictions (SD') of the "Aachen-Karlsgraben" and "Münster-Aasee" test cases, respectively. Values in brackets indicate results derived from alternative ANN models using input variables excluding acoustic data.

OL	"Aachen-Karlsgraben"				"Münster-Aasee"			
	$PM_{(0.25–1)}$	$PM_{(0.25–2.5)}$	$PM_{(0.25–10)}$	$PNC_{(0.25–2.5)}$	$PM_{(0.25–1)}$	$PM_{(0.25–2.5)}$	$PM_{(0.25–10)}$	$PNC_{(0.25–2.5)}$
RMSE	5.97 (4.27) [µg·m^{-3}]	6.88 (5.09) [µg·m^{-3}]	7.78 (9.35) [µg·m^{-3}]	167 (208) [#·dm^{-3}]	12.29 (10.11) [µg·m^{-3}]	5.71 (5.66) [µg·m^{-3}]	6.50 (8.92) [µg·m^{-3}]	205 (259) [#·dm^{-3}]
FB	−0.17 (0.14)	−0.22 (−0.09)	−0.02 (−0.04)	−0.02 (−0.01)	0.30 (0.16)	−0.04 (0.00)	0.06 (0.06)	0.13 (0.37)
MEF	−1.15 (−0.27)	−0.89 (−0.41)	0.31 (0.05)	0.25 (0.26)	−0.01 (0.11)	0.82 (0.67)	0.64 (0.13)	0.85 (0.78)
R^2	0.05 (0.16)	0.13 (0.35)	0.48 (0.14)	0.28 (0.26)	0.70 (0.11)	0.85 (0.65)	0.78 (0.69)	0.89 (0.90)
slope	0.24 (0.01)	0.02 (0.81)	0.18 (0.02)	0.11 (0.17)	0.03 (0.11)	1.02 (0.62)	0.43 (0.03)	1.04 (0.93)
SD'	4.34 (0.02) [µg·m^{-3}]	0.32 (5.93) [µg·m^{-3}]	2.43 (0.62) [µg·m^{-3}]	41 (82) [#·dm^{-3}]	0.54 (1.06) [µg·m^{-3}]	14.84 (7.66) [µg·m^{-3}]	5.21 (0.36) [µg·m^{-3}]	591 (539) [#·dm^{-3}]
SD	4.07 (3.78) [µg·m^{-3}]	5.01 (4.29) [µg·m^{-3}]	9.39 (9.62) [µg·m^{-3}]	194 (241) [#·dm^{-3}]	12.24 (10.78) [µg·m^{-3}]	13.39 (9.91) [µg·m^{-3}]	10.79 (9.57) [µg·m^{-3}]	538 (554) [#·dm^{-3}]
$\overline{C_O}$	16.3 (15.6) [µg·m^{-3}]	20.0 (19.2) [µg·m^{-3}]	30.0 (31.8) [µg·m^{-3}]	518 (542) [#·dm^{-3}]	18.6 (15.5) [µg·m^{-3}]	21.7 (17.3) [µg·m^{-3}]	27.3 (27.7) [µg·m^{-3}]	652 (662) [#·dm^{-3}]

OL: Output Layer; RMSE: Root Mean Squared Error; FB: Fractional Bias; MEF: Model Efficiency score; R^2: coefficient of determination; slope: slope of the regression line between observation and prediction samples; SD': Standard Deviations of predictions; SD: Standard Deviation of observations; $\overline{C_O}$: mean concentration of observations

Figure 8 represents the testing results of all ANN models developed for the prediction of $PM_{(0.25–1)}$, $PM_{(0.25–2.5)}$, $PM_{(0.25–10)}$ and $PNC_{(0.25–2.5)}$ concentrations using the graphical approach of the target diagram as described in Section 2.5. Despite the fact that the CRMSE becomes always positive by its own mathematical definition (cf. Equation (5)), a minus-sign has been allocated to distinguish those situations when the standard deviation of predictions was lower than σ_O [54]. Most target values calculated from ANN model results are located in the left side of the diagram, i.e., the normalized CRMSE values are negative, indicating that those ANN model predictions vary within a narrower range than observations. The predictions for $PM_{(0.25–1.0)}$ and $PM_{(0.25–2.5)}$ from the "Aachen-Karlsgraben" test case as well as predictions for $PM_{(0.25–1)}$ from the "Münster-Aasee" test case feature negative MEF values (c.f. Table 4) so that respective target values are consequently plotted outside the boundary circle of the target diagram. Thus, a positive MEF was reached for predictions of $PM_{(0.25–10)}$ and

$PNC_{(0.25–2.5)}$ in the "Aachen-Karlsgraben" test case (MEF: 0.31–0.25) as well as for predictions of $PM_{(0.25–2.5)}$, $PM_{(0.25–10)}$ and $PNC_{(0.25–2.5)}$ in the "Münster-Aasee" test case (MEF: 0.64–0.85) resulting in depictions of target values inside the circumference of the target diagram. Considering MEF ANN models using the complete input incorporating SPL_{eq} almost always outperformed ANN models using input without acoustic data in especially for target results depicted within the boundary circle of the diagram (see Figure 8). For test cases where model results feature positive MEF scores ANN models using SPL_{eq} were almost always more accurate indicated by lower RMSEs in comparison to ANN models using input without acoustic data except for the case of $PM_{(0.25–2.5)}$ predictions (see Table 4).

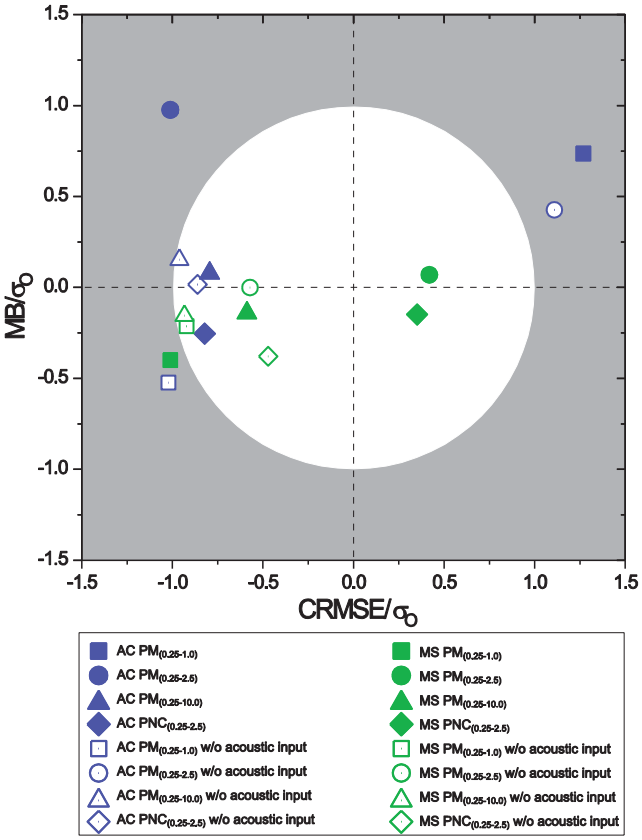

Figure 8. Target diagram of Artificial Neural Network (ANN) model results for $PM_{(0.25–1)}$ (rectangles), $PM_{(0.25–2.5)}$ (circles), $PM_{(0.25–10)}$ (triangles) and $PNC_{(0.25–2.5)}$ (rhombuses). Purple markers depict "Aachen-Karlsgraben" test case results. Green markers depict "Münster-Aasee" test case results. Filled and hollow markers differentiate between model results using acoustic input data and calculations without acoustic data input.

4. Discussion

4.1. Interpretation of ANN Model Results

The proposed ANN models using inputs of background particle transport, meteorology and acoustics to predict atmospheric concentrations of $PM_{(0.25–1)}$, $PM_{(0.25–2.5)}$, $PM_{(0.25–10)}$ and $PNC_{(0.25–2.5)}$ show mixed results regarding their performance within two test cases, i.e., by the use of a dataset that was collected in an isolated street canyon ("Aachen-Karlsgraben") as well as with data from a park area containing complex terrain ("Münster-Aasee"). Best performing ANN models within the "Aachen-Karlsgraben" test case were found to be for predicting concentrations of $PM_{(0.25–10)}$ and $PNC_{(0.25–2.5)}$ indicated by positive MEF values (MEF: 0.25–0.31), coefficients of determinations of 0.28 and 0.48, respectively, and nearly perfect FBs of −0.02. However, the variation within the prediction

sample was considerably lower in comparison to observations. Using data of the "Münster-Aasee" test case, the ANN model to predict concentrations of $PM_{(0.25–10)}$ turned out to perform fairly good featuring a MEF of 0.64, a R^2 of 0.78 and a FB of 0.01. Models to predict concentrations of $PM_{(0.25–2.5)}$ and $PNC_{(0.25–2.5)}$ reproduced observations rather accurate over the entire concentration range considering high MEF scores (MEF: 0.82–0.85) and coefficients of determination close to 1.0 (R^2: 0.87–0.89). However, up to now air quality modelers have not yet agreed upon the magnitude of standards for judging model performance [58]. As advised by [59], a model should be considered acceptable when most of its predictions are within a factor of two of the observations. The JRC of the European Commission has formulated an approach towards a more exhaustive indication of model response taking into account a consensus set of statistical measures by the development of the MEF and the graphical approach of the target value, as described in Section 2.5. In this regard the best performing ANN models developed in this study, i.e., to predict concentrations of $PM_{(0.25–10)}$ and $PNC_{(0.25–2.5)}$ within the "Aachen-Karlsgraben" test case and to estimate concentrations of $PM_{(0.25–2.5)}$, $PNC_{(0.25–2.5)}$ and $PM_{(0.25–10)}$ concentration within the "Münster-Aasee" campaign, yielded acceptable results meeting the quality objectives concerning MEF. According to [60] it is guaranteed that the ANN model is a better predictor of the observations than a constant value set to $\overline{C_O}$ when target values are depicted inside the circumference of the target diagram, i.e., when the MEF is >0. In the context of the European Framework Air Quality Directive, the proposed methodology, with regard to $PM_{(0.25–10)}$ and $PNC_{(0.25–2.5)}$ within the case of the street-canyon and $PM_{(0.25–2.5)}$, $PNC_{(0.25–2.5)}$ and $PM_{(0.25–10)}$ within the Münster park area test case, fulfills the requirements for estimations in terms of uncertainty and accuracy for mean value predictions [56]. Furthermore, the ANN model using additional acoustic data input proposed to predict concentrations of $PM_{(0.25–10)}$ within the "Münster-Aasee" test case produced better results regarding RMSE (7.78 $\mu g \cdot m^{-3}$) than the approach of [30], who were calculating hourly averages of PM_{10} using an ANN model approach with input data of traffic counts derived from motion picture in the city of Guangzhou. They reached RMSEs of 20.7–57.5 $\mu g \cdot m^{-3}$ for different locations, however, with no mention about the mean concentration of observations. Still, there is room for improvement concerning both the overall uncertainty of the ANN models considered, determined by the RMSE (see Table 4), and the narrower range of variation of predictions over observations, in particular in the street canyon test case, indicated by negative normalized CRMSE (see Figure 8). Concentration predictions of $PM_{(0.25–1.0)}$ and $PM_{(0.25–2.5)}$ within the test case "Aachen-Karlsgraben" as well as of $PM_{(0.25–1)}$ within the "Münster-Aasee" test case cannot be considered satisfactory, given negative MEF values throughout (see Table 4) as well as a seriously limited variation range of prediction values over observations (see Figures 6 and 7).

For the isolated street canyon of the "Aachen-Karlsgraben" test case predictions of particle fractions represented by $PM_{(0.25–1)}$ and $PM_{(0.25–2.5)}$ could not be successfully reproduced by the proposed methodology. In general, motor traffic emits both secondary and primary aerosols [8,61,62]. However, particles are underlying several aging processes, like e.g., the processes of coagulation or impaction [42], and therefore accrue over time. In an isolated street canyon under conditions of inhibited dilution (cf. Section 2.3) it can be stated that the local particle size distribution transforms over time due to e.g., growth processes resulting in a loss of total particle number towards a gain for the total volume concentration [63,64]. This effect was expected to occur especially when traffic-induced particle emissions decreased during evening hours or at night. Besides, the particle source of domestic heating could have had an influence on local background particle concentration of PM_{10} since the measurement campaign took place during the winter season. The input variables considered for the development of the ANN model only partly account for the particle source of local domestic heating by the use of PM_{10} (bc) (cf. Section 2.2.2). All these processes could have led to decreasing levels of concentrations of $PM_{(0.25–1)}$ (and partly of $PM_{(0.25–2.5)}$) not in the same extent as the decrease of concentrations of $PNC_{(0.25–2.5)}$ in the street canyon at times where the total motor traffic was decreasing. At those times a critical amount of noise was added to the sample so that the ANN models, using the considered input variables, were consequently not able to reproduce observations. Overall, the results presented for the

"Aachen-Karlsgraben" campaign reflect the findings that correlations between sound pressure levels and aerosol concentrations are generally higher for small particle fractions [7,10–14], here represented by $PNC_{(0.25–2.5)}$ in comparison to coarse particle fractions where the correlation in general was found to be weak [12,14,15]. Good model performance regarding the prediction of $PM_{(0.25–2.5)}$, $PM_{(0.25–10)}$ and $PNC_{(0.25–2.5)}$ within the "Münster-Aasee" test case was expected due to the spatial variation of measurement locations (cf. Section 2.1.2). The relationship of decreasing concentrations of particle mass and number concentrations as well as of motor traffic sound with increasing spatial distance to respective sources in particular downwind from emissions [65] is well documented [14,20,66] and could be reproduced with the ANN model approach. The poor performance of the ANN models concerning predictions of $PM_{(0.25–1)}$ using the "Münster-Aasee" data set could have been due to both physical reasons, as mentioned above for the street canyon test case, or methodical reasons. The size of the sample of the "Münster-Aasee" test case is rather small (cf. Section 2.3). Concerning the recommendations of [47], in consequence, the size of the training data set within the "Münster-Aasee" test case might have been critical for the number of weights and biases apparent in the network used to predict concentrations of $PM_{(0.25–1)}$ (cf. Section 2.2.4). However, due to the small size of the "Münster-Aasee" data set further analysis of subsets of data, i.e., according to separated measurement locations, wind directions or different seasons, has not been possible.

4.2. Limitations and Future Aspects

Attention must be paid to ANN models, besides that those models can often represent relationships with surprising accuracy, which are not fully understood by the traditional theory, due to the inherent "black-box" nature of the neural network approach. The "black-box" nature of ANN models restricts the usefulness in regard to increase the knowledge of physical processes, and the interaction of driving mechanisms [25]. Furthermore, by definition, ANN models work only for a variety of data the network is trained for. Extrapolation is not possible [33], i.e., extreme or uncommon events cannot be reproduced. Hence, for an operational application, ANN models should be repeatedly updated with observational data to guarantee that they are not out of range [22]. Overall, the methodology proposed is far from an operational type of model to predict aerosol concentrations yet. Several simplifying assumptions have been made in the process of the ANN model development: (I) The data set that was used to develop the ANN models was collected during winter time in an isolated street-canyon. For simplifying purposes the research site has been deliberately defined to keep effects of potential particle sources besides motor traffic emissions due to resuspension, sometimes found in areas characterized by surfaces of dried-out soil [66], Volatile Organic Compound (VOC) emissions or nearby industrial activities to a minimum. (II) Local domestic heating was potentially underrepresented by the input variables that were considered as representatives for particle sources (cf. Section 4.1). (III) The ANN models were developed under conditions avoiding periods of precipitation. Changed sound characteristics (e.g., changed rolling sound of motor traffic on wet lanes of traffic) as well as a dramatic influence on particle concentrations due to take-off mechanisms like the "wash-out" effect after precipitation events [42] can be expected. All these shortcomings could lead to an addition of a critical amount of noise to input data, when the approach is applied at locations where the simplified conditions of an isolated street canyon may not hold, and could consequently result in unsatisfactory ANN model predictions. In future research regarding the improvement of the proposed ANN model approach towards an operational model those issues as raised above should be addressed. Further refinement concerning the meteorological input of the ANN model could be possible by using information about atmospheric stability parameters like e.g., the Richardson number or mixing height [22,29]. Future viability of the approach is likely, although a transformation of the vehicle fleet, potentially towards a bigger share of electric vehicles, will continue. There is proved to be an impact on PM concentrations with an estimated future decrease in particle concentrations due to a transformed vehicle fleet composition, particularly affecting fine and ultrafine particle fraction as well as the total number concentration [67]. However, even a change towards 100% electric vehicles will

cause a merely small decrease in concentrations of coarse particles (3–4 $\mu g \cdot m^{-3}$ regarding PM_{10} in Germany according to [8]) due to the fact that the major part of traffic-induced emissions of particle mass originates from non-exhaust sources [61,62].

5. Conclusions

In this study, a methodology of a statistical model based on the ANN approach for predictions of particle concentration metrics in the urban roughness layer near road arterials using input data of sound, background concentration of PM_{10} and meteorology is presented. ANN models were developed and tested using a data set that was collected in a street canyon in the city of Aachen. The approach was tested against an ANN model using the more traditional method of using inputs of only meteorology and background concentration of PM_{10}. Given the particular consideration of sound input variable selection using PMI it turned out that the metric of SPL_{eq} includes the maximum predictive information regarding motor traffic-induced aerosol sources. Results highlight that the ANN models considered within the "Aachen-Karlsgraben" test case were able to reproduce observations of $PM_{(0.25–10)}$ and $PNC_{(0.25–2.5)}$ satisfactorily, even though results reveal some difficulties in estimating the individual sample concentrations. The prediction samples showed less variation than observations. Still, in this case, ANN models were able to meet the standards of the European Commission regarding MEF and the approach of the target diagram, respectively and can be considered valid for the estimation of mean values also indicated by almost perfect mean value reproduction represented through FBs of around zero. The ANN approach considered was furthermore carried out to a park area in the city of Münster to test the performance of the ANN models developed beyond an isolated street canyon by the use of a data set that was collected in an intra urban park area at three different locations up to 100 m away from a main road arterial. Results highlight that predictions of $PM_{(0.25–2.5)}$, $PM_{(0.25–10)}$ and $PNC_{(0.25–2.5)}$within the "Münster-Aasee" test case show very good agreement in comparison to observations fulfilling also the requirements regarding MEF. However, the ANN models left also room for improvement especially when it comes to the prediction of $PM_{(0.25–1)}$ and $PM_{(0.25–2.5)}$ within the street canyon of the "Aachen-Karlsgraben" test case as well as of $PM_{(0.25–1)}$ within the "Münster-Aasee" test case. Reasons were estimated to be inherent limitations during the input stage of the ANN models, i.e., several source categories of particles, which were not covered with the input variables considered such as sources of local domestic heating, which added a critical amount of stochastic effects to the data set in order that a reproduction of observations was impossible. It has to be mentioned that especially in the "Münster-Aasee" test case the samples used to develop the ANN models were rather small. Thus, model performance could have had been weak in consequence. Moreover, data collection took place under simplified conditions only. Rainy periods as well as high wind speeds were avoided. In order to refine the ANN models proposed towards operational applications data samples should be extended and include all relevant real world meteorological conditions. Overall, it could be proved that acoustic data input contributes to ANN model performance regarding the prediction of particle concentrations for almost all test cases.

It can be concluded that the ANN model approach developed in this study can be useful and at least in parts a fairly accurate tool of assessment in predicting particle concentrations. Given that input variables were carefully chosen using appropriate site- and time-specific data as well as recommended variable selection techniques by the use of PMI and after successful network training, its application requires less effort than performing deterministic model computations. However, the ANN models developed also feature several limitations, namely the "black-box" character inherent in the ANN approach and the restriction to work only for a variety of data the network is trained for in order that predictions of uncommon or extreme events is impossible. Another important limitation for practical applications is the dependency on training with locally measured data. Initial measurements of particle concentrations, permanent collection of acoustic data—although cost-effective in relation to particle measurement equipment—data of background particle transport and meteorological data are still needed. As another result, the model is restricted to "now-cast". For the purpose of particle

concentration forecasting future development basing on the presented ANN model approach could use forecasts of urban acoustic models, numerical weather prediction models as well as meso-scale background particle transport models as input vectors. In comparison to ANN model approaches that are basing on inputs of traffic counts this study demonstrates the application of ANN models for predicting spatial concentration distributions in urban areas due to the model input of sound.

Acknowledgments: This study has been carried out within the project Urban Future Outline (UFO) as part of the interdisciplinary Project House HumTec (Human Technology Center) at RWTH Aachen University funded by the Excellence Initiative of the German federal and state governments. We acknowledge O. Klemm and G. Ketzler for providing measurement data of the weather stations operated by the University of Münster and the RWTH Aachen University, respectively. This study would not have been possible without the data. We thank all students who supported the field work as well as two anonymous reviewers and the scientific editor of this special issue for very helpful comments that helped to improve the quality of the manuscript.

Author Contributions: Bastian Paas designed and performed the experiments, developed the model, analyzed the data and wrote the paper. Jonas Stienen contributed to the experiments through acoustic data collection, calibration and pre-processing. Jonas Stienen, Michael Vorländer and Christoph Schneider reviewed and edited the paper.

Conflicts of Interest: The authors declare no conflict of interest.

References

1. Babisch, W. *Chronischer Lärm als Risikofaktor für den Myokardinfarkt*; Ergebnisse der "NaRoMI"-Studie; Umweltbundesamt: Wien, Austria, 2004; pp. 1–159.
2. Raaschou-Nielsen, O.; Andersen, Z.J.; Beelen, R.; Samoli, E.; Stafoggia, M.; Weinmayr, G.; Hoffmann, B.; Fischer, P.; Nieuwenhuijsen, M.J.; Brunekreef, B.; et al. Air pollution and lung cancer incidence in 17 European cohorts: Prospective analyses from the European Study of Cohorts for Air Pollution Effects (ESCAPE). *Lancet Oncol.* **2013**, *14*, 813–822. [CrossRef]
3. Belis, C.A.; Karagulian, F.; Larsen, B.R.; Hopke, P.K. Critical review and meta-analysis of ambient particulate matter source apportionment using receptor models in Europe. *Atmos. Environ.* **2013**, *69*, 94–108. [CrossRef]
4. Morawska, L.; Thomas, S.; Gilbert, D.; Greenaway, C.; Rijnders, E. A study of the horizontal and vertical profile of submicrometer particles in relation to a busy road. *Atmos. Environ.* **1999**, *33*, 1261–1274. [CrossRef]
5. Kassomenos, P.A.; Kelessis, A.; Paschalidou, A.K.; Petrakakis, M. Identification of sources and processes affecting particulate pollution in Thessaloniki, Greece. *Atmos. Environ.* **2011**, *45*, 7293–7300. [CrossRef]
6. Karagulian, F.; Belis, C.A.; Dora, C.F.C.; Prüss-Ustün, A.M.; Bonjour, S.; Adair-Rohani, H.; Amann, M. Contributions to cities' ambient particulate matter (PM): A systematic review of local source contributions at global level. *Atmos. Environ.* **2015**, *120*, 475–483. [CrossRef]
7. Weber, S. Spatio-temporal covariation of urban particle number concentration and ambient noise. *Atmos. Environ.* **2009**, *43*, 5518–5525. [CrossRef]
8. Wurzler, S.; Hebbinghaus, H.; Steckelbach, I.; Schulz, T.; Pompetzki, W.; Memmesheimer, M.; Jakobs, H.; Schöllnhammer, T.; Nowag, S.; Diegmann, V. Regional and local effects of electric vehicles on air quality and noise. *Meteorol. Z.* **2016**, *25*, 319–325.
9. Dekoninck, L.; Botteldooren, D.; Decoensel, B.; Int Panis, L. Spectral noise measurements supply instantaneous traffic information for multidisciplinary mobility and traffic related projects. In Proceedings of the 45th International Congress and Exposition on Noise Control Engineering (Internoise 2016): Towards a Quieter Future, Hamburg, Germany, 21–24 August 2016.
10. Fernández-Camacho, R.; Brito Cabeza, I.; Aroba, J.; Gómez-Bravo, F.; Rodríguez, S.; de la Rosa, J. Assessment of ultrafine particles and noise measurements using fuzzy logic and data mining techniques. *Sci. Total Environ.* **2015**, *512–513*, 103–113. [CrossRef] [PubMed]
11. Allen, R.W.; Davies, H.; Cohen, M.A.; Mallach, G.; Kaufman, J.D.; Adar, S.D. The spatial relationship between traffic-generated air pollution and noise in 2 US cities. *Environ. Res.* **2009**, *109*, 334–342. [CrossRef] [PubMed]
12. Boogaard, H.; Borgman, F.; Kamminga, J.; Hoek, G. Exposure to ultrafine and fine particles and noise during cycling and driving in 11 Dutch cities. *Atmos. Environ.* **2009**, *43*, 4234–4242. [CrossRef]
13. Can, A.; Rademaker, M.; van Renterghem, T.; Mishra, V.; van Poppel, M.; Touhafi, A.; Theunis, J.; de Baets, B.; Botteldooren, D. Correlation analysis of noise and ultrafine particle counts in a street canyon. *Sci. Total Environ.* **2011**, *409*, 564–572. [CrossRef] [PubMed]

14. Shu, S.; Yang, P.; Zhu, Y. Correlation of noise levels and particulate matter concentrations near two major freeways in Los Angeles, California. *Environ. Pollut.* **2014**, *193*, 130–137. [CrossRef] [PubMed]
15. Weber, S.; Litschke, T. Variation of particle concentrations and environmental noise on the urban neighbourhood scale. *Atmos. Environ.* **2008**, *42*, 7179–7183. [CrossRef]
16. International Organization for Standardization. *ISO Acoustics—Normal Equal-Loudness-Level Contours*; International Organization for Standardization, Technical Committee ISO/TC 43, Acoustics; International Organization for Standardization: Geneva, Switzerland, 2003; p. 15.
17. Borrego, C.; Costa, A.M.; Ginja, J.; Amorim, M.; Coutinho, M.; Karatzas, K.; Sioumis, T.; Katsifarakis, N.; Konstantinidis, K.; de Vito, S.; et al. Assessment of air quality microsensors versus reference methods: The EuNetAir joint exercise. *Atmos. Environ.* **2016**, *147*, 246–263. [CrossRef]
18. Daly, A.; Zannetti, P. Air Pollution Modeling–An Overview. In *Chapter 2 of AMBIENT AIR POLLUTION*; Zannetti, P., Al-Ajmi, D., Al-Rashied, S., Eds.; The Arab School for Science and Technology (ASST); The EnviroComp Institute: Fremont, CA, USA, 2007.
19. Lateb, M.; Meroney, R.N.; Yataghene, M.; Fellouah, H.; Saleh, F.; Boufadel, M.C. On the use of numerical modelling for near-field pollutant dispersion in urban environments—A review. *Environ. Pollut.* **2016**, *208*, 271–283. [CrossRef] [PubMed]
20. Paas, B.; Schneider, C. A comparison of model performance between ENVI-met and Austal2000 for particulate matter. *Atmos. Environ.* **2016**, *145*, 392–404. [CrossRef]
21. Vlachogianni, A.; Kassomenos, P.; Karppinen, A.; Karakitsios, S.; Kukkonen, J. Evaluation of a multiple regression model for the forecasting of the concentrations of NO_x and PM_{10} in Athens and Helsinki. *Sci. Total Environ.* **2011**, *409*, 1559–1571. [CrossRef] [PubMed]
22. Santos, G.; Fernández-Olmo, I. A proposed methodology for the assessment of arsenic, nickel, cadmium and lead levels in ambient air. *Sci. Total Environ.* **2016**, *554–555*, 155–166. [CrossRef] [PubMed]
23. Merbitz, H.; Buttstädt, M.; Michael, S.; Dott, W.; Schneider, C. GIS-based identification of spatial variables enhancing heat and poor air quality in urban areas. *Appl. Geogr.* **2012**, *33*, 94–106. [CrossRef]
24. Merbitz, H.; Fritz, S.; Schneider, C. Mobile measurements and regression modeling of the spatial particulate matter variability in an urban area. *Sci. Total Environ.* **2012**, *438*, 389–403. [CrossRef] [PubMed]
25. Gardner, M.W.; Dorling, S.R. Artificial neural networks (the multilayer perceptron)—A review of applications in the atmospheric sciences. *Atmos. Environ.* **1998**, *32*, 2627–2636. [CrossRef]
26. Kukkonen, J. Extensive evaluation of neural network models for the prediction of NO_2 and PM_{10} concentrations, compared with a deterministic modelling system and measurements in central Helsinki. *Atmos. Environ.* **2003**, *37*, 4539–4550. [CrossRef]
27. Wu, W.; Dandy, G.C.; Maier, H.R. Protocol for developing ANN models and its application to the assessment of the quality of the ANN model development process in drinking water quality modelling. *Environ. Model. Softw.* **2014**, *54*, 108–127. [CrossRef]
28. Gardner, M.W.; Dorling, S.R. Neural network modelling and prediction of hourly NO_x and NO_2 concentrations in urban air in London. *Atmos. Environ.* **1999**, *33*, 709–719. [CrossRef]
29. Hooyberghs, J.; Mensink, C.; Dumont, G.; Fierens, F.; Brasseur, O. A neural network forecast for daily average PM concentrations in Belgium. *Atmos. Environ.* **2005**, *39*, 3279–3289. [CrossRef]
30. Cai, M.; Yin, Y.; Xie, M. Prediction of hourly air pollutant concentrations near urban arterials using artificial neural network approach. *Transp. Res. Part Transp. Environ.* **2009**, *14*, 32–41. [CrossRef]
31. Kraftfahrtbundesamt Zentrales Fahrzeugregister. Available online: http://www.kba.de/cln_031/nn_191172/DE/Statistik/Fahrzeuge/Bestand/FahrzeugklassenAufbauarten/b__fzkl__zeitreihe.html (accessed on 15 October 2016).
32. Hájek, P.; Olej, V. Ozone prediction on the basis of neural networks, support vector regression and methods with uncertainty. *Ecol. Inform.* **2012**, *12*, 31–42. [CrossRef]
33. Maier, H.R.; Jain, A.; Dandy, G.C.; Sudheer, K.P. Methods used for the development of neural networks for the prediction of water resource variables in river systems: Current status and future directions. *Environ. Model. Softw.* **2010**, *25*, 891–909. [CrossRef]
34. Günther, F.; Fritsch, S. neuralnet: Training of Neural Networks. *R J.* **2016**, *2*, 30–38.
35. Razavi, S.; Tolson, B.A. A New Formulation for Feedforward Neural Networks. *IEEE Trans. Neural Netw.* **2011**, *22*, 1588–1598. [CrossRef] [PubMed]

36. Stamenković, L.J.; Antanasijević, D.Z.; Ristić, M.Đ.; Perić-Grujić, A.A.; Pocajt, V.V. Modeling of ammonia emission in the USA and EU countries using an artificial neural network approach. *Environ. Sci. Pollut. Res.* **2015**, *22*, 18849–18858. [CrossRef] [PubMed]
37. May, R.J.; Maier, H.R.; Dandy, G.C.; Fernando, T.M.K.G. Non-linear variable selection for artificial neural networks using partial mutual information. *Environ. Model. Softw.* **2008**, *23*, 1312–1326. [CrossRef]
38. Manousakas, M.; Papaefthymiou, H.; Diapouli, E.; Migliori, A.; Karydas, A.G.; Bogdanovic-Radovic, I.; Eleftheriadis, K. Assessment of PM2.5 sources and their corresponding level of uncertainty in a coastal urban area using EPA PMF 5.0 enhanced diagnostics. *Sci. Total Environ.* **2017**, *574*, 155–164. [CrossRef] [PubMed]
39. Morelli, X.; Foraster, M.; Aguilera, I.; Basagana, X.; Corradi, E.; Deltell, A.; Ducret-Stich, R.; Phuleria, H.; Ragettli, M.S.; Rivera, M.; et al. Short-term associations between traffic-related noise, particle number and traffic flow in three European cities. *Atmos. Environ.* **2015**, *103*, 25–33. [CrossRef]
40. Merbitz, H. Feinstaubkonzentration in Abhängigkeit von Witterung und Großwetterlagen im Raum Aachen. *Aachen. Geogr. Arb.* **2009**, *46*, 121–134.
41. Merbitz, H.; Ketzler, G.; Schneider, C. Untersuchungen zu den Windverhältnissen im Innenstadtbereich von Aachen. *Aachen. Geogr. Arb.* **2010**, *Heft 46*, 97–116.
42. Seinfeld, J.H.; Pandis, S.N. *Atmospheric Chemistry and Physics: From Air Pollution to Climate Change*, 2nd ed.; John Wiley: Hoboken, NJ, USA, 2006.
43. Sandberg, U.; Ejsmont, J.A. *Tyre/Road Noise Reference Book*; INFORMEX: Kisa, Sweden; Harg, Sweden, 2002.
44. Bowden, G.J.; Dandy, G.C.; Maier, H.R. Input determination for neural network models in water resources applications. Part 1—background and methodology. *J. Hydrol.* **2005**, *301*, 75–92. [CrossRef]
45. Fernando, T.M.K.G.; Maier, H.R.; Dandy, G.C. Selection of input variables for data driven models: An average shifted histogram partial mutual information estimator approach. *J. Hydrol.* **2009**, *367*, 165–176. [CrossRef]
46. May, R.J.; Maier, H.R.; Dandy, G.C. Data splitting for artificial neural networks using SOM-based stratified sampling. *Neural Netw.* **2010**, *23*, 283–294. [CrossRef] [PubMed]
47. Johnson, S.R.; Jurs, P.C. Prediction of the Clearing Temperatures of a Series of Liquid Crystals from Molecular Structure. *Chem. Mater.* **1999**, *11*, 1007–1023. [CrossRef]
48. Rumelhart, D.E.; Hinton, G.E.; Williams, R.J. Learning representations by back-propagating errors. *Nature* **1986**, *323*, 533–536. [CrossRef]
49. Bishop, C.M. *Neural Networks for Pattern Recognition*; Clarendon Press: Oxford, UK; Oxford University Press: Oxford, UK; New York, NY, USA, 1995.
50. Grimm, H.; Eatough, D.J. Aerosol Measurement: The Use of Optical Light Scattering for the Determination of Particulate Size Distribution, and Particulate Mass, Including the Semi-Volatile Fraction. *J. Air Waste Manag. Assoc.* **2009**, *59*, 101–107. [CrossRef] [PubMed]
51. LANUV Umgebungslärm in NRW. Available online: http://www.umgebungslaerm-kartierung.nrw.de/ (accessed on 5 December 2016).
52. Schneider, C.; Ketzler, G. *Klimamessstation Aachen-Hörn—Monatsberichte Februar, Mai, September/2014*; Lehr- und Forschungsgebiet Physische Geographie und Klimatologie, Geographisches Institut, RWTH Aachen: Aachen, Germany, 2016.
53. Sousa, S.; Martins, F.; Alvimferraz, M.; Pereira, M. Multiple linear regression and artificial neural networks based on principal components to predict ozone concentrations. *Environ. Model. Softw.* **2007**, *22*, 97–103. [CrossRef]
54. Pederzoli, A.; Thunis, P.; Georgieva, E.; Borge, R.; Carruthers, D. Performance criteria for the benchmarking of air quality model regulatory applications: The "target" aproach. In Proceedings of the 14th Conference on Harmonisation within Atmospheric Dispersion Modelling for Regulatory Purposes Kos, Greece, 2–6 October 2011; pp. 297–301.
55. Taylor, K.E. Summarizing multiple aspects of model performance in a single diagram. *J. Geophys. Res. Atmos.* **2001**, *106*, 7183–7192. [CrossRef]
56. Thunis, P.; Georgieva, E.; Pederzoli, A. A tool to evaluate air quality model performances in regulatory applications. *Environ. Model. Softw.* **2012**, *38*, 220–230. [CrossRef]
57. Cox, W.M.; Tikvart, J.A. A statistical procedure for determining the best performing air quality simulation model. *Atmos. Environ. Part Gen. Top.* **1990**, *24*, 2387–2395. [CrossRef]
58. Yassin, M.F. Numerical modeling on air quality in an urban environment with changes of the aspect ratio and wind direction. *Environ. Sci. Pollut. Res.* **2013**, *20*, 3975–3988. [CrossRef] [PubMed]

59. Chang, J.C.; Hanna, S.R. Air quality model performance evaluation. *Meteorol. Atmos. Phys.* **2004**, *87*, 167–196. [CrossRef]
60. Stow, C.A.; Jolliff, J.; McGillicuddy, D.J.; Doney, S.C.; Allen, J.I.; Friedrichs, M.A.M.; Rose, K.A.; Wallhead, P. Skill assessment for coupled biological/physical models of marine systems. *J. Mar. Syst.* **2009**, *76*, 4–15. [CrossRef]
61. Ketzel, M.; Omstedt, G.; Johansson, C.; Düring, I.; Pohjola, M.; Oettl, D.; Gidhagen, L.; Wåhlin, P.; Lohmeyer, A.; Haakana, M.; et al. Estimation and validation of PM2.5/PM10 exhaust and non-exhaust emission factors for practical street pollution modelling. *Atmos. Environ.* **2007**, *41*, 9370–9385. [CrossRef]
62. Amato, F.; Cassee, F.R.; Denier van der Gon, H.A.C.; Gehrig, R.; Gustafsson, M.; Hafner, W.; Harrison, R.M.; Jozwicka, M.; Kelly, F.J.; Moreno, T.; et al. Urban air quality: The challenge of traffic non-exhaust emissions. *J. Hazard. Mater.* **2014**, *275*, 31–36. [CrossRef] [PubMed]
63. Gidhagen, L.; Johansson, C.; Langner, J.; Olivares, G. Simulation of NO_x and ultrafine particles in a street canyon in Stockholm, Sweden. *Atmos. Environ.* **2004**, *38*, 2029–2044. [CrossRef]
64. Ketzel, M.; Berkowicz, R. Multi-plume aerosol dynamics and transport model for urban scale particle pollution. *Atmos. Environ.* **2005**, *39*, 3407–3420. [CrossRef]
65. Zhu, Y.; Kuhn, T.; Mayo, P.; Hinds, W.C. Comparison of Daytime and Nighttime Concentration Profiles and Size Distributions of Ultrafine Particles near a Major Highway. *Environ. Sci. Technol.* **2006**, *40*, 2531–2536. [CrossRef] [PubMed]
66. Paas, B.; Schmidt, T.; Markova, S.; Maras, I.; Ziefle, M.; Schneider, C. Small-scale variability of particulate matter and perception of air quality in an inner-city recreational area in Aachen, Germany. *Meteorol. Z.* **2016**, *25*, 305–317.
67. Soret, A.; Guevara, M.; Baldasano, J.M. The potential impacts of electric vehicles on air quality in the urban areas of Barcelona and Madrid (Spain). *Atmos. Environ.* **2014**, *99*, 51–63. [CrossRef]

Appendix A

Micro-scale variability of PM10 – Influence of vegetation elements on ground-level aerosol concentrations

Micro-scale variability of PM_{10} – Influence of vegetation elements on ground-level aerosol concentrations

Paas, Bastian [1) 3)], Schneider, Christoph [2)]

1) Department of Geography, RWTH Aachen University, Aachen, Germany
2) Department of Geography, Humboldt-Universität zu Berlin, Berlin, Germany
3) Project House HumTec, RWTH Aachen University, Aachen, Germany

Area under study / Test cases

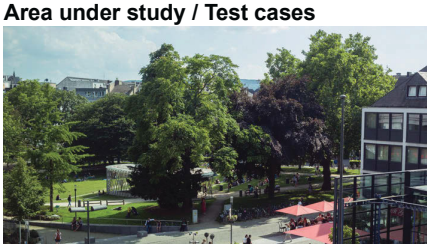

Fig. 1: Photograph of the research site from the northern end pointing to the south with the camera.

- Inner-city park area in the city of Aachen (Fig. 1), Germany
- Remote from industrial areas, complex terrain with numerous obstacles i.e. houses, vegetation elements, varying ground levels and 3 traffic lines (Fig. 2, Fig. 3)
- Six receptor points, where measurements were carried out (Fig. 2) in February and July 2014 (n = 46 hourly averages)
- Two simulation test cases: with and without vegetation elements

Fig. 2: Map of the research site with marked monitoring locations (A-F) where measurements with the OPC were carried out (black dots) and marked location where meteorological measurements as inflow boundary conditions for the model were conducted (blue dot).

The modelling software – ENVI-met

- prognostic 3d microclimate model based on CFD (κ-ε model) [1]
- pollution dispersion module to simulate the dispersion of numerous point, line and area sources of substances, e.g. PM.
- Includes particle sedimentation and deposition at surfaces
- Upstream advection approach

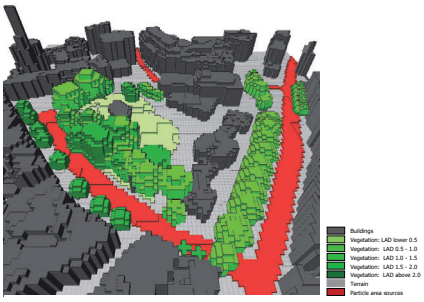

Fig. 3: 3d rendering of the used ENVI-met model domain representing the area under study.

Data handling and processing

- Measurements were carried out with a Grimm optical particle counter (OPC), model EDM107G. Background concentrations were deducted from PM_{10} measurement data using data from government air quality sites.
- Two performance measures were calculated to compare simulation results to measurement data:

1. Fractional Bias (FB) as a dimensionless and normalized measure which varies between -2 and +2 for extreme over- or under-prediction of the model. The formula is given by [2]:

$$FB = \frac{2\,(\bar{C}_P - \bar{C}_O)}{(\bar{C}_P + \bar{C}_O)}$$

$\bar{C}_P$ = predicted PM_{10} concentration
$\bar{C}_O$ = observed PM_{10} concentration

2. Robust Highest Concentration (RHC) as a criterion proofing the important high-end concentration range. A good model will provide RHCs close to RHCs calculated from observation data. The formula is given by [3]:

$$RHC = x^{(n)} + \left(x - x^{(n)}\right)\ln\left(\frac{3n-1}{2}\right)$$

n = number of values of the upper end of the concentration distribution, we used n = 15
x = average of the n-1 largest concentration values
$x^{(n)}$ = nth largest concentration value

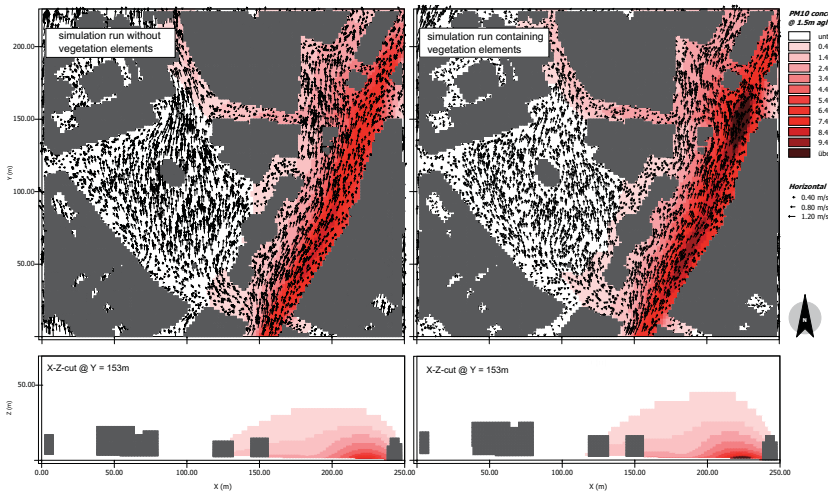

Fig 4: Predicted PM_{10} concentration distributions for depicted simulation runs without vegetation elements (left illustrations) and simulation runs containing vegetation elements (right illustrations) as 1-hr averages. Upper illustrations show results of X-Y-cuts in 1.5m agl with horizontal wind vectors. Lower illustrations show simulation results of X-Z-cuts (@ Y = 153m).

Results and Discussion

- Simulation results of runs that contained vegetations elements, i.e. trees and shrubs > 1m, indicate higher ground level (1.5m agl) PM_{10} concentrations in particular close to the particle sources (Fig. 4, Fig. 6).
- Wind speeds decreased when considering vegetation (Fig. 4).
- The model in both test cases considerably under predicted observed concentrations indicated by a high FB (Tab.1) and a rank correlation that indicates an under prediction at the lowest by the factor of 2 (Fig. 5).

Tab. 1: FB for all test cases and RHC in µg m^{-3} of observed and predicted PM_{10} concentration data.

	Observations	Simulations containing vegetation elements	Simulations without vegetation elements
Fractional bias (FB)		1.60	1.65
PM_{10} Robust highest concentration (RHC)	56.0 µg m^{-3}	11.2 µg m^{-3}	9.6 µg m^{-3}

- The model produced marginally better results when considering vegetation elements compared to measurement data espacially in the important high-end concentration range indicated by RHCs that are closer to RHCs calculated out of observation data (Tab.1) and a rank correlation that is closer to the 1:1 line in the upper concentration range.
- At average, the simulation runs without vegetation elements produced a higher number of grid-cells with mid-range PM_{10} concentration ranges (3.5 - 5.5 µg m^{-3}); the simulations containing shrubs and trees calculated results with ground-level grid-cells featuring less mid-range concentration values but in comparison featuring more high-end concentration values (5.5 - 8.5 µg m^{-3}).
- Overall, the comparison of simulation runs that were initiated with similar input data (particle sources and meteorological boundary conditions) but were conducted in different domains with and without vegetation elements shows that the effect of vegetation on ground-level PM_{10} concentrations is small. Our results indicate the influence of vegetation elements on the distribution of PM_{10} in the same magnitude of findings from other studies, e.g. [4].

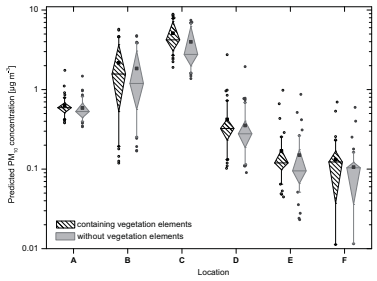

Fig. 6: Boxplot diagramm of predicted PM_{10} concentrations for all monitoring locations (A-F) comparing data of simulation runs that were conducted without vegetation elements (grey boxes) to data of simulation runs that were conducted containing vegetation elements (black boxes). Filled squares represent arithmetic means; Boxes show 25-75 percentiles; Whisker represent 10-90 percentiles; Outliers are marked with circles.

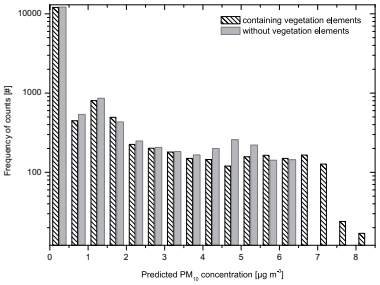

Fig. 7: Histogramm of averaged PM_{10} concentration data featuring all simulation runs over the whole study period (n = 46) at 1.5m agl simulated without vegetation elements (grey bars) and of simulation runs containing vegetation elements (black bars).

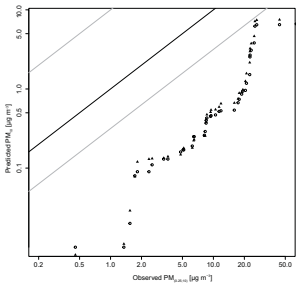

Fig. 5: Q-Q plot for predicted vs. observed PM_{10} concentrations of all the receptor points (A-F) and all the test cases as 1-hr averages. Circles represent results of the simulation runs without vegetation elements. Triangles show results of simulation runs containing vegetation elements. The black line indicates the 1:1 rank correlation of the distributions. The grey lines depict the factor of 2 over and under estimates.

Conclusions – Take home messages

- Simulation results indicate that trees and shrubs have an influence on ground-level particle distributions. PM_{10} concentrations at 1.5m agl were simulated to be marginally higher when considering vegetation elements.
- The impact of vegetation elements on the particle distribution was higher more close to the sources (traffic lines) and more pronounced in the mid- to high-end concentration range.
- Output data of ENVI-met must, as in any other case of predictive models, be interpreted with caution. Observation data were seriously under predicted in all test cases.

References

[1] Bruse, M., and H. Fleer, 1998: Simulating surface–plant–air interactions inside urban environments with a three dimensional numerical model. Environmental Modelling & Software, 13, 373–384, doi:10.1016/S1364-8152(98)00042-5.
[2] Hanna, S. R., 1988: Air Quality Model Evaluation and Uncertainty. JAPCA, 38, 406–412, doi:10.1080/08940630.1988.10466390.
[3] Perry, S. G., and Coauthors, 2005: AERMOD: A Dispersion Model for Industrial Source Applications. Part II: Model Performance against 17 Field Study Databases. Journal of Applied Meteorology, 44, 694–708, doi:10.1175/JAM2228.1.
[4] Gromke, C., and B. Blocken, 2015: Influence of avenue-trees on air quality at the urban neighborhood scale. Part II: Traffic pollutant concentrations at pedestrian level. Environmental Pollution, 196, 176–184, doi:10.1016/j.envpol.2014.10.015.

Acknowledgements

This project is part of the interdisciplinary Project House HumTec (Human Technology Center) at RWTH Aachen University. The financial support from the German federal and state governments through the German Research Foundation (Deutsche Forschungsgemeinschaft DFG) is gratefully acknowledged.

Bastian Paas, M.Sc.
Department of Geography
Wüllnerstr. 5b | 52062 Aachen | GERMANY
Telefon: +49 241 80-96454
E-Mail: bastian.paas@geo.rwth-aachen.de

Department of Geography

RWTH AACHEN UNIVERSITY

References

Abohela, I., Hamza, N., Dudek, S., 2013. Effect of roof shape, wind direction, building height and urban configuration on the energy yield and positioning of roof mounted wind turbines. Renewable Energy 50, 1106–1118. doi:10.1016/j.renene.2012.08.068

Ahmad, K., Khare, M., Chaudhry, K.K., 2005. Wind tunnel simulation studies on dispersion at urban street canyons and intersections—a review. Journal of Wind Engineering and Industrial Aerodynamics 93, 697–717. doi:10.1016/j.jweia.2005.04.002

Amato, F., Cassee, F.R., Denier van der Gon, H.A.C., Gehrig, R., Gustafsson, M., Hafner, W., Harrison, R.M., Jozwicka, M., Kelly, F.J., Moreno, T., Prevot, A.S.H., Schaap, M., Sunyer, J., Querol, X., 2014. Urban air quality: The challenge of traffic non-exhaust emissions. Journal of Hazardous Materials 275, 31–36. doi:10.1016/j.jhazmat.2014.04.053

Ambrosini, D., Galli, G., Mancini, B., Nardi, I., Sfarra, S., 2014. Evaluating Mitigation Effects of Urban Heat Islands in a Historical Small Center with the ENVI-Met® Climate Model. Sustainability 6, 7013–7029. doi:10.3390/su6107013

Andersson-Sköld, Y., Thorsson, S., Rayner, D., Lindberg, F., Janhäll, S., Jonsson, A., Moback, U., Bergman, R., Granberg, M., 2015. An integrated method for assessing climate-related risks and adaptation alternatives in urban areas. Climate Risk Management 7, 31–50. doi:10.1016/j.crm.2015.01.003

Badland, H.M., Duncan, M.J., 2009. Perceptions of air pollution during the work-related commute by adults in Queensland, Australia. Atmospheric Environment 43, 5791–5795. doi:10.1016/j.atmosenv.2009.07.050

Baumgardner, D., Varela, S., Escobedo, F.J., Chacalo, A., Ochoa, C., 2012. The role of a peri-urban forest on air quality improvement in the Mexico City megalopolis. Environmental Pollution 163, 174–183. doi:10.1016/j.envpol.2011.12.016

Bekö, G., Kjeldsen, B.U., Olsen, Y., Schipperijn, J., Wierzbicka, A., Karottki, D.G., Toftum, J., Loft, S., Clausen, G., 2015. Contribution of various microenvironments to the daily personal exposure to ultrafine particles: Personal monitoring coupled with GPS tracking. Atmospheric Environment 110, 122–129. doi:10.1016/j.atmosenv.2015.03.053

Birmili, W., Alaviippola, B., Hinneburg, D., Knoth, O., Tuch, T., Borken-Kleefeld, J., Schacht, A., 2009. Dispersion of traffic-related exhaust particles near the Berlin urban motorway – estimation of fleet emission factors. Atmospheric Chemistry and Physics 9, 2355–2374. doi:10.5194/acp-9-2355-2009

Birmili, W., Rehn, J., Vogel, A., Boehlke, C., Weber, K., Rasch, F., 2013a. Micro-scale variability of urban particle number and mass concentrations in Leipzig, Germany. Meteorol. Z. 22, 155–165. doi:10.1127/0941-2948/2013/0394

Birmili, W., Tomsche, L., Sonntag, A., Opelt, C., Weinhold, K., Nordmann, S., Schmidt, W., 2013b. Variability of aerosol particles in the urban atmosphere of Dresden (Germany): Effects of spatial scale and particle size. Meteorol. Z. 22, 195–211. doi:10.1127/0941-2948/2013/0395

Blocken, B., Tominaga, Y., Stathopoulos, T., 2013. CFD simulation of micro-scale pollutant dispersion in the built environment. Building and Environment 64, 225–230. doi:10.1016/j.buildenv.2013.01.001

Borrego, C., Costa, A.M., Ginja, J., Amorim, M., Coutinho, M., Karatzas, K., Sioumis, T., Katsifarakis, N., Konstantinidis, K., De Vito, S., Esposito, E., Smith, P., André, N., Gérard, P., Francis, L.A., Castell, N., Schneider, P., Viana, M., Minguillón, M.C., Reimringer, W., Otjes, R.P., von Sicard, O., Pohle, R., Elen, B., Suriano, D., Pfister, V., Prato, M., Dipinto, S., Penza, M., 2016. Assessment of air quality microsensors versus reference methods: The EuNetAir joint exercise. Atmospheric Environment 147, 246–263. doi:10.1016/j.atmosenv.2016.09.050

Brody, S.D., Peck, B.M., Highfield, W.E., 2004. Examining Localized Patterns of Air Quality Perception in Texas: A Spatial and Statistical Analysis. Risk Analysis 24, 1561–1574. doi:10.1111/j.0272-4332.2004.00550.x

Broich, A.V., Gerharz, L.E., Klemm, O., 2012. Personal monitoring of exposure to particulate matter with a high temporal resolution. Environ. Sci. Pollut. Res. 19, 2959–2972. doi:10.1007/s11356-012-0806-3

Brunekreef, B., Holgate, S.T., 2002. Air pollution and health. Lancet 360, 1233–1242. doi:10.1016/S0140-6736(02)11274-8

Bruse, M., Fleer, H., 1998. Simulating surface–plant–air interactions inside urban environments with a three dimensional numerical model. Environmental Modelling & Software 13, 373–384. doi:10.1016/S1364-8152(98)00042-5

Buccolieri, R., Salim, S.M., Leo, L.S., Di Sabatino, S., Chan, A., Ielpo, P., de Gennaro, G., Gromke, C., 2011. Analysis of local scale tree–atmosphere interaction on pollutant concentration in idealized street canyons and application to a real urban junction. Atmospheric Environment 45, 1702–1713. doi:10.1016/j.atmosenv.2010.12.058

Cai, M., Yin, Y., Xie, M., 2009. Prediction of hourly air pollutant concentrations near urban arterials using artificial neural network approach. Transportation Research Part D: Transport and Environment 14, 32–41. doi:10.1016/j.trd.2008.10.004

Can, A., Rademaker, M., Van Renterghem, T., Mishra, V., Van Poppel, M., Touhafi, A., Theunis, J., De Baets, B., Botteldooren, D., 2011. Correlation analysis of noise and ultrafine particle counts in a street canyon. Science of the Total Environment 409, 564–572. doi:10.1016/j.scitotenv.2010.10.037

Chang, C.-H., Meroney, R.N., 2001. Numerical and physical modeling of bluff body flow and dispersion in urban street canyons. Journal of Wind Engineering and Industrial Aerodynamics 89, 1325–1334. doi:10.1016/S0167-6105(01)00129-5

Chang, J.C., Hanna, S.R., 2004. Air quality model performance evaluation. Meteorology and Atmospheric Physics 87. doi:10.1007/s00703-003-0070-7

Chen, L., Ng, E., 2012. Outdoor thermal comfort and outdoor activities: A review of research in the past decade. Cities 29, 118–125. doi:10.1016/j.cities.2011.08.006

Chow, J.C., Watson, J.G., Mauderly, J.L., Costa, D.L., Wyzga, R.E., Vedal, S., Hidy, G.M., Altshuler, S.L., Marrack, D., Heuss, J.M., Wolff, G.T., Arden Pope III, C., Dockery, D.W., 2006. Health Effects of Fine Particulate Air Pollution: Lines that Connect. Journal of the Air & Waste Management Association 56, 1368–1380. doi:10.1080/10473289.2006.10464545

Cox, W.M., Tikvart, J.A., 1990. A statistical procedure for determining the best performing air quality simulation model. Atmospheric Environment. Part A. General Topics 24, 2387–2395. doi:10.1016/0960-1686(90)90331-G

Daly, A., Zannetti, P., 2007. Air Pollution Modeling–An Overview, in: Zannetti, P., Al-Ajmi, D., Al-Rashied, S. (Eds.), Chapter 2 of AMBIENT AIR POLLUTION. Published by The Arab School for Science and Technology (ASST) (http://www.arabschool.org.sy) and The EnviroComp Institute (http://www.envirocomp.org/).

Dias, D., Tchepel, O., Antunes, A.P., 2016. Integrated modelling approach for the evaluation of low emission zones. Journal of Environmental Management 177, 253–263. doi:10.1016/j.jenvman.2016.04.031

Dons, E., Int Panis, L., Van Poppel, M., Theunis, J., Willems, H., Torfs, R., Wets, G., 2011. Impact of time–activity patterns on personal exposure to black carbon. Atmospheric Environment 45, 3594–3602. doi:10.1016/j.atmosenv.2011.03.064

DWD, 2012. Temperatur und Niederschlag: Langjährige Mittel 1981 - 2010 [WWW Document]. URL http://www.dwd.de/DE/leistungen/klimadatendeutschland/langj_mittelwerte.html?nn=16102&lsbId=343278 (accessed 6.15.16).

EEA, E.E.A., 2016. Air quality in Europe - 2016 report (No. 28/2016). European Union, Luxembourg.

El-Harbawi, M., 2013. Air quality modelling, simulation, and computational methods: a review. Environmental Reviews 21, 149–179. doi:10.1139/er-2012-0056

Gardner, M.W., Dorling, S.R., 1998. Artificial neural networks (the multilayer perceptron)—a review of applications in the atmospheric sciences. Atmospheric Environment 32, 2627–2636. doi:10.1016/S1352-2310(97)00447-0

Gidhagen, L., Johansson, C., Langner, J., Olivares, G., 2004. Simulation of NOx and ultrafine particles in a street canyon in Stockholm, Sweden. Atmospheric Environment 38, 2029–2044. doi:10.1016/j.atmosenv.2004.02.014

Gosling, S.N., McGregor, G.R., Páldy, A., 2007. Climate change and heat-related mortality in six cities Part 1: model construction and validation. International Journal of Biometeorology 51, 525–540. doi:10.1007/s00484-007-0092-9

Grimmond, C.S.B., King, T.S., Roth, M., Oke, T.R., 1998. Aerodynamic roughness of urban areas derived from wind observations. Boundary-Layer Meteorology 89, 1–24. doi:10.1023/A:1001525622213

Gromke, C., Blocken, B., 2015. Influence of avenue-trees on air quality at the urban neighborhood scale. Part II: Traffic pollutant concentrations at pedestrian level. Environmental Pollution 196, 176–184. doi:10.1016/j.envpol.2014.10.015

Gromke, C., Buccolieri, R., Di Sabatino, S., Ruck, B., 2008. Dispersion study in a street canyon with tree planting by means of wind tunnel and numerical investigations – Evaluation of CFD data with experimental data. Atmospheric Environment 42, 8640–8650. doi:10.1016/j.atmosenv.2008.08.019

Hájek, P., Olej, V., 2012. Ozone prediction on the basis of neural networks, support vector regression and methods with uncertainty. Ecological Informatics 12, 31–42. doi:10.1016/j.ecoinf.2012.09.001

Hooyberghs, J., Mensink, C., Dumont, G., Fierens, F., Brasseur, O., 2005. A neural network forecast for daily average PM concentrations in Belgium. Atmospheric Environment 39, 3279–3289. doi:10.1016/j.atmosenv.2005.01.050

Huang, Y., Hu, X., Zeng, N., 2009. Impact of wedge-shaped roofs on airflow and pollutant dispersion inside urban street canyons. Building and Environment 44, 2335–2347. doi:10.1016/j.buildenv.2009.03.024

IT.NRW, 2015. Einwohnerzahlen im Regierungsbezirk Köln und Münster - Fortschreibung des Bevölkerungsstandes auf Basis des Zensus vom 09.05.2011 [WWW Document]. URL https://www.it.nrw.de/statistik/a/daten/bevoelkerungszahlen_zensus/zensus_rp3_juni15.html (accessed 6.15.16).

Janhäll, S., 2015. Review on urban vegetation and particle air pollution – Deposition and dispersion. Atmospheric Environment 105, 130–137. doi:10.1016/j.atmosenv.2015.01.052

Janicke, 2011. Austal2000 - Program Documentation of Version 2.4. Janicke Consulting, Dunum, Germany.

Jänicke, B., Meier, F., Hoelscher, M.-T., Scherer, D., 2015. Evaluating the Effects of Façade Greening on Human Bioclimate in a Complex Urban Environment. Advances in Meteorology 2015, 1–15. doi:10.1155/2015/747259

Johansson, E., Thorsson, S., Emmanuel, R., Krüger, E., 2014. Instruments and methods in outdoor thermal comfort studies – The need for standardization. Urban Climate 10, 346–366. doi:10.1016/j.uclim.2013.12.002

Johnson, S.R., Jurs, P.C., 1999. Prediction of the Clearing Temperatures of a Series of Liquid Crystals from Molecular Structure. Chemistry of Materials 11, 1007–1023. doi:10.1021/cm980674x

Karagulian, F., Belis, C.A., Dora, C.F.C., Prüss-Ustün, A.M., Bonjour, S., Adair-Rohani, H., Amann, M., 2015. Contributions to cities' ambient particulate matter (PM): A systematic review of local source contributions at global level. Atmospheric Environment 120, 475–483. doi:10.1016/j.atmosenv.2015.08.087

Keller, M., de Hahn, (Eds.), 2004. Handbuch Emissionsfaktoren des Straßenverkehrs 2.1. INFRAS, UBA Berlin, BUWAL Bern, UBA Wien.

Kelly, F.J., Fussell, J.C., 2012. Size, source and chemical composition as determinants of toxicity attributable to ambient particulate matter. Atmospheric Environment 60, 504–526. doi:10.1016/j.atmosenv.2012.06.039

Ketzel, M., Berkowicz, R., 2005. Multi-plume aerosol dynamics and transport model for urban scale particle pollution. Atmospheric Environment 39, 3407–3420. doi:10.1016/j.atmosenv.2005.01.058

Ketzel, M., Omstedt, G., Johansson, C., Düring, I., Pohjola, M., Oettl, D., Gidhagen, L., Wåhlin, P., Lohmeyer, A., Haakana, M., Berkowicz, R., 2007. Estimation and validation of PM2.5/PM10 exhaust and non-exhaust emission factors for practical street pollution modelling. Atmospheric Environment 41, 9370–9385. doi:10.1016/j.atmosenv.2007.09.005

Köppen, W., 1936. Das geographische System der Klimate, in: Köppen, W., Geiger, R. (Eds.), Handbuch Der Klimatologie. Gebrüder Bornträger, Berlin, pp. 1–44.

Kraftfahrtbundesamt, 2012. Zentrales Fahrzeugregister [WWW Document]. URL http://www.kba.de/cln_031/nn_191172/DE/Statistik/Fahrzeuge/Bestand/FahrzeugklassenAufbauarten/b__fzkl__zeitreihe.html (accessed 10.15.16).

Kreyling, W.G., Semmler-Behnke, M., Möller, W., 2006. Ultrafine Particle–Lung Interactions: Does Size Matter? Journal of Aerosol Medicine 19, 74–83. doi:10.1089/jam.2006.19.74

Kukkonen, J., 2003. Extensive evaluation of neural network models for the prediction of NO2 and PM10 concentrations, compared with a deterministic modelling system and measurements in central Helsinki. Atmospheric Environment 37, 4539–4550. doi:10.1016/S1352-2310(03)00583-1

Kumar, P., Garmory, A., Ketzel, M., Berkowicz, R., Britter, R., 2009. Comparative study of measured and modelled number concentrations of nanoparticles in an urban street canyon. Atmospheric Environment 43, 949–958. doi:10.1016/j.atmosenv.2008.10.025

Langner, C., Klemm, O., 2011. A Comparison of Model Performance between AERMOD and AUSTAL2000. J. Air Waste Manage. Assoc. 61, 640–646. doi:10.3155/1047-3289.61.6.640

LANUV, 2015. Bericht über die Luftqualität im Jahre 2014. LANUV-Fachbericht 60 (No. 60). Landesamt für Natur, Umwelt und Verbraucherschutz Nordrhein-Westfalen (LANUV), Recklinghausen.

Lateb, M., Meroney, R.N., Yataghene, M., Fellouah, H., Saleh, F., Boufadel, M.C., 2016. On the use of numerical modelling for near-field pollutant dispersion in urban environments – A review. Environmental Pollution 208, 271–283. doi:10.1016/j.envpol.2015.07.039

Lee, S.-H., Park, S.-U., 2007. A Vegetated Urban Canopy Model for Meteorological and Environmental Modelling. Boundary-Layer Meteorology 126, 73–102. doi:10.1007/s10546-007-9221-6

Lenschow, P., 2001. Some ideas about the sources of PM10. Atmospheric Environment 35, 23–33. doi:10.1016/S1352-2310(01)00122-4

Letzel, M., Fallsak, T., Angel, D., 2012. Improvement of AUSTAL2000 results due to flow and turbulence input from MISKAM. Gefahrstoffe - Reinhalt. Luft 72, 329–334.

Li, X., Liu, C., Leung, D., Lam, K., 2006. Recent progress in CFD modelling of wind field and pollutant transport in street canyons. Atmospheric Environment 40, 5640–5658. doi:10.1016/j.atmosenv.2006.04.055

Lien, F.-S., Yee, E., Ji, H., Hsieh, K.-J., 2008. Partially resolved numerical simulation and RANS modeling of flow and passive scalar transport in an urban environment. Journal of Wind Engineering and Industrial Aerodynamics 96, 1832–1842. doi:10.1016/j.jweia.2008.02.042

Litschke, T., Kuttler, W., 2008. On the reduction of urban particle concentration by vegetation – a review. Meteorologische Zeitschrift 17, 229–240. doi:10.1127/0941-2948/2008/0284

Lohmeyer, A., Stockhauser, M., Moldenhauer, A., Nitzsche, E., Düring, I., 2004. Berechnung der KFZ-bedingten Feinstaubemissionen infolge Aufwirbelung und Abrieb für die Emissionskataster Sachsen (No. Arbeitspakete 1 und 2). Dresden.

Maier, H.R., Jain, A., Dandy, G.C., Sudheer, K.P., 2010. Methods used for the development of neural networks for the prediction of water resource variables in river systems: Current status and future directions. Environmental Modelling & Software 25, 891–909. doi:10.1016/j.envsoft.2010.02.003

Manousakas, M., Papaefthymiou, H., Diapouli, E., Migliori, A., Karydas, A.G., Bogdanovic-Radovic, I., Eleftheriadis, K., 2017. Assessment of PM2.5 sources and their corresponding level of uncertainty in a coastal urban area using EPA PMF 5.0 enhanced diagnostics. Science of The Total Environment 574, 155–164. doi:10.1016/j.scitotenv.2016.09.047

Massmeyer, K., 1999. Modelle zur Ausbreitung von Luftbeimengungen., in: Helbig, A., Baumüller, J., Kerschgens, M.J. (Eds.), Stadtklima und Luftreinhaltung. Springer, Berlin, Heidelberg, pp. 353–378.

Mauderly, J.L., Burnett, R.T., Castillejos, M., Özkaynak, H., Samet, J.M., Stieb, D.M., Vedal, S., Wyzga, R.E., 2010. Is the air pollution health research community prepared to support a multipollutant air quality management framework? Inhalation Toxicology 22, 1–19. doi:10.3109/08958371003793846

May, R.J., 2014. Neural Network Development Workflow. [WWW Document] URL http://www.ecms.adelaide.edu.au/civeng/research/water/software/neural-network-excel-add-in/gallery/workflow-image2.jpg (accessed 3.21.17).

May, R.J., Maier, H.R., Dandy, G.C., 2010. Data splitting for artificial neural networks using SOM-based stratified sampling. Neural Networks 23, 283–294. doi:10.1016/j.neunet.2009.11.009

Merbitz, H., Buttstädt, M., Michael, S., Dott, W., Schneider, C., 2012a. GIS-based identification of spatial variables enhancing heat and poor air quality in urban areas. Applied Geography 33, 94–106. doi:10.1016/j.apgeog.2011.06.008

Merbitz, H., Detalle, F., Ketzler, G., Schneider, C., Lenartz, F., 2012b. Small scale particulate matter measurements and dispersion modelling in the inner city of Liège, Belgium. Int. J. Environ. Pol. 50, 234. doi:10.1504/IJEP.2012.051196

Merbitz, H., Fritz, S., Schneider, C., 2012c. Mobile measurements and regression modeling of the spatial particulate matter variability in an urban area. Science of The Total Environment 438, 389–403. doi:10.1016/j.scitotenv.2012.08.049

Merbitz, H., Ketzler, G., Schneider, C., 2010. Untersuchungen zu den Windverhältnissen im Innenstadtbereich von Aachen. Aachener Geographische Arbeiten, Sonderband: 30 Jahre Klimamessstation Aachen-Hörn des Geographischen Instituts - Beiträge zu Geschichte und Regionalbezug der Klimaforschung in Aachen Heft 47, 97–116.

Moonen, P., Defraeye, T., Dorer, V., Blocken, B., Carmeliet, J., 2012. Urban Physics: Effect of the micro-climate on comfort, health and energy demand. Frontiers of Architectural Research 1, 197–228. doi:10.1016/j.foar.2012.05.002

Morakinyo, T.E., Lam, Y.F., 2016. Simulation study of dispersion and removal of particulate matter from traffic by road-side vegetation barrier. Environmental Science and Pollution Research 23, 6709–6722. doi:10.1007/s11356-015-5839-y

Morawska, L., Thomas, S., Gilbert, D., Greenaway, C., Rijnders, E., 1999. A study of the horizontal and vertical profile of submicrometer particles in relation to a busy road. Atmospheric Environment 33, 1261–1274. doi:10.1016/S1352-2310(98)00266-0

Nikolopoulou, M., Kleissl, J., Linden, P.F., Lykoudis, S., 2011. Pedestrians' perception of environmental stimuli through field surveys: Focus on particulate pollution. Science of The Total Environment 409, 2493–2502. doi:10.1016/j.scitotenv.2011.02.002

Nikolova, I., Janssen, S., Vos, P., Vrancken, K., Mishra, V., Berghmans, P., 2011. Dispersion modelling of traffic induced ultrafine particles in a street canyon in Antwerp, Belgium and comparison with observations. Science of The Total Environment 412–413, 336–343. doi:10.1016/j.scitotenv.2011.09.081

Ning, Z., Sioutas, C., 2010. Atmospheric Processes Influencing Aerosols Generated by Combustion and the Inference of Their Impact on Public Exposure: A Review. Aerosol and Air Quality Research 10, 43–58. doi:10.4209/aaqr.2009.05.0036

Oberndorfer, E., Lundholm, J., Bass, B., Coffman, R.R., Doshi, H., Dunnett, N., Gaffin, S., KöHler, M., Liu, K.K.Y., Rowe, B., 2007. Green Roofs as Urban

Ecosystems: Ecological Structures, Functions, and Services. BioScience 57, 823. doi:10.1641/B571005

Oke, T.R., 1987. Boundary layer climates, 2nd ed. Cambridge University Press, London.

Pascal, M., Corso, M., Chanel, O., Declercq, C., Badaloni, C., Cesaroni, G., Henschel, S., Meister, K., Haluza, D., Martin-Olmedo, P., Medina, S., 2013. Assessing the public health impacts of urban air pollution in 25 European cities: Results of the Aphekom project. Science of The Total Environment 449, 390–400. doi:10.1016/j.scitotenv.2013.01.077

Pederzoli, A., Thunis, P., Georgieva, E., Borge, R., Carruthers, D., 2011. Performance criteria for the benchmarking of air quality model regulatory applications: The "target" aproach. Presented at the 14th Conference on Harmonisation within Atmospheric Dispersion Modelling for Regulatory Purposes, Kos, Greece, pp. 297–301.

Pepe, N., Pirovano, G., Lonati, G., Balzarini, A., Toppetti, A., Riva, G.M., Bedogni, M., 2016. Development and application of a high resolution hybrid modelling system for the evaluation of urban air quality. Atmospheric Environment 141, 297–311. doi:10.1016/j.atmosenv.2016.06.071

Perry, S.G., Cimorelli, A.J., Paine, R.J., Brode, R.W., Weil, J.C., Venkatram, A., Wilson, R.B., Lee, R.F., Peters, W.D., 2005. AERMOD: A Dispersion Model for Industrial Source Applications. Part II: Model Performance against 17 Field Study Databases. Journal of Applied Meteorology 44, 694–708. doi:10.1175/JAM2228.1

Peters, J., Van den Bossche, J., Reggente, M., Van Poppel, M., De Baets, B., Theunis, J., 2014. Cyclist exposure to UFP and BC on urban routes in Antwerp, Belgium. Atmospheric Environment 92, 31–43. doi:10.1016/j.atmosenv.2014.03.039

Pope, C.A., Burnett, R.T., Thun, M.J., Calle, E.E., Krewski, D., Ito, K., Thurston, G.D., 2002. Lung cancer, cardiopulmonary mortality, and long-term exposure to fine particulate air pollution. Journal of the American Medical Association 287, 1132–1141.

Raaschou-Nielsen, O., Andersen, Z.J., Beelen, R., Samoli, E., Stafoggia, M., Weinmayr, G., Hoffmann, B., Fischer, P., Nieuwenhuijsen, M.J., Brunekreef, B., Xun, W.W., Katsouyanni, K., Dimakopoulou, K., Sommar, J., Forsberg, B., Modig, L., Oudin, A., Oftedal, B., Schwarze, P.E., Nafstad, P., De Faire, U., Pedersen, N.L., Östenson, C.-G., Fratiglioni, L., Penell, J., Korek, M., Pershagen, G., Eriksen, K.T., Sørensen, M., Tjønneland, A., Ellermann, T., Eeftens, M., Peeters, P.H., Meliefste, K., Wang, M., Bueno-de-Mesquita, B., Key, T.J., de Hoogh, K., Concin, H., Nagel, G., Vilier, A., Grioni, S., Krogh, V., Tsai, M.-Y., Ricceri, F., Sacerdote, C., Galassi, C., Migliore, E., Ranzi, A., Cesaroni, G., Badaloni, C., Forastiere, F., Tamayo, I., Amiano, P., Dorronsoro, M., Trichopoulou, A., Bamia, C., Vineis, P., Hoek, G., 2013. Air pollution and lung cancer incidence in 17 European cohorts: prospective analyses from the European Study of Cohorts for Air Pollution Effects (ESCAPE). The Lancet Oncology 14, 813–822. doi:10.1016/S1470-2045(13)70279-1

Razavi, S., Tolson, B.A., 2011. A New Formulation for Feedforward Neural Networks. IEEE Transactions on Neural Networks 22, 1588–1598. doi:10.1109/TNN.2011.2163169

Roupsard, P., Amielh, M., Maro, D., Coppalle, A., Branger, H., Connan, O., Laguionie, P., Hébert, D., Talbaut, M., 2013. Measurement in a wind tunnel of dry deposition velocities of submicron aerosol with associated turbulence onto rough and smooth urban surfaces. Journal of Aerosol Science 55, 12–24. doi:10.1016/j.jaerosci.2012.07.006

Rumelhart, D.E., Hinton, G.E., Williams, R.J., 1986. Learning representations by back-propagating errors. Nature 323, 533–536. doi:10.1038/323533a0

Sæbø, A., Popek, R., Nawrot, B., Hanslin, H.M., Gawronska, H., Gawronski, S.W., 2012. Plant species differences in particulate matter accumulation on leaf surfaces. Science of The Total Environment 427–428, 347–354. doi:10.1016/j.scitotenv.2012.03.084

Santos, G., Fernández-Olmo, I., 2016. A proposed methodology for the assessment of arsenic, nickel, cadmium and lead levels in ambient air. Science of The Total Environment 554–555, 155–166. doi:10.1016/j.scitotenv.2016.02.182

Schiavon, M., Redivo, M., Antonacci, G., Rada, E.C., Ragazzi, M., Zardi, D., Giovannini, L., 2015. Assessing the air quality impact of nitrogen oxides and benzene from road traffic and domestic heating and the associated cancer risk in an urban area of Verona (Italy). Atmospheric Environment 120, 234–243. doi:10.1016/j.atmosenv.2015.08.054

Shu, S., Yang, P., Zhu, Y., 2014. Correlation of noise levels and particulate matter concentrations near two major freeways in Los Angeles, California. Environmental Pollution 193, 130–137. doi:10.1016/j.envpol.2014.06.025

Spinazzè, A., Cattaneo, A., Scocca, D.R., Bonzini, M., Cavallo, D.M., 2015. Multi-metric measurement of personal exposure to ultrafine particles in selected urban microenvironments. Atmospheric Environment 110, 8–17. doi:10.1016/j.atmosenv.2015.03.034

Stamenković, L.J., Antanasijević, D.Z., Ristić, M.Đ., Perić-Grujić, A.A., Pocajt, V.V., 2015. Modeling of ammonia emission in the USA and EU countries using an artificial neural network approach. Environmental Science and Pollution Research 22, 18849–18858. doi:10.1007/s11356-015-5075-5

Steinle, S., Reis, S., Sabel, C.E., 2013. Quantifying human exposure to air pollution—Moving from static monitoring to spatio-temporally resolved personal exposure assessment. Science of the Total Environment 443, 184–193. doi:10.1016/j.scitotenv.2012.10.098

Stow, C.A., Jolliff, J., McGillicuddy, D.J., Doney, S.C., Allen, J.I., Friedrichs, M.A.M., Rose, K.A., Wallhead, P., 2009. Skill assessment for coupled biological/physical models of marine systems. Journal of Marine Systems 76, 4–15. doi:10.1016/j.jmarsys.2008.03.011

Stull, R.B., 1988. An Introduction to Boundary Layer Meteorology. Springer.

Taylor, K.E., 2001. Summarizing multiple aspects of model performance in a single diagram. Journal of Geophysical Research: Atmospheres 106, 7183–7192. doi:10.1029/2000JD900719

Thunis, P., Georgieva, E., Pederzoli, A., 2012. A tool to evaluate air quality model performances in regulatory applications. Environmental Modelling & Software 38, 220–230. doi:10.1016/j.envsoft.2012.06.005

Tominaga, Y., Stathopoulos, T., 2013. CFD simulation of near-field pollutant dispersion in the urban environment: A review of current modeling techniques. Atmospheric Environment 79, 716–730. doi:10.1016/j.atmosenv.2013.07.028

United Nations, 2014. Population Division, Department of Economic and Social Affairs. World urbanization prospects: the 2014 revision.

Van den Bossche, J., Theunis, J., Elen, B., Peters, J., Botteldooren, D., De Baets, B., 2016. Opportunistic mobile air pollution monitoring: A case study with city wardens in Antwerp. Atmospheric Environment 141, 408–421. doi:10.1016/j.atmosenv.2016.06.063

Venkatram, A., 2008. Computing and displaying model performance statistics. Atmospheric Environment 42, 6862–6868. doi:10.1016/j.atmosenv.2008.04.043

Venkatram, A., Brode, R., Cimorelli, A., Lee, R., Paine, R., Perry, S., Peters, W., Weil, J., Wilson, R., 2001. A complex terrain dispersion model for regulatory applications. Atmospheric Environment 35, 4211–4221. doi:10.1016/S1352-2310(01)00186-8

Venn, A.J., Lewis, S.A., Cooper, M., Hubbard, R., Britton, J., 2001. Living Near a Main Road and the Risk of Wheezing Illness in Children. American Journal of Respiratory and Critical Care Medicine 164, 2177–2180. doi:10.1164/ajrccm.164.12.2106126

Vlachogianni, A., Kassomenos, P., Karppinen, A., Karakitsios, S., Kukkonen, J., 2011. Evaluation of a multiple regression model for the forecasting of the concentrations of NOx and PM10 in Athens and Helsinki. Science of The Total Environment 409, 1559–1571. doi:10.1016/j.scitotenv.2010.12.040

Vlachokostas, C., Achillas, C., Michailidou, A.V., Moussiopoulos, V., 2012. Measuring combined exposure to environmental pressures in urban areas: An air quality and noise pollution assessment approach. Environment International 39, 8–18. doi:10.1016/j.envint.2011.09.007

Vlachokostas, C., Banias, G., Athanasiadis, A., Achillas, C., Akylas, V., Moussiopoulos, N., 2014. Cense: A tool to assess combined exposure to environmental health stressors in urban areas. Environment International 63, 1–10. doi:10.1016/j.envint.2013.10.014

von Klot, S., 2005. Ambient Air Pollution Is Associated With Increased Risk of Hospital Cardiac Readmissions of Myocardial Infarction Survivors in Five European Cities. Circulation 112, 3073–3079. doi:10.1161/CIRCULATIONAHA.105.548743

Vos, P.E.J., Maiheu, B., Vankerkom, J., Janssen, S., 2013. Improving local air quality in cities: To tree or not to tree? Environmental Pollution 183, 113–122. doi:10.1016/j.envpol.2012.10.021

Wania, A., Bruse, M., Blond, N., Weber, C., 2012. Analysing the influence of different street vegetation on traffic-induced particle dispersion using microscale simulations. Journal of Environmental Management 94, 91–101. doi:10.1016/j.jenvman.2011.06.036

Weber, S., 2009. Spatio-temporal covariation of urban particle number concentration and ambient noise. Atmospheric Environment 43, 5518–5525. doi:10.1016/j.atmosenv.2009.06.055

WHO, 2013. Health risks of air pollution in Europe – HRAPIE project [WWW Document]. URL http://www.euro.who.int/__data/assets/pdf_file/0017/234026/e96933.pdf?ua=1 (accessed 3.18.15).

Wilson, J.G., Kingham, S., Pearce, J., Sturman, A.P., 2005. A review of intraurban variations in particulate air pollution: Implications for epidemiological research. Atmospheric Environment 39, 6444–6462. doi:10.1016/j.atmosenv.2005.07.030

Wu, W., Dandy, G.C., Maier, H.R., 2014. Protocol for developing ANN models and its application to the assessment of the quality of the ANN model development process in drinking water quality modelling. Environmental Modelling & Software 54, 108–127. doi:10.1016/j.envsoft.2013.12.016

Wurzler, S., Hebbinghaus, H., Steckelbach, I., Schulz, T., Pompetzki, W., Memmesheimer, M., Jakobs, H., Schöllnhammer, T., Nowag, S., Diegmann, V., 2016. Regional and local effects of electric vehicles on air quality and noise. Meteorologische Zeitschrift 25, 319–325. doi:10.1127/metz/2016/0707

Yassin, M.F., 2013. Numerical modeling on air quality in an urban environment with changes of the aspect ratio and wind direction. Environmental Science and Pollution Research 20, 3975–3988. doi:10.1007/s11356-012-1270-9

Yli-Pelkonen, V., Setälä, H., Viippola, V., 2017. Urban forests near roads do not reduce gaseous air pollutant concentrations but have an impact on particles levels. Landscape and Urban Planning 158, 39–47. doi:10.1016/j.landurbplan.2016.09.014

Zhu, Y., Kuhn, T., Mayo, P., Hinds, W.C., 2006. Comparison of Daytime and Nighttime Concentration Profiles and Size Distributions of Ultrafine Particles near a Major Highway. Environmental Science & Technology 40, 2531–2536. doi:10.1021/es0516514

Acknowledgements

I thank Prof. Dr. Christoph Schneider who gave me the opportunity for this PhD thesis within the multi-disciplinary project house HumTec at RWTH Aachen University. He placed huge confidence in my decisions regarding the lead of the subproject FuEco, as well as the content-related direction of this thesis. Concerning the questions that matter I always had his ear, even in difficult times including Christoph's change of professorship from RWTH Aachen University to HU Berlin. I am thankful for him pointing me always wisely in the right direction. Thank you for your great supervision.

I acknowledge the support from the involved persons at HU Berlin that made my change with the PhD proposition from RWTH Aachen University to HU Berlin straightforward and gave me the feeling of being in the right place with the thesis.

I want to thank all my colleagues at the home institution at RWTH Aachen University and at the interdisciplinary project house HumTec, as well as former colleagues from the University of Münster and the University of Tübingen, in particular Andy, Barbara, Benni, Cathrin, Dani, Degefie, Elisa, Eva, Frank, Gunnar, Ina, Isa, Jens, Joe, Jonas, Julian, Lars, Martina, Martina, Michael, Milad, Richard, Stanimira, Steffi, Tarek, Teresa and Timo. You inspired me, gave me confidence to go further, and showed me the ability to think outside the box.

Special thanks go to Alice, Arne, Beate, Burkard, Chris, Dominique, Erik, Falk, Florenz, Florian, Franziska, Friederike, Gerhard, Ilse, Isa, Jochen, Jutta, Laura, Lino, Manu, Michael, Mika, Nino, Phil, Resi, Richard, Rumpel, Sebastian, Simon, Tabea, Thomas, Uwe, Warron, and Yanik for their support as friends and family through the good and the hard times.

Thank you Prof. Dr. Stefan Weber and Prof. Dr. Wilfried Endlicher for the consent to survey this thesis as external referees and as known experts in the research fields of urban climate and air pollution.

Last but not least I want to thank Prof. Dr. Otto Klemm who first introduced me to the discipline of atmospheric science and aroused my interest and passion for the topic of climatology when I was a young undergraduate student at the University of Münster. Up to the point of now finishing my PhD thesis I can still say that a lot of what I know about academic working in the field of atmospheric science I learned from him.

Selbständigkeitserklärung

Ich erkläre, dass ich die Dissertation selbständig und nur unter Verwendung der von mir gemäß § 7 Abs. 3 der Promotionsordnung der Mathematisch-Naturwissenschaftlichen Fakultät, veröffentlicht im Amtlichen Mitteilungsblatt der Humboldt-Universität zu Berlin Nr. 126/2014 am 18.11.2014 angegebenen Hilfsmittel angefertigt habe.

Aachen, den 25.06.2017